# POTENTIAL PFAS PRODUCTS FROM THERMAL DECOMPOSITION OF MUNITIONS: A DFT ANALYSIS OF PYROLYSIS PRODUCTS OF FLUOROPOLYMERS IN THE PRESENCE OF ENERGETIC COMPOUNDS

by

Zachary C. Triumph

A thesis submitted to the Faculty and the Board of Trustees of the Colorado School of Mines in partial fulfillment of the requirements for the degree of Master of Science (Applied Chemistry).

Golden, Colorado

Date _____

Signed: _____

Zachary C. Triumph

Signed: _____

Dr. Shubham Vyas
Thesis Advisor

Golden, Colorado

Date _____

Signed: _____

Dr. Tom Gennett
Professor and Department Head
Department of Chemistry

# ABSTRACT

Per- and polyfluoralkyl substances (PFAS) are one of the most recalcitrant anthropogenic chemicals that can bioaccumulate and have carcinogenic properties. Their ubiquity in environmental matrices and resistance toward traditional disposal techniques pose a serious threat to the environment and public health. This thesis serves as a preliminary analysis of a novel source of PFAS, the disposal of munitions. Most munitions contain energetic compounds, to serve as the source of energy in detonation events, and fluoropolymers, to bind formulations as a means of stabilization, to seal the formulation away from the elements, or to serve as a fluorine source in pyrolants. Energetic compounds degrade through a variety of pathways, but the major pathways involve the formation of radicals and extreme heat. Despite the extreme recalcitrance of fluoropolymers, the conditions of detonation events are more than sufficient to initiate thermal decomposition in even the most robust fluoropolymers. The thermal decomposition of fluoropolymers involves highly reactive radical intermediates too. Since both energetic compounds and fluoropolymers undergo radical degradation mechanisms, PFAS radical recombination products are expected to be formed. There is little known about such potential PFAS products since they contain functionalities not seen in other sources of PFAS, so a summary of the synthesis and degradation reactions that these species are known to undergo from synthesis work is provided. This work also contains a detailed computational investigation of chemical bonding in such potential PFAS products from the pyrolysis of fluoropolymers in the presence of energetic compounds. Such investigations provide insight to the mechanisms of PFAS production and the types of functional groups to expect which provide guidance to the future analytical work by narrowing the scope of the system. The more that computational work is able to mimic experimental results, the more efficient future laboratory work will be. Thus, this thesis concludes by proposing possible future directions for this work, which includes a wide variety of ways to expand the system to be a more comprehensive representation of reality.

TABLE OF CONTENTS

LIST OF FIGURES

ACKNOWLEDGMENTS

In this space, I would like to thank my advisor, Shubham, for his constant support throughout this process. Shubham's guidance and constructive criticism helped me grow into the person I am today, and for that, I will be eternally grateful. Additionally, I would like to recognize the rest of the Vyas group who are living examples to the testament of Shubham's character as an advisor and as a person; I could not have imagined a better advisor to be my mentor, guide, and role model throughout this process. Each and every member of the Vyas group is a beautiful human being and many are dear friends. Their support and encouragement through every step of the research process is appreciated more than they can ever know. Their openness and kindness promoted an environment conducive to learning, camaraderie, and ,most importantly, progress on research! I thank my family, especially Mom, Dad, and Ty, for being a constant source of encouragement and support throughout my time at Mines. Last, but most certainly not least, I would like to thank my committee for their feedback and questions which serve as a source of inspiration my future as a scientist.

For those that came before and those who shall follow after.

# CHAPTER 1
# INTRODUCTION

## 1.1 Introduction

Per- and polyfluoroalkyl substances (PFAS) are one of the most recalcitrant manmade environmental contaminants. The robustness of PFAS is dedicated to the strong C-F bonds which coupled with PFAS' hydrophobic and lipophobic abilities provided them numerous applications. However, several recent studies have linked perfluorooctane sulfonic acid (PFOS) and perfluorooctanoic acid (PFOA) content in the bloodstream to various types of cancer [1, 2]. PFAS are also known to bioaccumulate in species at the top of their respective food chains, such as polar bears [3]. Thus, PFAS in environmental matrices is a serious public health hazard that is becoming more publicized as of late. The EPA report from October 2021 classified PFAS with a hazardous sub-stance designation, which will give the organization more legal grounding to hold polluters accountable and help to deal with the problem of PFAS in environmental matrices [4]. As of June $15^{th}$, 2022, the EPA confirmed the outline, and placed much stricter guidelines on four PFAS: PFOS, PFOA, hexafluoropropylene oxide (HFPO) dimer acid and its ammonium salt (GenX chemicals), and perfluorobutane sulfonic acid and its potassium salt (PFBS) [5]. While these most common PFAS have the largest body of research devoted to demonstrating their harm, the unifying component to their chemistry is the presence of C-F bonds which are ubiquitous in all PFAS. Therefore, the generation of novel compounds with C-F bonds is of particular concern from both the environmental and public health standpoints. Thus, this thesis will begin with the identification of a previously uninvestigated possible source of PFAS, munitions, followed by a description of the degradation pathways some of the most widely used energetic or explosive compounds in energetic devices. This will be followed by followed by a discussion of another important component of many energetic formulations, fluoropolymers, and the degradation pathways of some of the most common fluoropolymers used in energetic devices. The major hypothesis of this thesis that intermediates from the degradation pathways of energetic compounds and fluoropolymers will react to form novel PFAS. A discussion of what is known about the synthesis and reactions of such compounds and a brief summary as well as the purpose of and methods used in the work for this thesis will conclude this introduction chapter.

## 1.2 Degradation Mechanisms of Energetic Compounds

The National Academy of Sciences, Engineering, and Medicine (NASEM), the Division on Engineering and Physical Sciences (DEPS), and the Board on Army Science and Technology (BAST) determined that

there are 400,000 tons of expired or outdated munitions in the US alone that need to be disposed of safely and sustainably [6]. The two primary current disposal methods are open burns and controlled detonations. Open burns involve the combustion of munitions through deflagration processes rather than a detonation event, which sustains much lower temperatures and pressures for an extended period of time. There is a gap in the literature concerning the exact temperature ranges, pressures, and timescales of this process, but deflagration for energetic compounds such as the solid-state rocket fuel cyclotrimethylenetrinitramine, commonly called hexogen, Royal Demolition eXplosive, or Research Department eXplosive (RDX) can be sustained at temperatures as low as 477 K in systems where RDX deflagration is used to clean pipes such as by McLean *et al.* [7], but it can become as high as 1200-3000 K depending on the exact conditions as proposed by Sakano *et al.* [8]. The uncertainty of deflagration temperatures adds complexity to determination of the range of temperature relevant to each system, thus requiring an understanding of the mechanisms of thermal decomposition of energetic compounds. The key energetic compounds are trinitrotoluene (TNT), RDX, and cyclotetramethylenetetranitramine, which is commonly called octagen, Her Majesty's eXplositve, or High Melting eXplosive (HMX), the structures of which are shown in Figure 1.1.

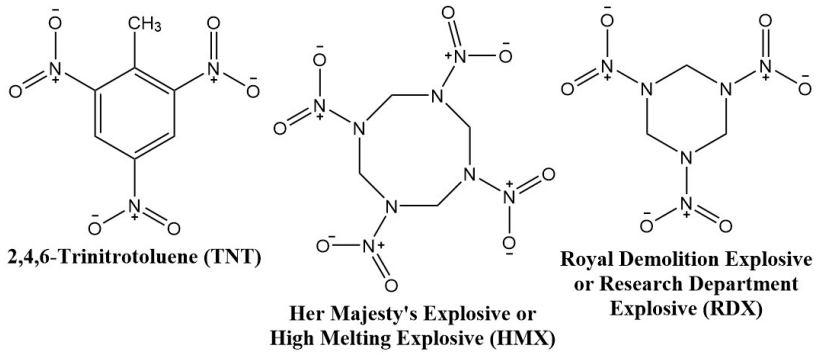


Figure 1.1 Chemical structures of TNT, HMX, and RDX.

### 1.2.1 Initiation Mechanisms of TNT Degradation

The degradation of TNT is characterized by three major initiation pathways, C-$NO_2$ homolysis [9–13], C-H $\alpha$ attack, which generates water and 2,4-dinitro-anthranil [9–12], and $CH_3$ removal [11, 12] (see Figure 1.2). In 2014, Furman *et al.* performed reactive force field simulations with corrections for London dispersion forces (ReaxFF-lg) on this system, which allowed for the modeling of pyrolysis mechanisms while accounting for each atom that began in the simulation and its fate [12]. The three major pathways encompass much of the reactivity and product distribution expected in the detonation of TNT, but other minor pathways are necessary to understand the generation of the major species over time as shown by

Furman *et al.* [12]. Such pathways are the isomerization from the nitro compound, R-$NO_2$, into the aromatic nitrite, R-ONO, and it subsequent dissociation to form R-O and NO radicals [10–12], O elimination, H escape, OH removal, and HONO elimination [11, 12]. There is still fervent discussion of the details of TNT degradation even though the compound was discovered over well over a century ago and has been in use as an energetic compound for almost as long. For example, there is some contention about each minor pathway's relative importance, which is discussed in detail below. Despite the extent of the use of TNT for the timescale it has been in use, there is much unknown in the details of its degradation. C-$NO_2$ homolysis leads to the generation of $NO_2$ radicals, and it is the most prevalent degradation pathway of TNT at the high temperatures most relevant to detonation events [10–13]. The generation of $NO_2$ radicals is typical for many energetic compounds [13]; the R-$NO_2$ bond is relatively weak, and the cleavage of this bond is very entropically favorable, so it is the most likely bond to break once sufficient temperatures are reached [10–12]. A 2007 study by Cohen *et al.* found that the temperature needed for this pathway to become accessible are between 1250-1500 K [10], and, in 2010, Chen *et al.* determined that the exact temperature needed for C-$NO_2$ cleavage to become kinetically accessible was 1335 K [11]. While these temperatures are moderately high, they are easily achievable during detonation events, where temperatures can exceed 3000 K [14]. C-H $\alpha$ attack, which produces a bicyclic intermediate and water, is the most prevalent degradation pathway of TNT at low temperatures, and it is a minor pathway at higher temperatures [11, 12]. Although $CH_3$ removal is not the most prevalent degradation pathway of TNT no matter the temperature, it is the second most important pathway for the high temperature degradation associated with detonation events [11]. This pathway become kinetically accessible at temperatures above 2112 K and remains the second most important reaction as temperatures increase [11]. While each major reaction is relevant to determine the major products and intermediates that result from the degradation of TNT, $NO_2$ radicals are likely to be the most impactful and prevalent [10–13]. Minor pathways are relevant for a number of reasons, but as demonstrated by Furman *et al.*, the foremost reason is that the species distribution over time reflects the timescales at which each becomes important [12]. Additionally, kinetic investigation [11] implicate R-$NO_2$ isomerization, O elimination, H escape, OH removal, and HONO elimination to various degrees at different temperatures. Using first-principles Density Functional Theory (DFT) to investigate the unimolecular decomposition of TNT, it is expected that the HONO elimination reaction will only be kinetically relevant in a very narrow temperature window (1200-1335 K) [11], but the species distributions over time show in ReaxFF-Ig simulations show a different story where HONO molecules are a relevant minor intermediate 3500 K [12]. Additionally, NO radicals were found to be very common in simulations [12], but kinetics of the isomerization thought to be the major source of NO radicals is much too slow compared to other initiation pathways of TNT decomposition to account for such

significant concentrations [10, 11]. This result was thoroughly demonstrated by Cohen *et al.* in a DFT study where the isomerization and subsequent cleavage of the O-NO bond was found to be thermodynamically favorable at all temperatures but was also kinetically unfavorable at all temperatures compared to C-H $\alpha$ attack or C-$NO_2$ depending on the specific temperature [10]. Even so, the reasoning for this surprising result suggested by Furman *et al.* was to be tied to the importance of bimolecular decomposition in TNT [12], which was unaccounted for in both kinetics studies [10, 11]. In any case, there is some agreement about the importance of the three major pathways in literature, but there is contention about the relevance and impact of each of the minor pathways of the thermal decomposition of energetic compounds.

### 1.2.2 Initiation Mechanisms of RDX Degradation

The degradation of RDX is characterized by two major classes of initiation pathways: unimolecular reactions dominated by HONO elimination [15–21] and N-N bond homolysis [15–22], or bimolecular reactions where RDX reacts with other small radicals [17]. There are many other minor pathways such as concerted ring cleavage [15–18, 21], and, more recently, $NO_2$-ONO isomerization [18, 21, 22], followed by O-NO homolytic cleavage to produce R-O radical and NO, but such pathways are beyond the scope of this work. The relative importance of the major pathways is highly dependent on the phase of RDX [15–22]. In the solid phase, a 2008 study by Miao *et al.* used time-dependent DFT with a 6-311+G(d,p) basis set. This study suggests that unimolecular decomposition through N-N bond homolysis and HONO elimination dominates at stresses below 10 GPa while bimolecular reactions between radical decomposition products and unreacted RDX become the dominant pathways at stresses above 10 GPa [17]. In 2019, Zheng *et al.* used reactive force field (ReaxFF) to study of nanocrystalline RDX showed that N-N bond homolysis is the dominant initiation pathway, but that HONO elimination mechanisms are significant the degradation pathways of the intermediates formed from N-N bond homolysis [22]. In the liquid phase, the only major initiation pathways that were discussed thoroughly by Patidar *et al.* were N-N bond homolysis and HONO elimination [19]. Using Fourier Transform Infrared spectroscopy (FTIR) and time-of-flight mass spectrometry (ToFMS) in conjunction with a DFT analysis at the B3LYP/6-311++G(d,p) level of theory, this 2017 study concluded that HONO elimination is the most likely initiation step for RDX decomposition in the liquid phase [19]. This study goes on to claim that successive HONO elimination is less likely than ring-opening reactions after the initial HONO elimination reaction, and the resulting degradation pathways help elucidate the formation of formaldehyde and $N_2O$ shown in experiments [19]. In a following study of liquid-phase RDX decomposition, Patidar *et al.* proposed a reduced reaction mechanism that accounts for the observed kinetics and again conclude that HONO elimination is the dominant initiation mechanism

[20]. The calculations show that N-N bond homolysis is not relevant to the liquid-phase decomposition of RDX [20], which is in stark contrast to both solid-state [17, 22] and gaseous [15, 16, 18, 21] mechanisms. Even so, the body of work discussing the solid-phase and liquid-phase decomposition of RDX is much more limited than the work spanning many decades detailing the gas phase decomposition of RDX. In the gas phase, unimolecular decomposition mechanisms are the most common, but some studies include bimolecular reactions with small and common radical intermediates [15, 16, 18, 21]. In 2000, Chakraborty *et al.* performed a DFT analysis using the B3LYP/6-31G(d) level of theory to investigate the potential energy surface of gas phase decomposition in RDX [15]. This study found that HONO elimination is thermodynamically dominant over the N-N bond homolysis pathway because it has the most favorable potential energy surface [15]. A follow-up study in 2001 not only provides a model that aligns more closely with experimental observations, but it also included important secondary reactions for cyclic nitramines, RDX and HMX, with the key reactive radical intermediates including but not limited to $CH_2NNO_2$, $CH_2N$, NO, $NO_2$, and OH that were unable to be included in their first investigations of RDX and HMX [16]. In 2016, Molt *et al.* used couple cluster theory at the CCSD(T)/CBS level of theory to determine electronic energies for structures in RDX decomposition pathways obtained with MBPT(2)/cc-pVTZ methodology [18]. The authors investigated the four major initiation pathways and concluded that HONO elimination is the preferred mechanism at STP, and the authors determined that, after the initial HONO elimination, the activation barrier for N-N bond homolysis is similar to that of a second HONO elimination [18]. The most recent study of gas phase thermal decomposition of RDX discussed here is from 2019, and it uses Variable Reaction Coordinate Transition State Theory with a combination of CASPT2(10e,7o)/jun-cc-pVTZ level of theory for the key atoms and M06-2X/jun-cc-pVTZ for the rest of the molecule [21]. This study finds N-N bond homolysis to be the most dominant kinetic pathway by far with HONO elimination as a distant second [21], which is in agreement with the results of Molt *et al.* [18]. These gas phase studies tell a confusing story, but it is clear that the HONO elimination pathway has a lower activation energy barrier which had led many researchers to conclude that it will be the more kinetically relevant pathway for the initiation of RDX decomposition in the gas phase. However, as demonstrated through the experimental results and computational kinetic analyses, the kinetics of N-N bond homolysis are much faster than that of HONO elimination and therefore dominate initiation of RDX decomposition in the gas phase. Overall, the state of RDX is very important to the question of "How does RDX decomposition start?" Depending on the unique conditions of the experiment, unimolecular reactions where N-N bond homolysis [17, 21, 22] or HONO elimination [15–20] can be found to dominate, or bimolecular decomposition where reactions between RDX and other radicals are the most important [17].

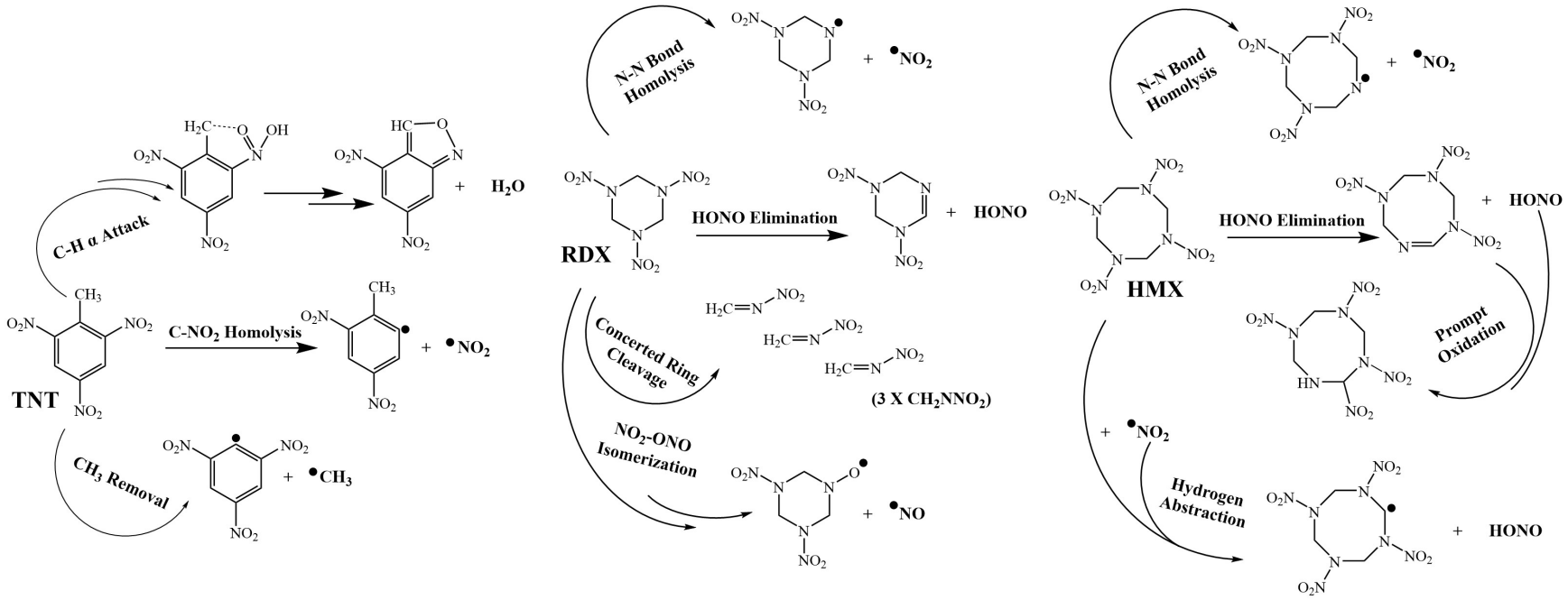


Figure 1.2 Initiation of TNT degradation through C-$NO_2$ homolysis, C-H $\alpha$ attack, and $CH_3$ removal mechanisms, initiation of RDX degradation through N-N bond homolysis, HONO elimination, concerted ring cleavage, and $NO_2$-ONO Isomerization, and initiation of HMX degradation through N-N bond homolysis, HONO elimination, prompt oxidation, and hydrogen abstraction.

### 1.2.3 Initiation Mechanisms of HMX Degradation

The degradation of HMX is characterized by two major initiation pathways: HONO elimination and N-N bond homolysis [16, 23–25]. Detailed analysis of minor pathways, such as O-migration from $NO_2$ to the adjacent carbon followed by ring-opening [23], and bimolecular reactions [24], such as oxygen abstraction by NO, prompt oxidation via HONO or $ONNO_2$ addition, and hydrogen abstraction by $NO_2$, are beyond the scope of this work. The conformation of HMX in the condensed phase, which is temperature dependent, is important for determining the most favorable initiation pathway [23, 24] [25]. Using DFT at the B3LYP/6-31G(d) level of theory, Chakraborty *et al.* performed a thorough investigation of the gas phase decomposition of HMX [23] and found it to be very similar to the gas phase decomposition of RDX, so a combined model including both species was made [16]. In HMX, HONO elimination is the dominant initiation pathway with N-N bond homolysis as a secondary pathway that is quite endothermic [16, 23]. This is reminiscent of their conclusions for RDX decomposition [15, 16], but, unlike RDX, HMX does not have a concerted ring cleavage initiation pathway as a significant secondary initiation pathway [16, 23]. The product distributions obtained from the updated kinetic model for thermal decomposition of RDX and HMX provided species distributions that aligned well with experimental observations [16]. In 2018 and using DFT at the B3LYP/6-311++G(d,p) level of theory, Patidar *et al.* determined that the liquid-phase decomposition of HMX mirrors that of RDX because HMX decomposition is likely to begin with HONO elimination and that ring-opening reactions are more likely than subsequent HONO eliminations [24, 25]. This study also calls for investigation of various bimolecular reactions that are likely to play important roles in the solid- and liquid-phase decomposition pathways of HMX [24]. In a 2020 study, Patidar *et al.* determined experimentally through differential scanning calorimetry (DSC), thermogravimetric analysis (TGA), and confined rapid thermolysis (CRT) that hydrogen abstraction (likely by $NO_2$) and prompt oxidation (likely through HONO or $ONNO_2$ addition) reactions play an important role in the liquid phase [25]. Overall, HONO elimination is thought to be the dominant pathway for the decomposition of both gas [16, 23] and liquid-phase HMX [24]. The major and minor initiation pathways in the degradation of TNT, RDX, and HMX are summarized in Figure 1.2. The initiation of TNT degradation primarily results in the formation of $NO_2$ radicals from the C-$NO_2$ bond homolysis pathway, and $CH_3$ radicals are made in through $CH_3$ removal. The body of research detailing HMX decomposition pathways is nowhere near as extensive as that of RDX, but both show HONO elimination and N-N bond homolysis being the most important initiation pathways in most scenarios relevant to detonation events for nitramines. These two major initiation pathways lead to the generation of reactive radical species that are unable to undergo further intramolecular degradation reactions: HONO is known to further decompose

into NO and OH radicals whereas N-N bond homolysis directly generates $NO_2$ radicals. Considering the parallels between RDX and HMX degradation mechanisms and the recent investigations of Molt *et al.* [18] and Chen *et al.* [21] showing the kinetic dominance of N-N bond homolysis in RDX, it would be interesting to see what the result would be if such an analysis were performed on HMX. Both possibilities for a major conclusion are intriguing: confirming that HONO elimination is the predominant pathway for HMX decomposition despite the opposite being true for RDX or contradicting previous HMX literature and showing that N-N bond homolysis is more kinetically relevant than HONO elimination in HMX.

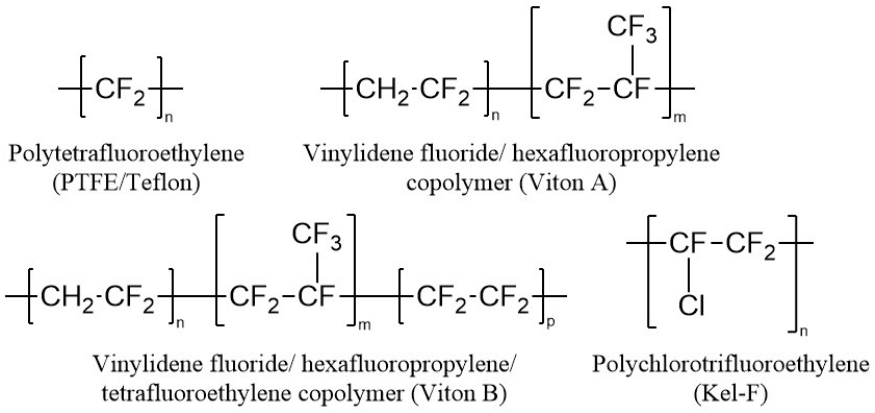


Figure 1.3 Chemical structures of PTFE, Viton A and B, and Kel-F.

### 1.3 Presence of Fluoropolymers in Munitions

Considering the current methods of disposal for munitions and the consequential products of thermal decomposition, it is important to note that munitions are more than the sum of energetic compounds. Fluoropolymers including polytetrafluoroethylene (PTFE, Teflon), vinylidene fluoride/ hexafluoropropylene copolymer (Viton A), vinylidene fluoride/ hexafluoropropylene/ tetrafluoroethylene copolymer (Viton B), and polychlorotrifluoroethylene (Kel-F) are commonly used as binders to stabilize the formulations, sealants to protect from the elements, and as fluorine sources in pyrolants, such as in pyrotechnic payloads based on magnesium, Teflon, and Viton called MTV formulations [14, 26]. MTV formulations use fluoropolymers as a fluorine source for the oxidation of magnesium into $MgF_2$, which is an incredibly exothermic process that generates a huge amount of heat and light and is very useful in flare technology and various other applications [14]. Viton O-rings are commonly used to seal formulations [27], and PTFE and Kel-F are often used to bind the energetic compounds to ensure that the devices only detonate when they are wanted to [28]. As can be seen below in Figure 1.3, all of these polymers contain fully fluorinated carbon centers, namely $CF_2$ moieties, as part of each monomer subunit. Thus, under the definition of per- and polyfluoroalkyl substances (PFAS) provided by Wang *et al.* in 2021, all of these polymers are classified

as PFAS, and many of their degradation products are also classified as PFAS [29]. PFAS are a class of persistent organic pollutants that have become a major problem for their carcinogenic properties [1, 2]. The EPA has heavily restricted the acceptable limits of the legacy PFAS, PFOA and PFOS, as well as some of their replacements including GenX chemicals and PFBS [4, 5]. Unfortunately, there was a list of over 4700 PFAS published by the Organisation for Economic Cooperation and Devolpement and the United Nations Environment Programme as of 2018, and there are likely many more yet to be classified [29]. Thus, the degradation products of PTFE, Viton, and Kel-F are of particular interest in the system of the disposal of expired munitions.

### 1.3.1 Thermal Degradation Mechanisms of PTFE

There is a massive variance in temperature ranges of deflagration depending on the exact conditions of the system [7, 8], and that variance makes it difficult to draw exact conclusions, so a minimum temperature of 1000 K was assumed. Although Viton has many classifications and there are thousands of formulations that are used for various industrial applications, some common Viton A copolymers [32–35] and Kel-F are known to completely degrade below 800 K [31, 34]. At 1000 K, complete degradation of the most recalcitrant fluoropolymer, PTFE, is observed [30, 34, 36, 37]. The first proposed mechanism for PTFE in 1947 by Lewis *et al.* proposed four-membered rings and $CF_2$ diradicals as possible intermediates to account for the formation of tetrafluoroethylene and hexafluoropropylene observed in their experiments [36]. Those experiments consisted of pyrolysis followed by the measurement of physical properties such as boiling points, flash points, and molecular weights for identification of the pyrolysis products [36]. Both the four-membered ring intermediated and $CF_2$ diradicals were confirmed with future pyrolysis and combustion experiments as important intermediates in PTFE degradation mechanisms [30, 37]. A 1967 combustion experiment performed by Mathias *et al.* confirmed the presence of $CF_2$ diradicals in part by the low reactivity between $CF_2$ diradicals and $O_2$ diradicals, but only 37% of the starting mass was recovered and identified despite none of the original polymer remaining in the chamber [37]. A number of other minor reactions and mechanisms for the formation of many of the major combustion products of PTFE, including $COF_2$, $CO_2$, and $CF_4$, were also proposed in this work [37]. A 1986 study of mechanisms of pyrolysis in a wide variety of fluoropolymers performed by Lonfei *et al.* investigated the formation of fluorinated alkyl chains that are likely to make up some portion of the weight unaccounted for by previous experiments [34]. The mechanism proposed by Lonfei *et al.* [34] in conjunction with the original mechanism proposed in 1947 by Lewis *et al.* [36] served as the basis for the mechanism of the combustion of PTFE proposed by Ellis *et al.* in 2001 shown in Figure 1.4 [30]. This mechanism of the thermolysis of PTFE showed that, in the presence of $O_2$ and $H_2O$ PTFE degradation can lead to the production of perfluoro carboxylic acids

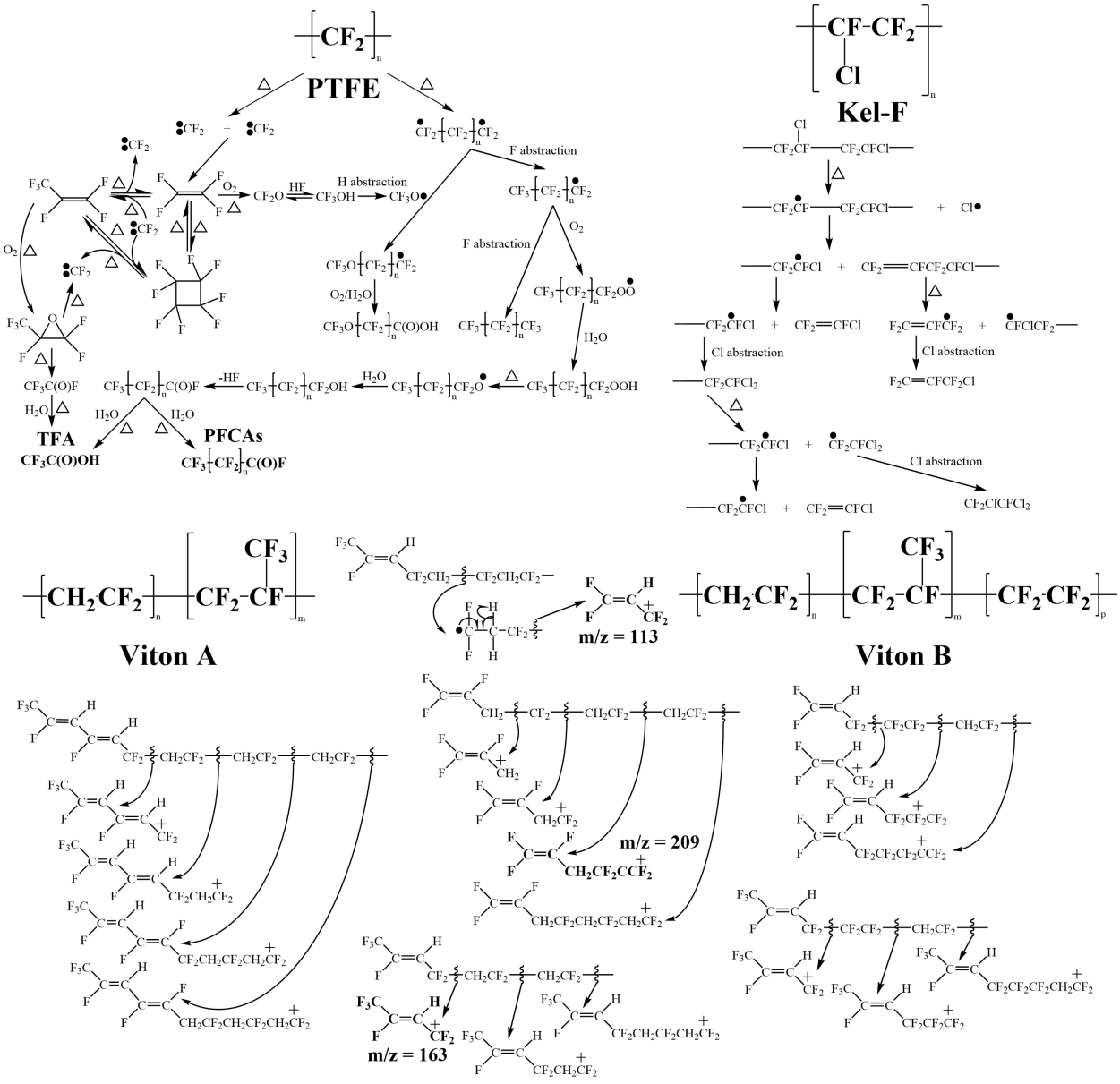


Figure 1.4 Decomposition pathways of PTFE [30], Kel-F [31], and Viton A and B [32]. For Viton B, the pathways below the polymers are unique to that polymer since tetrafluoroethylene is part of the copolymer formula [32]. The pathways shown in the center are most important for both Viton A and B since the largest peaks in each mass spectrum with m/z = 113, 163, and 209 are suspected to arise from these pathways [32].

including trifluoroacetic acid [30]. Such PFAS are of major environmental concern to the EPA [4, 5] and pose as a cancer risk to those exposed to moderate amounts of these carcinogenic compounds [1, 2].

### 1.3.2 Thermal Degradation Mechanisms of Viton and Kel-F

Viton has many, many classifications, but the two major categories are Viton A and Viton B. Viton A is a copolymer of vinylidene fluoride and hexafluoropropylene copolymer while Viton B also includes tetrafluoroethylene in its copolymer formula. The degradation mechanisms of various Viton types are not particularly well understood, but a 2014 paper by Hiltz proposes some pathways for the degradation of both Viton A and Viton B from pyrolysis gas chromatography/mass spectrometry (py-GC/MS) [32]. The degradation products observed in mass spectrometry experiments were identified as a combination partially fluorinated alkanes and alkenes with radical cation centers shown in Figure 1.4 [32]. These results match well with the proposed intermediates and products proposed by Lonfei *et al.* in their 1986 paper describing the degradation of various fluoropolymers [32, 34]. Lonfei *et al.* also used py-GC/MS to propose the production of short-chain alkanes and alkenes from polymers containing vinylidene fluoride monomer subunits [34]. Hiltz's analysis goes further by identifying individual peaks in the mass spectrums as a method of identifying unique fluoropolymers after they have been in service and contaminated by adulterants which could interfere with their IR spectra [32]. Kel-F is a chlorofluoropolymer with one chlorine for every three fluorines. Lonfei *et al.* investigated its decomposition in 1986, and they concluded that the mechanism would be much the same as perfluoropolymers such as PTFE except some fluorines would be replaced with chlorines [34]. According to their proposed mechanism for perfluoropolymers, the major reaction in the degradation of Kel-F would be monomers [34]. A slightly more recent study from 1994 that investigated the decomposition of partially chlorinated fluoropolymers written by Zulfiqar *et al.* found that, since chlorine abstraction is more favorable than fluorine abstraction, various products other than the monomer should be expected to form as seen in Figure 1.4 [31]. With the addition of hydrogenated carbons such as in the decomposition mechanism for the copolymers of chlorotrifluoroethylene and vinylidene fluoride, the system becomes exponentially more complex, and product such as HCl can be expected [31]. These limited mechanisms are difficult to substantiate given their preliminary nature and limited scope; none of the proposed mechanisms account for the presence of oxygen, and combustion is known to be more rapid, occur at lower temperatures, and be more complete than pyrolysis in the case of Viton A [33].

### 1.4 Possibility of PFAS Cross-Products

In the confined environment of the disposal of munitions through open burning and controlled detonation, it was hypothesized that the prevalent and long-lived radicals present in the degradation mechanisms of both energetic compounds and fluoropolymers will undergo radical recombination reactions with each other and molecular oxygen in air. Due to the speed of intramolecular degradation reactions for the complex organic radical intermediated in energetic compound degradation pathways, small volatile compounds produced in large quantities such as $NO_2$ and HONO. These compounds are produced in the competing initial degradation pathways of both RDX and HMX, N-N bond homolysis and HONO elimination respectively (see Figure 1.2) [15, 16, 23]. Such radicals cannot undergo rapid intramolecular degradation, but they are known to persist in the atmosphere and are associated with acid rain according to the US EPA [38]. $NO_2$ is already a radical, and HONO dissociates into OH and NO radicals, so these three radicals came into focus as the building blocks supplied by energetic compounds. The fluoropolymer system (see Figure 1.4) was not as straightforward because of factors like chain length and degree of unsaturation, but the simple universal intermediate chosen from the model system of PTFE was the primary perfluoropropyl radical because fully fluorinated alkyl radicals were proposed as an intermediate in the most robust degradation mechanism of PTFE to date [30]. The vinylidene fluoride component of both Viton A and B has hydrogenated carbon centers, so all permutations of polyfluoropropyl radicals were considered (see Figure 1.3). The addition of partial chlorination from including Kel-F has yet to be investigated because the addition of chlorine to the system would add orders of magnitude of complexity since partial fluorination, chlorination, and hydrogenation would need to be considered. Due to the possibility of 1,2-F shifts [39] and 1,2-H shifts [40], both primary and secondary per- and polyfluoropropyl radicals were considered as the inputs from fluoropolymers, but, for simplicity, each carbon center was either fully fluorinated or fully hydrogenated. The radical recombination products from these two sets of input radicals, gives PFAS analogs of nitroalkanes and alkyl nitrites from $NO_2$ radicals produced through C-N or N-N bond homolysis mechanisms as well as alcohols and nitrosoalkanes made from the NO and OH radicals formed from the degradation of HONO produced in HONO elimination mechanisms.


Figure 1.5 Synthesis reaction scheme for production of nitroso-PFAS [41, 42].

### 1.4.1 Synthesis and Degradation of Nitroso-PFAS

There is a surprisingly rich history in research of such cross-products in literature. In the 1950s and 1960s, compounds such as perfluoronitroalkanes (nitro-PFAS) and perfluoroalkyl nitrates (nitrito-PFAS) were of interest for a variety of synthetic applications including fluoropolymers [42, 42–50]. Perfluoronitrosoalkanes (nitroso-PFAS) have unique photodimerization reactions and decomposition products that were of interest [42, 42, 44, 48, 49]. A 1953 paper by Haszeldine discussed the synthesis of various nitroso-PFAS as shown in Figure 1.5 by reacting perfluoroalkyl radicals with NO gas [42]. Haszeldine's investigation of the oxidation products of trifluoronitrosomethane (TFNsM) and other nitroso-PFAS found that the major product obtained was the nitro-PFAS analog, trifluoronitromethane (TFNM) as seen in Figure 1.6 in the case of TFNsM [42]. Banus confirms these conclusions with a 1953 investigation of TFNsM and heptafluoronitrosopropane (HFNsP) which found that, when exposed to alkali or mercury and shaken, these compounds oxidized into their nitro-compound analogs [42]. Banus discovered the synthesis shown in Figure 1.5 used to make such perfluoroalkyl nitroso compounds earlier that same year, which involved abstracting iodine to make the carbocation analog and reacting that with NO gas [41].

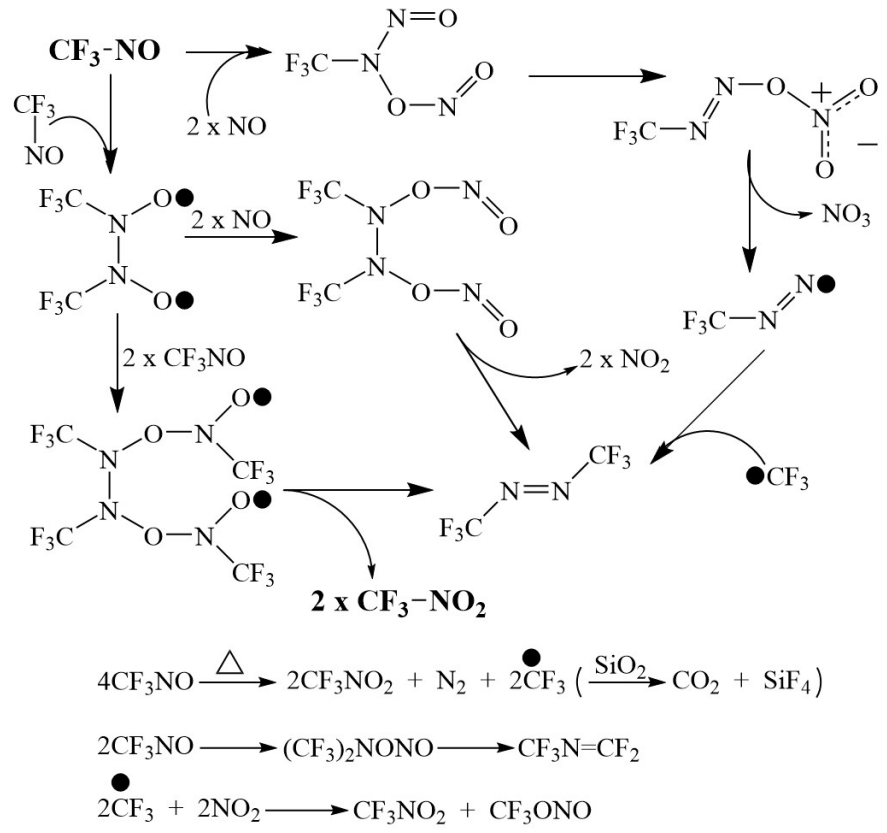


Figure 1.6 Prominent degradation mechanisms of TFNsM [49, 51, 52].

In 1961, Barr *et al.* investigated the synthesis of TFNsM-alkene copolymers and their degradation products [44]. These reactions were found to form oxazetidines and a 1:1 copolymer, the degradation of which made imines with various substitutions and chain lengths [44]. In 1965, Banks *et al.* investigated the thermal decomposition mechanism of HFNsP through pyrolysis and NMR [48]. This study determined some major products of HFNsP decomposition include trisubstituted hydroxylamines and aza-alkenes as shown in Figure 1.7 [48]. Banks *et al.* also probed the thermal decomposition of TFNsM in 1965 and determined that, in glass at 100°C as seen in Figure 1.6, TFNsM decomposed slowly into the major products TFNM, hexafluoroazomethane, perfluoro-(methylenemethylamine), and nitrogen [49]. This reaction was previously proposed to take only 14 days, but this study found that TFNsM is only destroyed after 6 months, and other major products, hexafluoroazomethane and perfluoro-(methylenemethylamine), were elucidated as shown in Figure 1.6 [49]. At 180°C, the same major products as at 100°C as well as $CO_2$ and $SiF_4$ were produced with 97% destruction of the TFNsM was completed in 24 hours [49]. A 1957 paper by Haszeldine *et al.* [51] and a 1963 paper by Mason (née Banus) [52] establish the accepted mechanism for the decomposition of TFNsM (Figure 1.6). The research into nitroso-PFAS in the 1950s and 1960s provided a fantastic basis for the research that followed, but, while the study of nitroso-PFAS was not limited to that twenty-year period, scientific interest in these compounds tapered off over the following decades. The next relevant paper was written in 1979 by Banks *et al.* investigating the photolysis and thermolysis of HFNsP [53]. In the photolysis experiments, HFNsP was constantly irradiated by 2737 Å UV light over 18 hours to yield about 30% nitroso dimers ($(n\text{-}C_3F_7)_2NONO$, $(n\text{-}C_3F_7)_2NNO_2$), which decomposed with preparative gas liquid chromatography and were identified with IR and mass spec, the trisubstituted hydroxylamine ($(n\text{-}C_3F_7)_2NOC_3F_7$), the trisubstituted amine ($(n\text{-}C_3F_7)_3N$), and the aza-alkene ($(n\text{-}C_3F_7)_2N{=}CFC_2F_5$) [53]. When HFNsP was flow-pyrolyzed in platinum at 250°C and 7-9 mmHg, the degradation products were determined to contain 88% hydroxylamine, 7% heptafluoronitropropane (HFNP), and 1.5% aza-alkene, but, thermal decomposition of HFNsP at 80°C for 24 hours in the absence of air resulted in 72% aza-alkene, 11% HFNP, and 8% hydroxylamine [53]. The mechanisms for the formation of these products are shown in Figure 1.7. A 1991 paper written by Pye *et al.* discussed the conversion of nitroso-PFAS into nitro-PFAS using a living free-radical copolymers as a catalyst, and it suggested some possible mechanisms for these reactions [54]. The reaction at room temperature in the absence of light also makes perfluoroazoalkanes, but, at 70°C in the absence of light, the reaction yields perfluoroaza-alkenes as a major product indicating that the $\beta$-cission reaction mechanism is temperature-dependent, and it likely has a high enough activation barrier as to make it inaccessible at room temperature [54].

Another paper written in the following year discussed the absolute rate constants of the reaction to make nitroso-PFAS from perfluoralkyl radicals and NO gas, which fundamentally investigated the

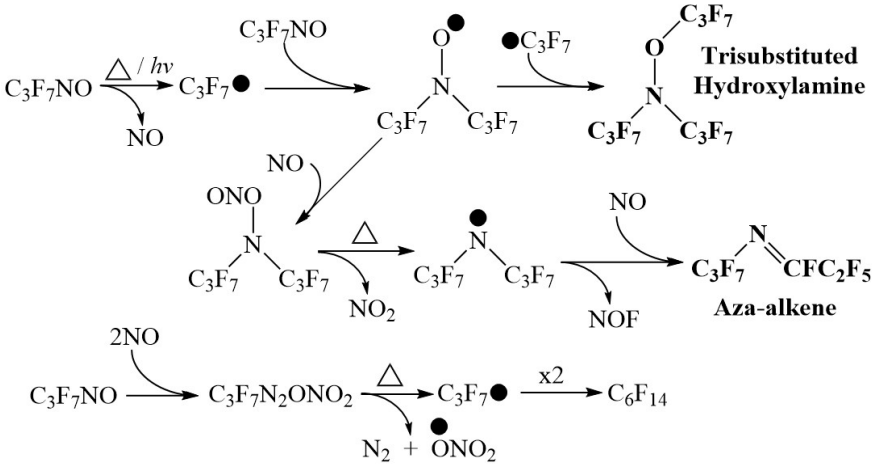


Figure 1.7 Prominent degradation mechanisms of HFNsP [48].

shock-wave dissociation of nitroso-PFAS under relatively mild conditions [55]. A 1995 paper written by Ludovici *et al.* describes the synthesis of nitroso-PFAS using the reaction between a fluoralkylzinc bromide with two associated cyanoalkanes and NOCl gas [56]. A 1996 study of the photolysis of TFNsM references the 1957 paper by Haszeldine *et al.* [51] and the 1963 paper by Mason (née Banus) [52] as the major sources for the mechanism shown in Figure 1.6 that was investigated in that work [57]. The experimental results agreed with the mechanisms established by these two experts in nitroso-PFAS chemistry [57], which further validates much of the early work done investigating nitroso-PFAS chemistry in the 1950s and 1960s. In 2014, a study used a similar ZnBr organozinc reagent to react $CF_2$ diradicals with NO gas in order to synthesis gem-difluorinated nitroso compounds [58]. Recently, there has been very little work done investigating nitroso-PFAS since such compounds were thoroughly investigated by Haszeldine [42, 44, 49] and Mason (née Banus) [41, 42, 52] in the 1950s and 1960s.

### 1.4.2 Synthesis and Degradation of Nitro-PFAS and Nitrito-PFAS

As previously mentioned, nitro-PFAS and nitrito-PFAS have also been thoroughly investigated since the 1950s and 1960s [43, 45–47, 50]. In 1958, Severson *et al.* investigated the use of perfluoroalkanesulfonyl fluorides to generate perfluoroalkyl radicals and the reactions with NO and $NO_2$ gas (Figure 1.8) [43]. These reactions led to the formation of nitro-PFAS and nitrito-PFAS whose subsequent degradation led to the generation of perfluoro acid fluorides (PFAFs) and perfluorocarboxylic acids (PFCAs) [43]. Both PFAFs and PFCAs were observed experimentally after being collected in cold traps from the anoxic reaction chamber, and the proposed mechanism for their formation is shown in Figure 1.9 [43]. A 1963 study by Knunyants *et al.* found that the addition of nitro and fluorine groups to alkenes allowed for

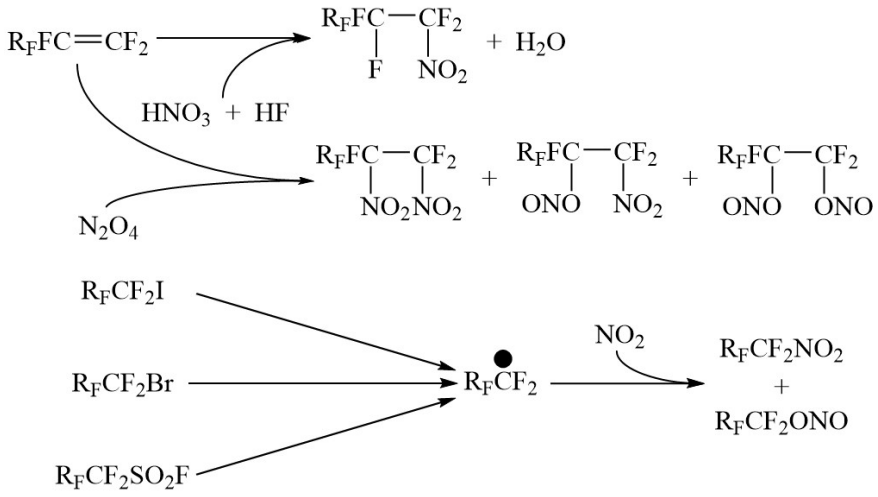


Figure 1.8 Synthesis reactions of nitro-PFAS and nitrito-PFAS [43, 45–47].

functionalization of both carbons participating in the double bond likely through Sn2 reactions replacing the fluorine groups (Figure 1.8) [45]. The following year, Scribner *et al.* [46] and Knunyants *et al.* [47] published papers on syntheses with nitro-PFAS and nitrito-PFAS as intermediates or products respectively. Scribner *et al.* reacted the staring material, polyfluoroalcohols with no fluorines on the carbon with the alcohol, with $N_2O_4$ gas in air through a mechanism which could involve both nitro-PFAS and nitrito-PFAS as intermediates; nitro-PFAS degraded at these temperatures through elimination reactions to form the aldehyde whereas nitrito-PFAS went through homolytic bond cleavage at the RO-NO bond to produce NO gas (see Figure 1.9) [46]. At 300-400°C, this reaction formed gem-diols and no carboxylic acids, but, when the reaction was performed at higher temperatures for longer periods of time, only carboxylic acids were formed as the final products [46]. The synthesis conducted by Knunyants *et al.* in 1964 was of the addition of $N_2O_4$ gas to the double bond in hexafluoroisobutene was expected to form the 1,2-dinitroalkane, 1-nitro-2-nitritoalkane, 1-nitrito-2-nitroalkane, and 1,2-dinitritoalkane (Figure 1.8), but the only products observed after treatment with water were pentafluoro-3-nitro-2-(trifluoromethyl)- 2-propanol and trifluoro-2-(trifluoromethyl)lactic acid (bistrifluoromethylglycolic acid) [47]. The species formed were determined to be pentafluoro-3-nitro-2-(trifluoromethyl)-2-propanol nitrite and pentafluoro-2-(trifluoromethyl)-l,2-propanediol dinitrite, the nitrito groups of which reacted vigorously with water to form the corresponding alcohol and carboxylic acid functionalities depending on whether the nitrito group was primary or secondary shown in Figure 1.9 [47]. In 1966, Knunyants *et al.* reinvestigated the addition of $N_2O_4$ to double bonds to form dinitro, nitro-nitrito, and dinitrito species as seen in Figure 1.8 with a new substrate, hexafluoropropylene, and were able to synthesize gem-diols [50]. These

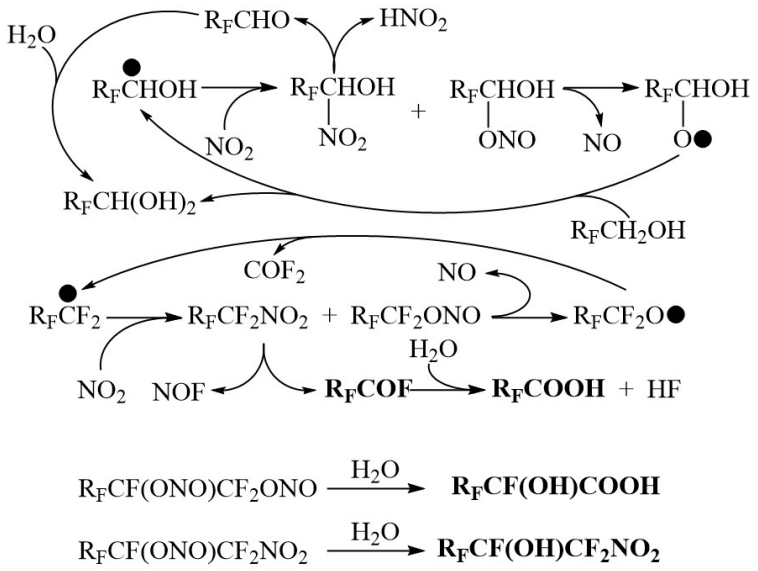


Figure 1.9 Degradation mechanisms of nitro-PFAS and nitrito-PFAS [43, 46, 47].

gem-diols were able to be dehydrated into their ketone analogs which underwent various other reactions to form cyanohydrins, hemiacetals, and other functionalities [50]. Following in the footsteps of Knunyants, Fokin *et al.* published a review of the products of nitration of fluoroalkenes using $N_2O_4$ and their reactions in 1982 [59]. This work was an incredibly detailed summary of the reactions of fluoroalkanes with a wide variety of substrate in reactions that could be used to synthesize various functional groups including carboxylic acids, acid fluorides, amides, alcohols, ketones, gem-diols, and sulfonamides [59]. Much like with nitroso-PFAS, the research interest in nitro-PFAS and nitrito-PFAS tapers off rapidly over the decades following the 1960s, but the foundational understanding of such compounds was already quite solid, so little work of note has been done since then.

### 1.4.3 Environmental Degradation and Fate of Per- and Polyfluoroalcohols

Perfluoroalcohols are an important intermediate in PTFE degradation [30], and fluorotelomer alcohols (FTOHs) have well-documented decomposition mechanisms in environmental matrices such as air [60] [61]. As can be seen in Figure 1.4 and Figure 1.10, in the degradation mechanism of PTFE, perfluoroalcohols decompose into their carboxylic acid analogs through successive reactions involving HF elimination and the addition of water to the acid fluoride [30]. This reaction is relatively slow in environmentally relevant conditions, but temperatures achieved in a detonation event are more than sufficient to catalyze this process assuming that water is available [30]. This process was also observed in environmental matrices such as air where the rate-limiting step, addition of water to the acid fluoride, occurred through

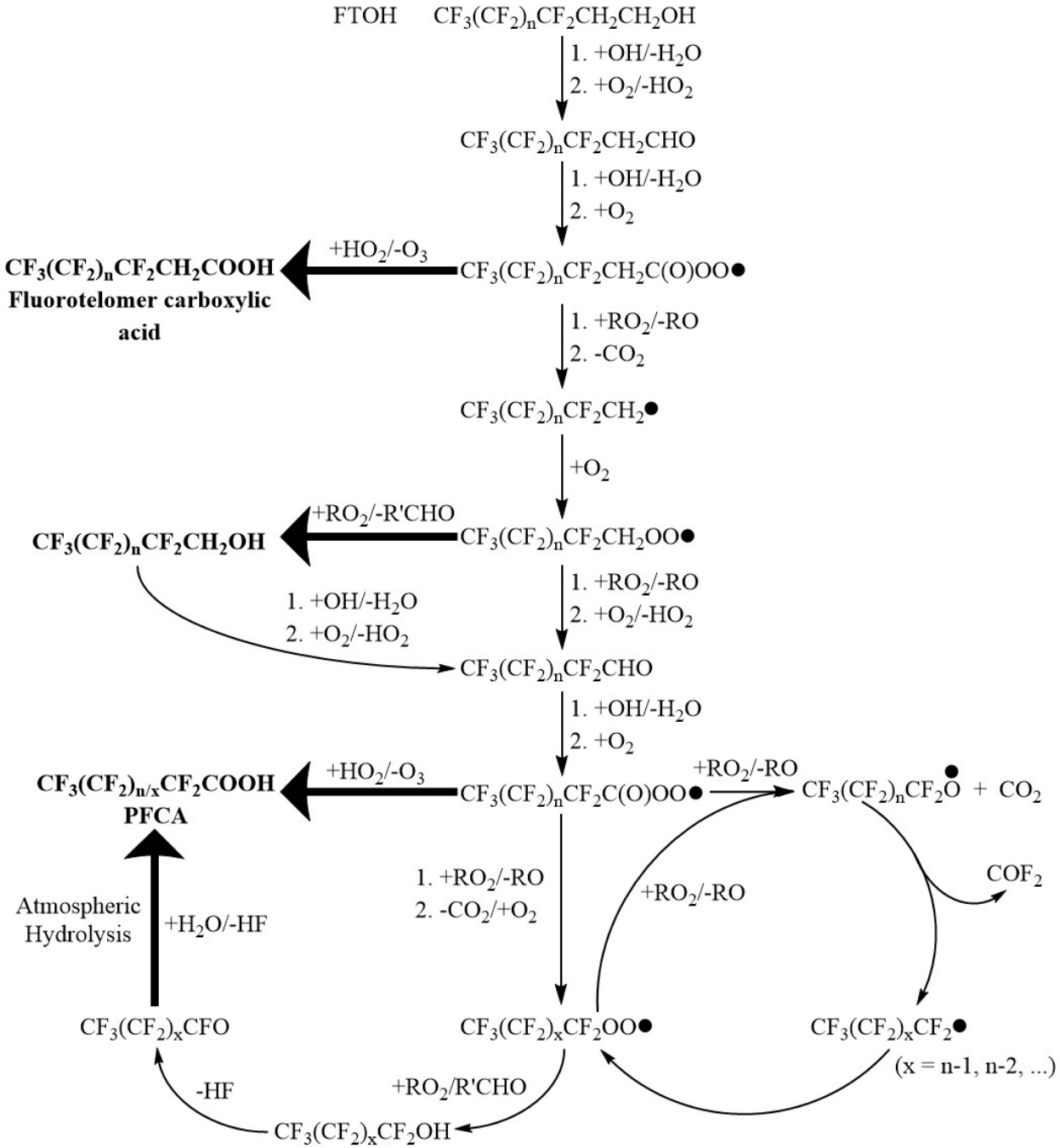


Figure 1.10 Atmospheric degradation mechanism of FTOHs and perfluoroalchohols [60].

atmospheric hydrolysis [60]. Ellis *et al.* [60] also set the precedent for investigation of FTOH decomposition in environmental matrices, and subsequent studies [61, 62] proposed very similar degradation mechanisms as those seen in Figure 1.10. The mechanism proposed by Ellis *et al.* involves the successive hydrogen abstraction by OH and $O_2$ followed by hydrogen abstraction by the PFAS and the loss of ozone [60]. Put simply, in the presence of oxygen and water, which are ubiquitous in environmental matrices, both perfluoroalcohols and FTOHs will eventually degrade into PFCAs in environmental matrices [30, 60–62]. As previously mentioned, per- and polyfluoroalcohols are not alone in their ability to generate PFCAs; nitro-PFAS and nitrito-PFAS have been used to synthesize PFCAs in procedures dating back to 1958 [43, 46, 47, 59]. The fact that these and other functionalized PFAS is one reason among many that PFCAs are one of the major focuses for PFAS contamination in the environment.

### 1.5 Conclusion and Outlook

To conclude, munitions are a possible source of novel PFAS. The components of energetic devices include both energetic compounds such as TNT, RDX, and HMX and fluoropolymers such as PTFE, Viton A and B, and Kel-F which undergo the radical degradation mechanisms discussed above. In the confined environment of the disposal of munitions through open burning and controlled detonation, it was hypothesized that the prevalent and long-lived radicals present in the degradation mechanisms of both energetic compounds and fluoropolymers will undergo radical recombination reactions with each other. Due to the magnitude of the number of possible products the scope of the following work was limited to a 3-carbon system, which reduced the number of species under study to 82 with 14 transition states, but, due to the difficulty of synthesizing these compounds and the lack of reliable standards for quantifying them, a computational approach was adopted. We probed the thermodynamic stability and kinetic accessibility of per- and polyfluoroalkyl adducts formed with OH, NO and $NO_2$ radicals using density functional theory (DFT) calculations and natural bond orbital (NBO) analyses. This work is discussed in full in the following chapter.

# CHAPTER 2

# CHEMICAL BONDING IN POTENTIAL PFAS PRODUCTS FROM THERMAL DEGRADATION OF ENERGETIC DEVICES, A DFT ANALYSIS

## 2.1 Abstract

This work investigates chemical bonding in possible per- and polyfluoroalkyl substances (PFAS) generated through the dis-posal of munitions in controlled detonations and open burns. Many munitions contain both fluoropolymers and energetic compounds that undergo radical degradation pathways when exposed to sufficient thermal stress. The purpose of this work is to serve as a preliminary product distribution analysis of the possible radical recombination products of intermediates from both pathways through analysis of bonding in these species. Due to the inordinate number of possible products, their detection and characterization via traditional analytical techniques are too time-intensive and expensive. The system was truncated to a 3-carbon system, and density functional theory (DFT), calculations were used to determine bond dissociation enthalpies (BDEs), activation enthalpies, and other physical properties. This DFT analysis investigated bonding through BDEs in order to determine the most likely functional groups to be present based on the level of fluorination and the position of those fluorines relative to said functional groups. This work expedites the analytical process to confirm that PFAS are cre-ated from current disposal methods of energetic devices by providing insight as to of what types of compounds should be expected in future analytical work. The PFAS generated in such reactions are expected to contain some functional groups (i.e., nitro and nitrite) that have not been known to exist as a result of the environmental degradation of industrially relevant PFAS, which may have been overlooked otherwise. These unique products are isomers, so an initial investigation of their isomerization reaction was investigated, but more work is needed to develop a deep understanding of this process.

## 2.2 Introduction

Fluoropolymers are incredibly resistant to chemical and thermal degradation and are both hydrophobic and oleophobic. These properties make them ideal for use in sealing energetic devices and preventing the energetic compounds within from being exposed to environmental elements or in binding the energetic compounds in a way that prevents the formulation from detonating prematurely [26]. Fluoropolymers are also used as a pyrolant for solid-state rocket fuels such as cyclotetramethylenetetranitramine, commonly called octogen, Her Majesty's eXplosive, or High Melting eXplosive (HMX), and cyclotrimethylene-trinitramine, commonly called hexogen, Royal Demolition eXplosive, or Research Department eXplosive

(RDX), since they provide a fluorine source for Mg metal oxidation [14, 26]. This mechanism of ignition has been in practice since the late 1950s, so there are munitions that were never used are now being disposed of by detonating them [14]. Common fluoropolymers used for this purpose such as the vinylidene fluoride/ hexafluoropropylene copolymer (Viton A), vinylidene fluoride/ hexafluoropropylene/ tetrafluoroethylene copolymer (Viton B), and polytetrafluoroethylene (PTFE) can be expected to degrade at temperatures under 1000 K [14, 30, 32, 34]. Although fluoropolymers are quite resistant to degradation, the extreme temperature, which can exceed 3000 K [14], pressure, and oxidative environment in a detonation event leads to their degradation. The homolytic cleavage of C-C bonds in fluoropolymers creates short chain radical precursors that are part of the per- and poly-fluoroalkyl substance (PFAS) family [30, 32, 34]. PFAS are one of the most recalcitrant manmade environmental contaminants. PFAS are carcinogenic. There are several studies linking perfluorooctane sulfonic acid (PFOS) and perfluorooctanoic acid (PFOA) content in the bloodstream to various types of cancer [1, 2]. PFAS are also known to bioaccumulate in species at the top of their respective food chains, such as polar bears [3]. Thus, PFAS in environmental matrices is a serious public health hazard that is becoming more publicized as of late. The EPA report from October 2021 classified PFAS with a hazardous substance designation, which will give the organization more legal grounding to hold polluters accountable and help to deal with the problem of PFAS in environmental matrices [4]. As of June 15th, 2022, the EPA confirmed the outline, and placed much stricter guidelines on four PFAS: PFOS, PFOA, hexafluoropropylene oxide (HFPO) dimer acid and its ammonium salt (GenX chemicals), and perfluorobutane sulfonic acid and its potassium salt (PFBS) [5]. While these most common PFAS have the largest body of research devoted to demonstrating their harm, the unifying component to their chemistry is the presence of C-F bonds which are ubiquitous in all PFAS. Since HMX [16, 23] and RDX [15, 16]] have identical functionalities on 6- and 8-membered rings respectively, their two major degradation pathways are also identical. The elimination of HONO species leads to the generation of OH and NO radicals, and the homolytic cleavage of N-$NO_2$ leads to the generation of $NO_2$ radicals. The degradation of PTFE leads to the generation of $CF_3CF_2CF_2$ and other short chain fluoroalkyl radicals [34]. Other fluoropolymers such as Viton comprise of hydrogenated carbons along with perfluorinated carbons. At the temperatures reached during detonation events, these primary radicals can readily interconvert with the secondary radicals through 1,2 fluorine transfers [39] or 1,2 hydrogen transfers [40]. Viton has many different forms, and it can have up to 3 different subunits with varying levels of fluorination, which implies that short chain PFAS radicals with greatly varied levels of fluorination from perfluoropropane radicals to propane radicals are possible in this system [33]. As a result, it is important to understand the bonding and formation of products formed upon radical recombination of per and polyfluoroalkyl radicals and relevant small radicals being generated by decomposition of HMX and

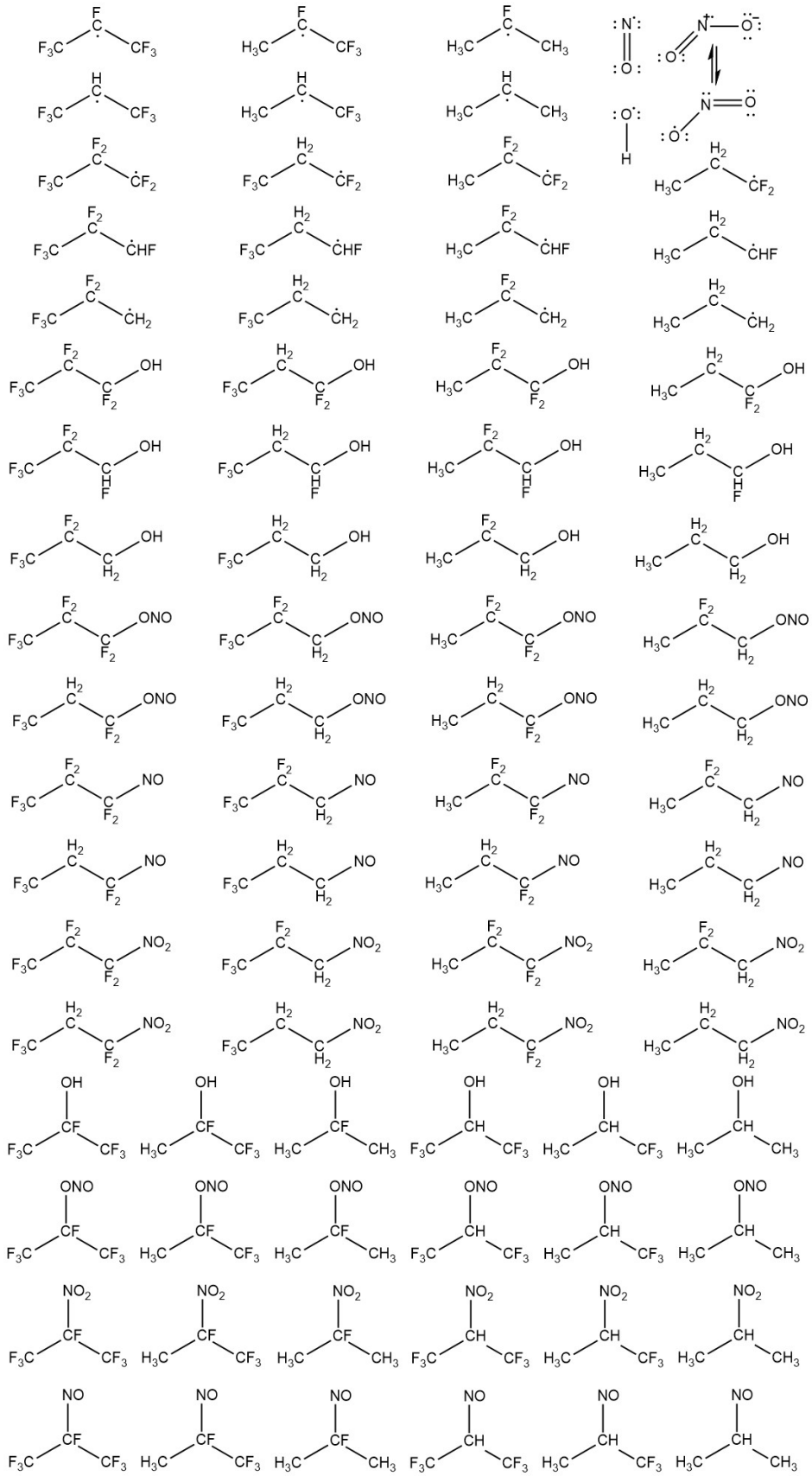

Figure 2.1 Structures of all compounds under study.

RDX. In this study, we probed the thermodynamic stability and kinetic accessibility of per- and polyfluoroalkyl adducts formed with OH, NO and $NO_2$ radicals using density functional theory (DFT) calculations and natural bond orbital (NBO) analyses. For simplicity, the species that were investigated in this work were limited to three-carbon systems.

### 2.3 Computational Methods

The quantum mechanical calculations used to determine the chemical properties of the compounds of interest were performed using Gaussian 16 software suite. Becke's 3 parameter exchange functional along with Lee-Yang-Parr correlation functional (B3LYP) was utilized as the DFT functional due to its widespread use and chemical accuracy of thermodynamic properties [63, 64] along with CBSB7 basis sets [65]. All the of the stationary points were identified as minimum energy structures or a transition state (TS) by the presence of zero or one imaginary vibrational mode, respectively. Intrinsic reaction coordinate (IRC) calculations were performed to characterize the true nature of the TS structures. NBO calculations and analyses were performed to probe spin density and partial atomic charges as implemented in Gaussian 16.

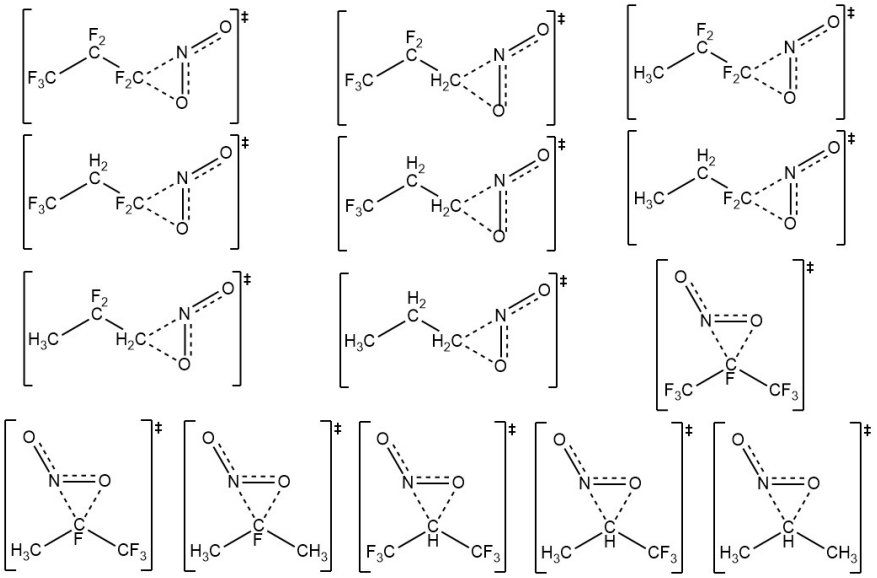

Figure 2.2 Structures of all transition states investigated in this work.

### 2.4 Results and Discussion

PFAS radicals produced from the decomposition of various fluoropolymers could have different degrees of fluorination, we therefore investigated a total of a total of 81 compounds with different fluorination on a 3-carbon backbone along with possible functional groups that may add from the decomposition of energetic

compounds (Figure 2.1). Furthermore, 14 TS structures were also investigated in this study (Figure 2.2). Specific functional groups investigated in this study are nitro, nitroso, alcohols, and nitrites. These classes of species will be referred to as R-$NO_2$, R-NO, R-OH, and R-ONO respectively in further discussion.

For simplicity, fluorines in the $\alpha$, $\beta$, and $\gamma$ positions will be referred to as $\alpha$-fluorines, $\beta$-fluorines, and $\gamma$-fluorines (Figure 2.3). In addition to bond dissociation enthalpies (BDEs), two other parameters were calculated: 1) the energy difference between the $\sigma$ and $\sigma^*$ energy level for the C-R bond and 2) the s-orbital versus p-orbital character of that bond, since they serve as measures of the bond strength. These values corroborate the direction and sometimes magnitude of all trends observed for the BDEs of all compounds studied (vide supra), and this reinforces the theory that the stability of the C-R bond is the direct cause of the trends we see in the stability of these species. All of the calculated values for both parameters can be found in the supporting information (Table A.1).

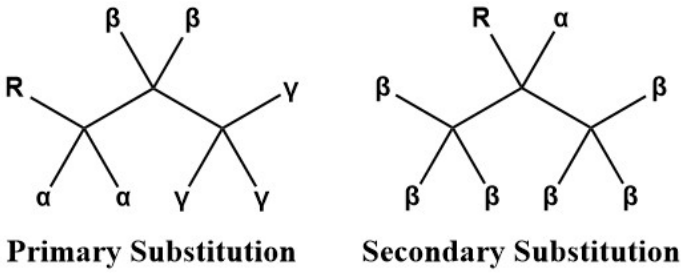


Figure 2.3 Generic layout of the two major classifications of analytes: primary and secondary substituted species. $\alpha$, $\beta$, and $\gamma$ are H or F, and R is $NO_2$, NO, OH, or ONO.

### 2.4.1 Trends in R-N Substitution

In Figure 2.5(a), the BDEs for the R-$NO_2$ compounds from top to bottom are the secondary substituted compounds fully hydrogenated to fully fluorinated and then the primary substituted compounds fully hydrogenated to fully fluorinated. All future figures of this style will have the exact same ordering of the alkyl groups. For R-$NO_2$ BDEs, replacement of fluorines with hydrogens is clearly favorable, i.e., availability of fluorines in these systems have a destabilizing effect. For example, comparison of 1-nitropropane with 1-nitroperfluoropropane shows the difference of 11.6 kcal/mol in C-$NO_2$ BDE. While this effect can be seen for both $\beta$-fluorines and $\gamma$-fluorines, the effect of the removal of $\alpha$-fluorines was the most significant. The stabilization caused by the removal of $\alpha$-fluorines ranged from 1.5-2.1 kcal/mol in secondary substituted species and from 3.4-5.4 kcal/mol in primary substituted species.

As seen in Table A.1, the $\sigma$ vs. $\sigma^*$ energies as well as the s-character of the C-N bond align well with these findings. The difference in $\sigma$ vs. $\sigma^*$ energies and the s-character of the C-N bond are expected to

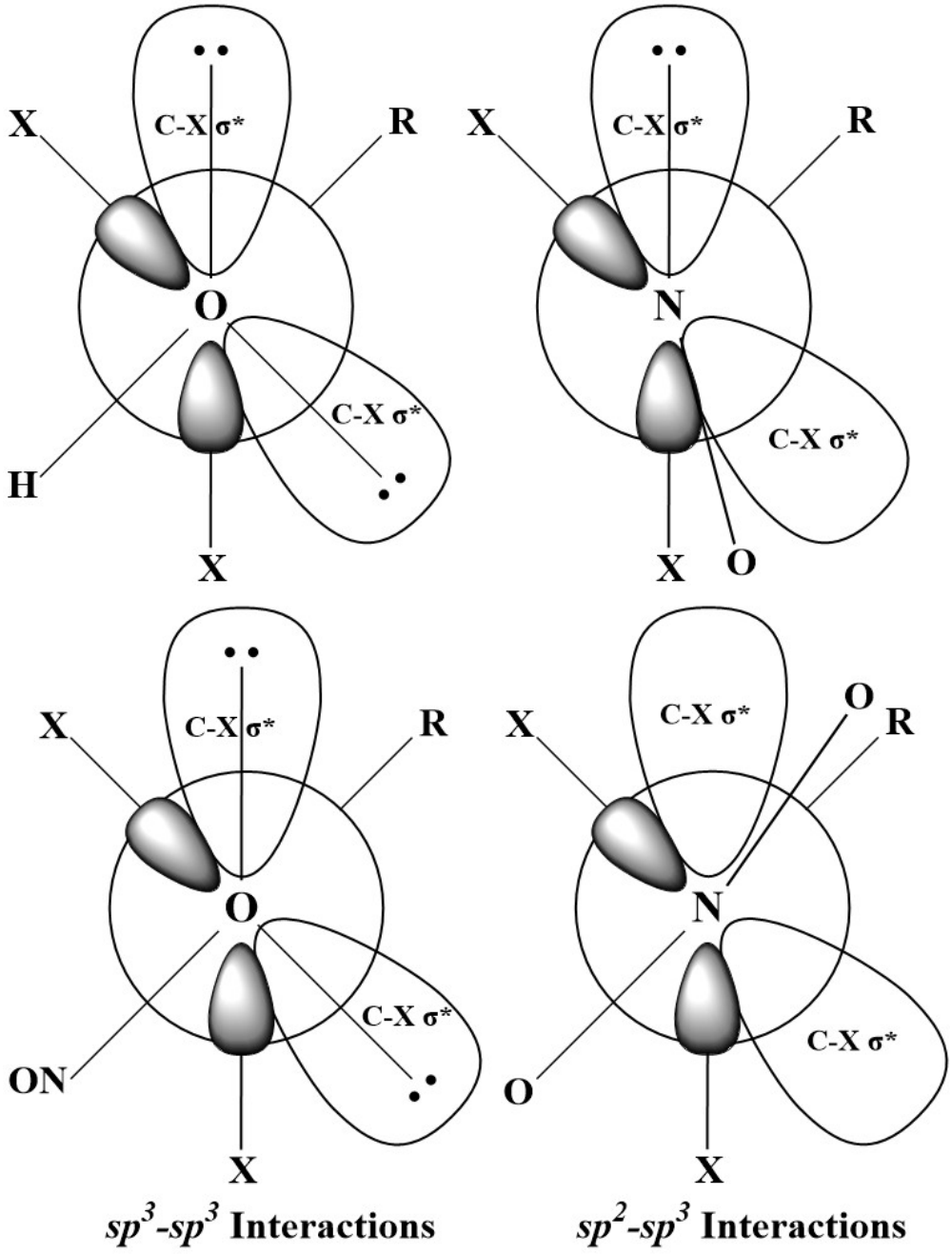


Figure 2.4 Differences in nature of intramolecular interactions between C-N ($sp^2$-$sp^2$ interactions) and C-O bonds ($sp^2$-$sp^2$ interactions) in primary-substituted species where X = H or F

increase with increasing C-N bond strength. For R-$NO_2$ compounds, both parameters indicate decreasing bond strength with higher levels of fluorination. One stereochemical explanation is that the symmetry necessitated by the $sp^2$-hybridization of the N atom in the nitro group prevents effective stabilization of the C-N bond through hyperconjugative interactions with adjacent fluorine substituents (Figure 2.4). Overlap between the electron pair delocalized between the oxygens and adjacent C-F $\sigma^*$ orbital(s) is limited due to the geometric constraints of trigonal planar versus tetrahedral geometry (Figure 2.4). Additionally, the electronegativity of fluorines creates an environment where electron donation to the strongly electron-withdrawing nitro group is very difficult. The more fluorinated the molecule, the more significant the effect.

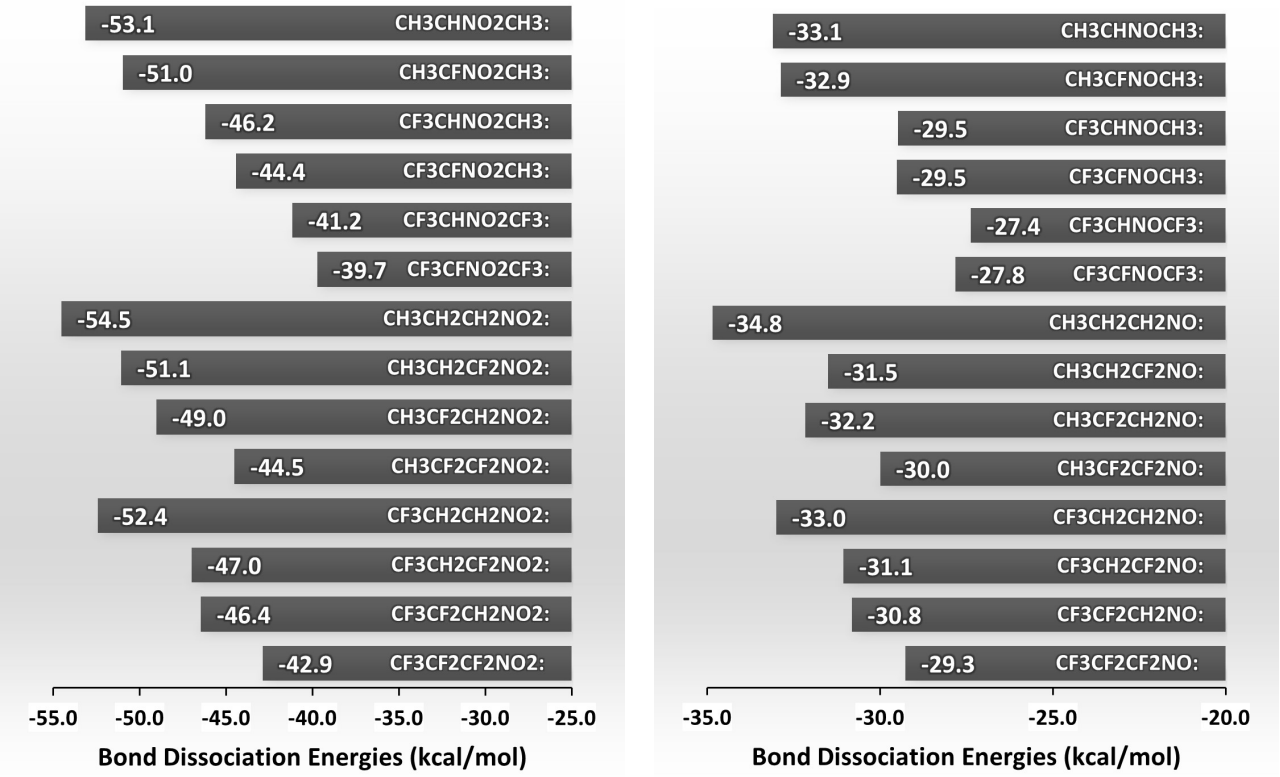


(a) BDEs for R-$NO_2$ Compounds.

(b) BDEs for R-NO Compounds.

Figure 2.5 BDEs for R-N Compounds.

In Figure 2.5(b), the BDEs for the R-NO compounds are shown. For R-NO compounds, nearly all fluorines in these systems have a destabilizing effect with the notable exception of those in partially fluorinated secondary substituted systems where the effect of replacing fluorines with hydrogens is quite minor. Furthermore, the effect of replacing both $\beta$-fluorines with hydrogens has a greater and more

consistent effect than that of replacing $\alpha$-fluorines. This is evident when comparing the difference in BDEs between $CH_3CH_2CH_2NO$ and $CH_3CF_2CH_2NO$ (5.5 kcal/mol) to the difference in BDEs between $CF_3CF_2CH_2NO$ and $CF_3CF_2CF_2NO$ (3.4 kcal/mol). Even so, it is important to note that the stabilization caused by the removal of $\alpha$-fluorines ranged from -0.4-+0.2 kcal/mol in secondary substituted species and from 1.5-3.3 kcal/mol in primary substituted species. The effect of fluorination in R-NO compounds is significantly less than that observed in R-$NO_2$ compounds. This can partly be attributed to the fact that the C-N bonds in R-NO compounds are much weaker than those in R-$NO_2$ compounds as indicated by the low BDEs for R-NO compounds and the low percent s-character of their C-N bond. Another component contributing to this discrepancy is the significant decrease in the partial atomic charge of the nitrogen atom in R-NO (+0.07-0.14) versus the nitrogen atom in R-$NO_2$ (+0.47-0.52); a nitrogen atom with a formal positive charge is much more electron-withdrawing than the one double-bonded to a single oxygen atom (Table A.1).

R-$NO_2$ and R-NO functionalities see the trend that all levels of fluorination are unfavorable to the stability of the resulting species; the addition of fluorine weakens the weakest bond in both sets of compounds: the C-N bond. The electron-withdrawing properties of these R-N substitutions have an antagonistic relationship with the electropositive carbons and electrophilic fluorines of fluorocarbons. The lack of high-energy lone pairs on these substitutions as well as geometric constraints effectively prevent HOMO stabilization through synergistic effects such as electron donation into the low-lying C-F$\alpha$ $\sigma^*$ orbitals seen in R-O compounds (Figure 2.4 and *vide infra*).

### 2.4.2 Trends in R-O Substitution

In Figure 2.6(a), the BDEs for the R-OH compounds are shown. For R-OH compounds, while all $\alpha$-fluorines in these systems have an extremely strong stabilizing force, the effect of replacing $\beta$-fluorines and $\gamma$-fluorines with hydrogens is a relatively minor destabilizing force. The destabilization caused by the removal of all $\alpha$-fluorines ranged from 4.8-5.2 kcal/mol in secondary substituted species and from 17.3-19.1 kcal/mol in primary substituted species. The stability changes for removing $\alpha$-fluorines in primary substituted species are significantly larger than it is in the secondary substituted species, and this can be accounted for by considering R-CFH-OH species as can be seen below. The destabilization caused by removing the first $\alpha$-fluorine ranged from 7.1-9.2 kcal/mol while the destabilization caused from removing the second $\alpha$-fluorine ranged from 9.5-12.0 kcal/mol.

In Figure 2.6(b), the BDEs for the R-ONO compounds are shown. For R-ONO compounds, while all $\alpha$-fluorines in these systems have an extremely strong stabilizing effect, the effect of replacing $\beta$-fluorines and $\gamma$-fluorines with hydrogens has a relatively minor effect. The destabilization caused by the removal of

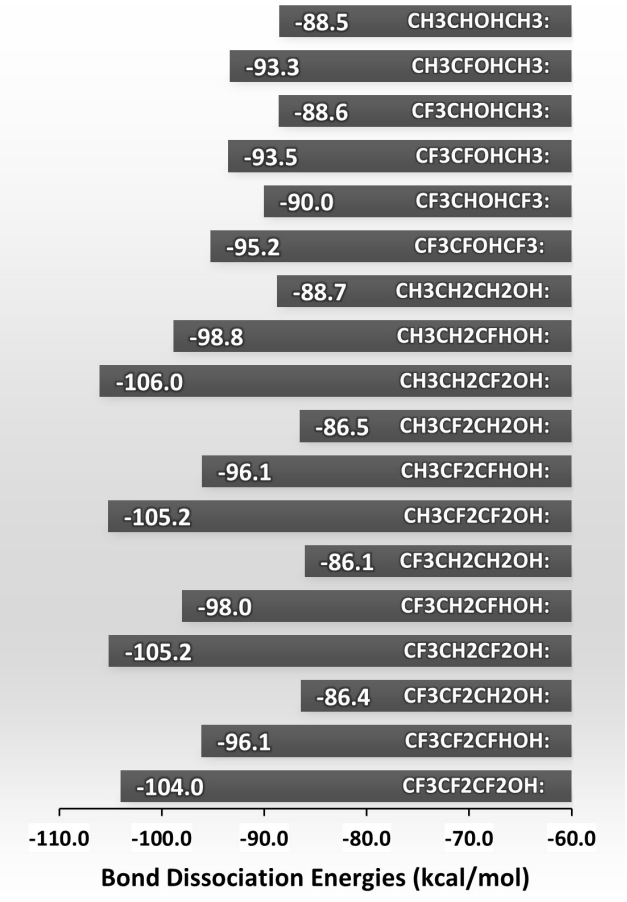


(a) BDEs for R-OH Compounds.

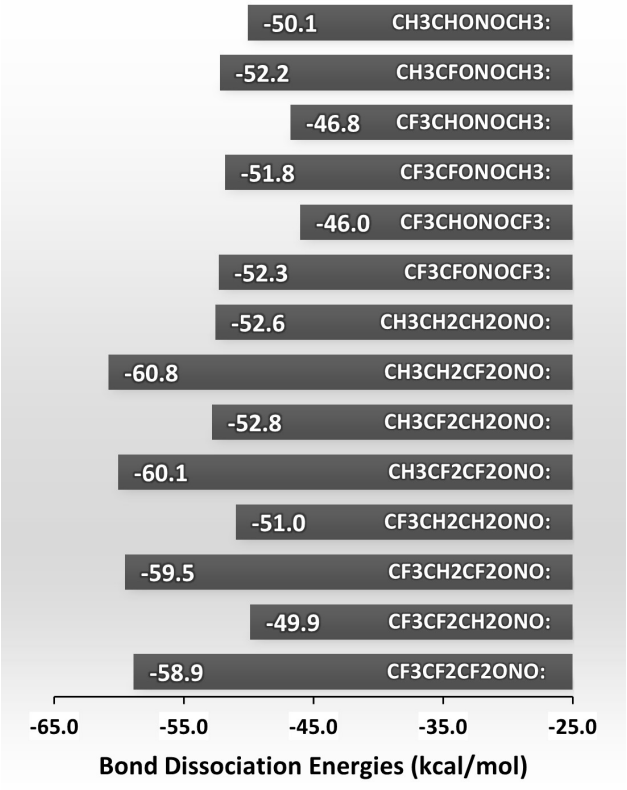


(b) BDEs for R-ONO Compounds.

Figure 2.6 BDEs for R-O Compounds.

$\alpha$-fluorines ranged from 2.2-6.3 kcal/mol in secondary substituted species and from 7.2-9.0 kcal/mol in primary substituted species. This is in stark contrast with the effects seen in R-$NO_2$ compounds where $\alpha$-fluorines were clearly unfavorable for BDEs, especially in primary substituted species. These drastically different trends in R-N and R-O compounds can simply be attributed to the electron-donating versus electron-withdrawing properties of the substituents, but a more robust explanation can be found by looking at the stereoelectronics of the interaction between fluorine and the orientation of the functional groups, specifically, the oxygen and nitrogen atoms in R-O and R-N compounds, respectively (see Figure 2.5(a)). The stabilization effect of fluorines in R-OH and R-ONO compounds can be explained by examining the highest occupied molecular orbital (HOMO). For example, the distribution of electron density in the HOMO of alcohols differs greatly based on the number of $\alpha$-fluorines. In R-$CF_2$-OH, the electron density is evenly distributed throughout the fluorinated portions of the molecule, and, in R-$CH_2$-OH, electron density

is focused around the C-O bond in a $\pi$*-type interaction. In R-CFH-OH, there is some delocalization throughout the fluorinated portions and some density focused around the C-O bond in a $\pi$*-type interaction. This effect is mirrored to a great extent by the R-ONO analogs of R-$CF_2$-OH and R-$CH_2$-OH (Figures S3 and S4). The favorable effects of $\alpha$-fluorines on the stability of R-OH and R-ONO compounds can be further explained using stereoelectronics where each additional $\alpha$-fluorine allows for another lone pair of oxygen to donate into a C-F $\sigma$* orbital. This assertion is further supported by the lengthening of C-F$\alpha$ bonds when compared to the C-F$\beta$ bonds in R-OH and R-ONO (Table A.1).

### 2.4.3 Isomerization of R-$NO_2$ into R-ONO

The combination of R-$NO_2$ compounds having a strong preference against $\alpha$-fluorines and R-ONO compounds having a strong preference for $\alpha$-fluorines is likely to have significant effects on the product distribution of R-$NO_2$ to R-ONO compounds. As can be seen in Figure 2.7(a), the presence of fluorines, especially $\alpha$-fluorines, is a strong driving force powerful enough to reverse the direction of the thermodynamic stability between the two species (R-$NO_2$ and R-ONO) by a significant amount. The removal of $\alpha$-fluorines caused a shift in the thermodynamic stability in the favor of R-$NO_2$ with a magnitude of 2.9-4.3 kcal/mol for secondary substituted compounds and 5.3-9.1 kcal/mol for primary substituted compounds. This appreciable difference in the BDEs of R-$NO_2$ and R-ONO is extremely significant because thermodynamic products will be favored at temperatures where the isomerization reaction is kinetically accessible.

In Figure 2.7(b), the same trend of $\alpha$-fluorines conferring preference for R-ONO species (Figure 2.7(b)) reflected in the reaction enthalpies of this isomerization are shown in the enthalpy barriers needed to access the TS. By comparing the BDEs of R-$NO_2$ (Figure 2.7(a)) bonds and RO-NO (Figure A.5) bonds to the activation enthalpy of this isomerization, C-N and O-NO bonds are easier to break and therefore more likely to happen than for the isomerization reaction. Nevertheless, it is interesting to note that the addition of fluorines decreases the activation barrier for the isomerization of R-$NO_2$ into R-ONO by 2.8-4.3 kcal/mol for secondary substituted compounds and 6.5-10.7 kcal/mol for primary substituted compounds. While the primary reaction pathways expected within the scope of this work would be homolytic cleavage of the R-$NO_2$ or RO-NO bond, it is possible that isomerization from R-$NO_2$ to R-ONO would be kinetically competitive with the homolytic cleavage of the R-$NO_2$ bond in species with $\alpha$-fluorines at sufficiently high temperatures and pressures. This possibility should not be ignored in future kinetic studies of this system.

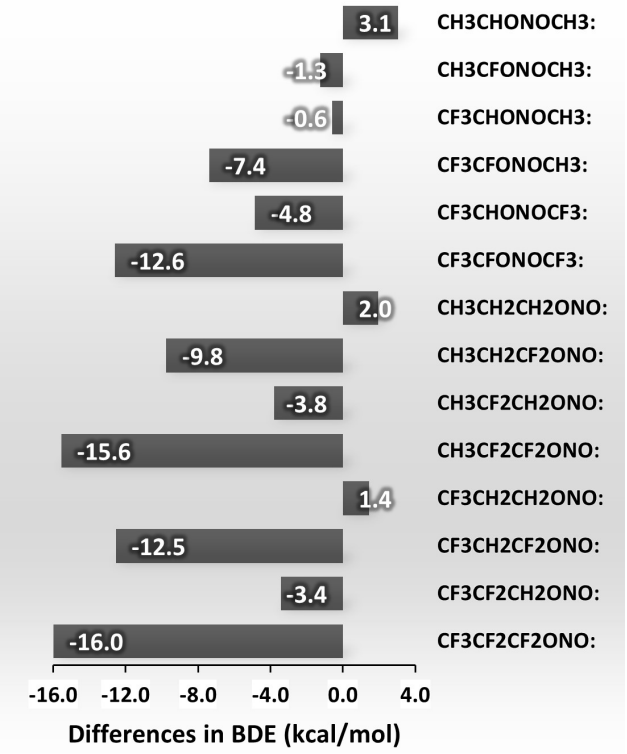


(a) Enthalpies of Isomerization from R-$NO_2$ Compounds into R-ONO Compounds.

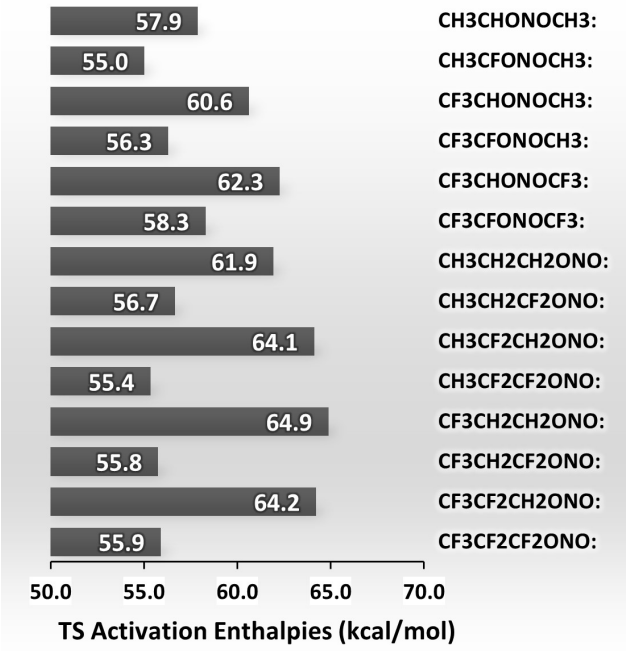


(b) Activation Enthalpies for Tight TS Isomerization from R-$NO_2$ Compounds to R-ONO Compounds.

Figure 2.7 Enthalpies Relevant to R-$NO_2$/R-ONO Isomerization

### 2.4.4 Kinetics of R-$NO_2$/R-ONO Isomerization

Isomerization between nitro-compounds and alkyl nitrites has been of interest in literature due to its implication in the degradation of nitro-compounds over time. Roaming-mediated isomerization (RMI), which is characterized by the homolytic cleavage of the C-$NO_2$ bond followed by drifting of the $NO_2$ radical to a distance of 3-4 Angstroms from the alkyl radical before reacting to form a C-ONO bond, is expected to play a major role in the decomposition of nitroalkanes [66, 67] as well as alkyl nitrites [68] and aromatic nitro-compounds [69]. In addition to this pathway, the other relevant pathways include tight TS isomerization (TTSI), where the C-$NO_2$ and C-ONO bonds are simultaneously broken and formed, respectively, while maintaining a distance of 1-2 Angstroms between the C atom and the $NO_2$/ONO group, concerted molecular elimination (CME), where a $\beta$-hydrogen is abstracted by the $NO_2$ group to form HONO and an alkene, and barrierless simple bond fission (SBF), the homolytic cleavage of the C-$NO_2$ bond which has no transition state and is therefore barrierless. These four decomposition pathways for nitroalkanes have similar enough activation barriers to be considered kinetic competitors in hydrogenated

alkanes [67]. We investigated the TTSI pathway where nitroalkane analogs isomerize into their alkyl nitrite isomers (Figure 2.7(b)), and, based on the lower reaction barriers in found in fluorinated nitroalkanes compared to their hydrogenated analogs, TTSI reactions may be possible in nitro-PFAS. Unfortunately, the scope of this study was limited to comparison between two of the four major pathways of nitro-compound decomposition, SBF and TTSI. In future kinetic studies, CME and RMI should be thoroughly investigated in order to elucidate the pathways that are both possible and likely for each PFAS.

$$k = \frac{k_b T}{h} e^{\frac{-E_a}{RT}} \tag{2.1}$$

The Arrhenius rate law, which is used to find the rate of a reaction based on the temperature and activation energy, was used with transition state theory pre-exponential theory to give Equation 1 to generate the graph of rate vs. temperature seen in Figure 2.8.

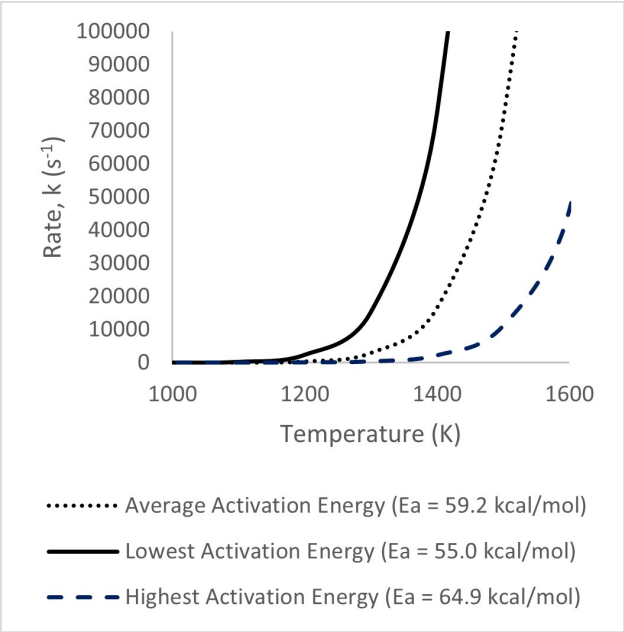


Figure 2.8 Rate vs. Temperature for the lowest (55.0 kcal/mol in $CH_3CFNO_2CH_3$), the highest (64.9 kcal/mol in $CF_3CH_2CH_2NO_2$), and average activation energies ($E_a$) of all species investigated for the isomerization of R-$NO_2$ into R-ONO (59.2 kcal/mol).

In Figure 2.8, appreciable rates of isomerization can be seen at temperatures as low as 1250 K for species with modest activation energies, but for the species with high activation energies, temperatures above 1400 K are needed for appreciable rates. On average, temperatures around 1325 K are sufficient for appreciable isomerization to be possible. These temperatures are easily achievable for controlled detonations [14], but it is unclear that they are achievable during open burns where deflagration is the primary pathway. This is due to the extremely wide temperature ranges achievable through deflagration

depending on the specific application. One study involving deflagration of RDX had a very temperature range from 1200-3000 K [8], which would increase the likelihood of isomerization occurring through that process, but others kept the temperature of the deflagration below 477 K to prevent spontaneous detonation [7]. As such, it is impossible to make definitive claims about the isomerization process without reliable data about the temperatures reached and maintained during the deflagration process in open burn disposal methods. Thus, accurate temperatures for the deflagration process in open burning disposal techniques need to be determined before more accurate predictions of the product distribution can be made.

### 2.5 Conclusion

The study highlights differences in chemical bonding and stabilities in four major classes of possible products of thermal degradation of fluoropolymer containing munitions with varied degree of fluorination. The bonding was dramatically affected by the presence of $\alpha$-fluorines and the impact of these fluorine atoms is significantly affected by the type of heteroatom connected to the carbon, e.g., R-$NO_2$ vs. R-ONO. The primary driving force for the changes in bonding and stability is driven by the geometrical arrangements of the functional group with respect to the C-$\alpha$-F bond, and ability of the heteroatom lone pair to interact with the $\sigma^*$ of C-F bond. An added factor is the electropositive or electronegative. In the aftermath of the deflagration or detonation of munitions containing fluoropolymers, novel PFAS with nitro, nitroso, alcohol, and nitrite functional groups as well as their environmental degradation products are likely to be found. Of these, R-NO compounds are known to oxidize readily into R-$NO_2$ under mild oxidative conditions or homolytically cleave along the C-N bond with exposure to visible light [53], but little is known about the environmental fate of such R-$NO_2$ compounds. Some studies [66, 67] suggest that isomerization and generation of NO will be a major pathway like it is in the fully hydrogenated alkane analogs, but that assessment is tentative. Primary-substituted alcohols with neither $\alpha$- or $\beta$-fluorines (fluorotelomer alcohols) have been known for the better part of two decades compounds degrade into the carboxylic acid analogs in environmental matrices such as the atmosphere [60]. Fully fluorinated primary alcohols are seen in the thermal degradation mechanism of PTFE, and, in the presence of water, are expected to oxidize into their carboxylic acid analogs [30]. However, little is known about the fate of R-ONO compounds, but the similar strength of the RO-NO bond to the C-N bond in R-NO compounds implies that homolytic cleavage is possible [68]. If homolytic cleavage occurs, then hydrogen abstraction from water to form the R-OH analog and subsequent degradation into the carboxylic acid analog and HF elimination is the most likely product [30, 60]]. Thus, the product distribution is expected to be weighted heavily towards carboxylic acids with $\alpha$-fluorines given that both possible R-O compounds are more thermodynamically stable than their R-N competitors when $\alpha$-fluorines are present. There will also likely

be some residual R-$NO_2$ PFAS since this reaction is highly influenced by kinetics due to the nature of the system. Even so, deflagration is suspected to be more likely to result in the larger preference towards thermodynamic products, R-O compounds, because this process is often done in the form of open burns, which can maintain high temperatures for quite some time. Controlled detonations, however, are more likely to result in a higher prevalence of the major set of kinetic products, R-$NO_2$ compounds despite the higher temperatures reached in this process because the time scale is so short.

# CHAPTER 3

# CONCLUSIONS AND FUTURE OUTLOOK

## 3.1 Possibility of Potential PFAS Cross-Products from Disposal of Munitions

As Chapter 1 described, according to NASEM, DEPS, and BAST, there are 400,000 tons of expired and outdated munitions in the US that need to be disposed of [6]. The current methods used to dispose of munitions, open burns and controlled detonations, involve the deflagration and detonation, respectively, of energetic compounds. The thermal degradation of TNT [10–12], RDX [15, 16, 18–22], and HMX [16, 23–25] leads to the production of $NO_2$, NO, and OH radicals that are reactive, but cannot undergo unimolecular decomposition. Throughout this process, the fluoropolymer binding agents, sealants, and pyrolants are exposed to extreme heat sufficient to induce the degradation of even the most recalcitrant fluoropolymer, PTFE [7, 8, 14, 30, 34, 36, 37]. The thermal degradation of PTFE produces perfluoroalkyl radicals [30, 34, 36, 37] that can recombine with radicals produced by energetic compounds degradation. Through such radical recombination mechanisms, the current methods used to dispose of munitions are likely to result in the formation of previously uncharacterized PFAS cross-products including nitroso-PFAS, nitro-PFAS, and nitrito-PFAS. PFAS are persistent organic pollutants of major concern the EPA [4], and strict guidelines are in place on four PFAS: PFOS, PFOA, GenX chemicals, and PFBS [5]. PFAS are ubiquitous in the blood of humans and carcinogenic [1, 2], and bioaccumulate in apex predators such as polar bears [3]. Novel sources of PFAS such as the disposal of munitions are of concern because of the threat they pose to both the environment and public health.

## 3.2 Nature of Bonding in Potential PFAS Cross-Products from Disposal of Munitions

As thoroughly demonstrated in Chapter 2, there are stark differences in the BDEs of bonds formed through radical recombination reactions between intermediates from energetic compound and fluoropolymer thermal degradation pathways. These BDEs depend on the level of fluorination and the presence of $\alpha$-fluorines as well as the atom bonded to carbon which can be oxygen (R-O compounds) or nitrogen (R-N compounds). For R-N compounds, the presence of any fluorines has a destabilizing effect on the BDE of the C-N bond, but this is not the case for R-O compounds. $\alpha$-fluorines have a strongly stabilizing effect on the BDE of the C-O bond. This effect, which is caused by hyperconjugative effects of oxygen lone pair donation into C-F $\sigma^*$ orbitals, leads to a reversal in trend of nitroalkane versus alkyl nitrite BDEs. In fully hydrogenated systems, the C-N bond created in the formation of a nitroalkane is stronger than the alternative, the formation of a C-O bond to make the alkyl nitrite analog. As $\alpha$-fluorines

are added to the systems, the alkyl nitrite C-O bond grows significantly stronger while the nitroalkane C-N bond grows weaker. Thus, alkyl nitrites are more likely to form in highly fluorinated systems than in hydrogenated ones. A subsequent investigation of the activation barriers for the TTSI of nitroalkanes into their alkyl nitrite analogs revealed the same trend as the C-O bond in alkyl nitrites; $\alpha$-fluorines lowered the activation barrier markedly. Investigation other possible degradation mechanisms for nitroalkanes such as RMI and CME was beyond the scope of that work, but future kinetic investigations of nitro-PFAS should elucidate the most prominent pathways in nitro-PFAS. Chapter 2 concluded that R-NO compounds would likely oxidize in air into R-$NO_2$ compounds or homolytically cleave along the C-N bond with exposure to visible light [53] due to the weakness of the C-N bond, and little is certain about the environmental fate of R-$NO_2$ compounds. FTOHs are known to degrade in PFCAs in environmental matrices such as air [60], and fully fluorinated primary alcohols also degrade into PFCAs in the presence of water [30].

## 3.3 Future Outlook

Since the system of the disposal of munitions as a novel source of PFAS has had minimal investigation to date, there are a wide variety of possible directions for future work. One avenue that has been investigated to some extent in conjunction with the work presented in Chapter 2 is the investigation of the reactions that molecular oxygen can have with fluoroalkyl radicals. This work aims to elucidate the role of spin delocalization on the stability of PFAS intermediates resulting from combustion of energetic devices and is discussed in Subsection 3.3.1. Other future work that has yet to be investigated include reactions with the relatively short-lived organic radical intermediates present in TNT, RDX, and HMX thermal degradation pathways as well as previously uninvestigated energetic compounds commonly used as solid-state propellants. Another possible direction would be to expand the scope of the fluoropolymers and their intermediates such as by investigating the reactions of $NO_2$, NO, and OH with the fluoroalkene products of fluoropolymer thermal degradation or fluoropolymer systems containing chlorine and/or oxygen including Kel-F and copolymers with perfluoromethyl vinyl ether subunits). Each of these possibilities concerning an expansion of the scope of the system is discussed in detail below in Subsection 3.3.2.

### 3.3.1 Impact of Spin Delocalization on Potential PFAS Products from Combustion of Energetic Devices

Per- and polyfluoroalkoxy (R-O) radicals are important intermediates in the study of the environmental fate of PFAS [53] and in the degradation of fluoropolymers in the presence of energetic compounds (See Subsection 2.4.2). The structural diversity of different fluoropolymers suggests that there could be different degrees of fluorination in R-O radicals. Therefore, it is important to understand how the degree of fluorination affects the properties of R-O radicals such as spin delocalization and stability. This is the first

topic of interest in this regard. R-O radicals have increasing stability proportional to the loss of spin on the oxygen radical center. As might be expected from the discussion of R-O compounds in Chapter 2, the trend for delocalization of spin on oxygen aligns with the fact that $\alpha$-fluorines have a significant stabilizing effect on R-O radicals. This effect is not as dramatic as that seen in R-OH species (Chapter 2), but it is nonetheless significant. R-O radicals can abstract hydrogen from a variety of natural sources, but the most likely candidate is $H_2O$, which will generate OH radicals. Thus, the products expected from the properties of R-O radicals agree strongly with the results from Chapter 2 which expects the generation of R-OH species that will eventually degrade into PFCAs. Since PFCAs are recalcitrant environmental contaminants, the most prominent production pathways of such species are of particular concern.

R-O radicals are known to be produced through a variety of mechanisms in the thermal degradation fluoropolymer and energetic compounds. There are two major classes of possibilities for the formation of R-O radicals in this system, and both will be discussed below. The first possibility is through the homolytic cleavage of a fluoroalkyl peroxide functionality (R-OO-R') or from the reaction of two fluoroalkyl peroxyl radicals (R-OO + R'-OO) to generate R-O and R'-O radicals and $O_2$. The other possibility is from the homolytic cleavage of the O-N bond in fluoroalkyl nitrites (R-ONO) or of the O-O bond in fluoroalkyl peroxynitrites (R-OONO), fluoroalkyl peroxynitrates (R-OO$NO_2$). In the first class of reactions, interactions between multiple fluoroalkyl radicals are necessary if R' is not $H_2O$, and the concentration of fluoroalkyl radicals is unlikely to be high in air. Thus, this option seems much less likely than the alternative in the system on the disposal of munitions. If R‘ is $H_2O$, then the homolytic cleavage of the O-O bond to generate R-O and OH radicals is reasonable given the presence of $H_2O$ in air as well as the generation of $H_2O$ from combustion reactions. R-ONO are already expected to be formed from the radical recombination of fluoroalkyl radicals and $NO_2$ as well as the isomerization of their nitroalkane analogs (see Chapter 2). Thus, R-ONO species are a likely candidate for the generation of R-O radicals. $O_2$ is in high concentrations in air, so fluoroalkyl radicals are likely to react with $O_2$ before they encounter NO or $NO_2$ and generate R-OO radicals. These radicals can recombine with NO or $NO_2$ present in the disposal of munitions to generate R-OONO and R-OO$NO_2$ species which can undergo homolytic cleavage to generate R-O radicals along with $NO_2$ or $NO_3$ radicals, respectively. The concentrations of the species in these possible formation mechanisms are likely to be the most important factor since most of these reactions will be moderately thermodynamically unfavorable and highly entropically favorable. Thus, further research is needed on the kinetics and species generation over time of these systems in order to develop a more robust understanding.

### 3.3.2 Increasing the Scope of the System

The system discussed in Chapter 2 is naturally quite limited in scope out of necessity; there are an incredible number of additional factors that could be considered. The most natural of these was the addition of molecular oxygen into the system as reviewed in Subsection 3.3.1, but there are many other possibilities including the inclusion of the large organic radical intermediates known to be present in TNT, RDX, and HMX degradation pathways. For TNT, the most obvious intermediate to include is the radical that results from the most prominent initiation pathway, C-$NO_2$ homolysis, 3,5-dinitro-2-methyl phenyl [11] which can be seen in Figure 1.2. Similarly, the radicals produced from the N-N bond homolysis pathway in RDX and HMX, RDR [15] and HMR [23], respectively, would be of note to include. Additionally, applying this style of analysis to other energetic compounds commonly used in energetic devices with fluoropolymers present could yield interesting results. For example, energetic compounds such as glycidyl azide polymer (GAP), nitroglycerine (NG), butane triol trinitrate (BTTN), and trimethylolethane trinitrate (TMETN) are commonly used in solid propellant formulations much like RDX and HMX [70]. The role that these components play in the possible generation of PFAS from the disposal of munitions is unknown and warrants investigation.

Another direction to expand the scope of this work would be in terms of the fluoropolymers known to be present in munitions. The products of pyrolysis of fluoropolymers such as PTFE [30, 34, 36, 37], Viton [32, 34], and Kel-F [31, 34] are fluoroalkenes. For PTFE, tetrafluoroethylene and hexafluoropropylene are the major products of pyrolysis [30, 34, 36, 37], and these compounds are highly reactive with radicals such as $NO_2$, NO, and OH [45, 47, 50]. Viton is an overarching distinction describing a myriad of copolymers that yield a wide variety of polyfluoroalkene products [32, 34], which are likely to be reactive with radicals. Lastly, Kel-F produces many fluoroalkenes and chlorofluoroalkenes through its pyrolysis [31, 34], and it is probable that these species are also reactive with the radicals produced by the thermal degradation of energetic compounds during the disposal of munitions. The work in Chapter 2 only discusses the degradation of fluoropolymers comprised of carbon, fluorine, and hydrogen, but the fluoropolymers used in munitions include chlorofluoropolymers such as Kel-F, copolymers of chlorofluoroalkenes monomers and partially hydrogenated fluoroalkene monomers, and copolymers that include oxygen functionalities such as ethers in one or more of their monomers. Such fluoropolymers are known to have radically different degradation pathways than the fluoropolymers investigated in Chapter 2 [34] which warrants further investigation of their thermal degradation mechanisms alone and in the presence of energetic compounds. The investigation of the disposal of munitions as a source of PFAS is in its infant stages, so there are countless other possibilities for future research directions that are scarcely related to the work presented in

this thesis.

REFERENCES


[1] Christopher Lau, John L Butenhoff, and John M Rogers. The developmental toxicity of perfluoroalkyl acids and their derivatives. *Toxicol. Appl. Pharmacol.*, 198(2):231–241, 2004.

[2] Raya I Boyd, Saeed Ahmad, Ratnakar Singh, Zeeshan Fazal, Gail S Prins, Zeynep Madak Erdogan, Joseph Irudayaraj, and Michael J Spinella. Toward a mechanistic understanding of poly- and perfluoroalkylated substances and cancer. *Cancers (Basel)*, 14(12):2919, 2022.

[3] Gabriel Boisvert, Christian Sonne, Frank F Rigét, Rune Dietz, and Robert J Letcher. Bioaccumulation and biomagnification of perfluoroalkyl acids and precursors in east greenland polar bears and their ringed seal prey. *Environ. Pollut.*, 252(Pt B):1335–1343, 2019.

[4] US EPA. EPA administrator regan announces comprehensive national strategy to confront PFAS pollution. 2021.

[5] US EPA. EPA announces new drinking water health advisories for PFAS chemicals, $1 billion in bipartisan infrastructure law funding to strengthen health protections. 2022.

[6] National Academies of Sciences, Engineering, and Medicine, Division on Engineering and Physical Sciences, Board on Army Science and Technology, and Committee on Alternatives for the Demilitarization of Conventional Munitions. *Alternatives for the demilitarization of conventional munitions*. National Academies Press, Washington, D.C., DC, 2019.

[7] K McLean, S J Zarrouk, and D Wilson. Application of numerical methods for geothermal pressure transient analysis: A deflagration case study from new zealand. In *41st Workshop on Geothermal Reservoir Engineering*, pages 1–10, Stanford, California, 2016. Stanford Geothermal Program.

[8] Michael N Sakano, Ahmed Hamed, Edward M Kober, Nicolo Grilli, Brenden W Hamilton, Md Mahbubul Islam, Marisol Koslowski, and Alejandro Strachan. Unsupervised learning-based multiscale model of thermochemistry in 1,3,5-trinitro-1,3,5-triazinane (RDX). *J. Phys. Chem. A*, 124 (44):9141–9155, 2020.

[9] Róbert Varga and Svatopluk Zeman. Decomposition of some polynitro arenes initiated by heat and shock part i. 2,4,6-trinitrotoluene. *J. Hazard. Mater.*, 132(2-3):165–170, 2006.

[10] Revital Cohen, Yehuda Zeiri, Elhanan Wurzberg, and Ronnie Kosloff. Mechanism of thermal unimolecular decomposition of TNT (2,4,6-trinitrotoluene): a DFT study. *J. Phys. Chem. A*, 111(43): 11074–11083, 2007.

[11] Xiao-Fang Chen, Ji-Feng Liu, Zi-Hui Meng, and Ke-Li Han. Thermal unimolecular decomposition mechanism of 2,4,6-trinitrotoluene: a first-principles DFT study. *Theor. Chem. Acc.*, 127(4):327–344, 2010.

[12] David Furman, Ronnie Kosloff, Faina Dubnikova, Sergey V Zybin, William A Goddard, 3rd, Naomi Rom, Barak Hirshberg, and Yehuda Zeiri. Decomposition of condensed phase energetic materials: interplay between uni- and bimolecular mechanisms. *J. Am. Chem. Soc.*, 136(11):4192–4200, 2014.

[13] Svatopluk Zeman. *Theoretical and Computational Chemistry: Energetic Materials, Part 2: Detonation, Combustion*. Elsevier Sci. BV, 2003.

[14] E.-C. Koch. Metal-fluorocarbon-pyrolants: III. development and application of magnesium. *Propellants Explos. Pyrotech.*, 27(5):262–266, 2002.

[15] Debashis Chakraborty, Richard P Muller, Siddharth Dasgupta, and William A Goddard. The mechanism for unimolecular decomposition of RDX (1,3,5-trinitro-1,3,5-triazine), an ab initio study. *J. Phys. Chem. A*, 104(11):2261–2272, 2000.

[16] Debashis Chakraborty, Richard P Muller, Siddharth Dasgupta, and William A Goddard, III. A detailed model for the decomposition of nitramines: RDX and HMX. *J. Comput.-aided Mater. Des.*, 8 (2/3):203–212, 2001.

[17] Maosheng Miao, Zbigniew A Dreger, James E Patterson, and Yogendra M Gupta. Shock wave induced decomposition of RDX: quantum chemistry calculations. *J. Phys. Chem. A*, 112(32):7383–7390, 2008.

[18] Robert W Molt, Thomas Watson, Alexandre P Bazanté, Rodney J Bartlett, and Nigel G J Richards. Gas phase RDX decomposition pathways using coupled cluster theory. *Phys. Chem. Chem. Phys.*, 18 (37):26069–26077, 2016.

[19] Lalit Patidar and Stefan T Thynell. Quantum mechanics investigation of initial reaction pathways and early ring-opening reactions in thermal decomposition of liquid-phase RDX. *Combust. Flame*, 178: 7–20, 2017.

[20] Mayank Khichar, Lalit Patidar, and Stefan T Thynell. Improvement and validation of a detailed reaction mechanism for thermal decomposition of RDX in liquid phase. *Combust. Flame*, 198:455–465, 2018.

[21] Xi Chen and C Franklin Goldsmith. Predictive kinetics for the thermal decomposition of RDX. *Proc. Combust. Inst.*, 37(3):3167–3173, 2019.

[22] Ke Zheng, Yushi Wen, Bing Huang, Jun Wang, Jin Chen, Gongnan Xie, Guoqing Lv, Jian Liu, Zhiqiang Qiao, and Guangcheng Yang. The solid phase thermal decomposition and nanocrystal effect of hexahydro-1,3,5-trinitro-1,3,5-triazine (RDX) via ReaxFF large-scale molecular dynamics simulation. *Phys. Chem. Chem. Phys.*, 21(31):17240–17252, 2019.

[23] Debashis Chakraborty, Richard P Muller, Siddharth Dasgupta, and William A Goddard. Mechanism for unimolecular decomposition of HMX (1,3,5,7-tetranitro-1,3,5,7-tetrazocine), an ab initio study. *J. Phys. Chem. A*, 105(8):1302–1314, 2001.

[24] Lalit Patidar, Mayank Khichar, and Stefan T Thynell. Identification of initial decomposition reactions in liquid-phase HMX using quantum mechanics calculations. *Combust. Flame*, 188:170–179, 2018.

[25] Lalit Patidar, Mayank Khichar, and Stefan T Thynell. A comprehensive mechanism for liquid-phase decomposition of 1,3,5,7-tetranitro-1,3,5,7-tetrazoctane (HMX): Thermolysis experiments and detailed kinetic modeling. *Combust. Flame*, 212:67–78, 2020.

[26] Yanjun Yin, Yue Dong, Mingling Li, and Zili Ma. Simultaneously altering the energy release and promoting the adhesive force of an electrophoretic energetic film with a fluoropolymer. *Langmuir*, 38 (8):2569–2575, 2022.

[27] DuPont Dow Elastomers. The viton ® a-type. 2000.

[28] G M Swallowe, J E Field, and C D Hutchinson. Impact experiments on thin layers of polymers and intermediate explosives. In *Shock Waves in Condensed Matter*, pages 891–896. Springer US, Boston, MA, 1985.

[29] Zhanyun Wang, Andreas M Buser, Ian T Cousins, Silvia Demattio, Wiebke Drost, Olof Johansson, Koichi Ohno, Grace Patlewicz, Ann M Richard, Glen W Walker, Graham S White, and Eeva Leinala. A new OECD definition for per- and polyfluoroalkyl substances. *Environ. Sci. Technol.*, 55(23): 15575–15578, 2021.

[30] D A Ellis, S A Mabury, J W Martin, and D C Muir. Thermolysis of fluoropolymers as a potential source of halogenated organic acids in the environment. *Nature*, 412(6844):321–324, 2001.

[31] S Zulfiqar, M Zulfiqar, Masroor Rizvi, Arshad Munir, and I C McNeill. Study of the thermal degradation of polychlorotrifluoroethylene, poly(vinylidene fluoride) and copolymers of chlorotrifluoroethylene and vinylidene fluoride. *Polym. Degrad. Stab.*, 43(3):423–430, 1994.

[32] John A Hiltz. Characterization of fluoroelastomers by various analytical techniques including pyrolysis gas chromatography/mass spectrometry. *J. Anal. Appl. Pyrolysis*, 109:283–295, 2014.

[33] G J Knight and W W Wright. The thermal degradation of hydrofluoro polymers. *J. Appl. Polym. Sci.*, 16(3):683–693, 1972.

[34] Jiang Lonfei, Wu Jingling, and Xue Shuman. Mechanisms of pyrolysis of fluoropolymers. *J. Anal. Appl. Pyrolysis*, 10(2):99–106, 1986.

[35] Madhuchhanda Maiti, Suman Mitra, and Anil K Bhowmick. Effect of nanoclays on high and low temperature degradation of fluoroelastomers. *Polym. Degrad. Stab.*, 93(1):188–200, 2008.

[36] E E Lewis and M A Naylor. Pyrolysis of polytetrafluoroethylene. *J. Am. Chem. Soc.*, 69(8): 1968–1970, 1947.

[37] Eckart Mathias and Glenn Miller. The decompostion of polytetrafluoroethylene in a glow discharge. *J. Phys. Chem.*, 71(8):2671–2675, 1967.

[38] US EPA. What is acid rain? 2022.

[39] Daniel J Van Hoomissen and Shubham Vyas. 1,2-fluorine radical rearrangements: Isomerization events in perfluorinated radicals. *J. Phys. Chem. A*, 121(45):8675–8687, 2017.

[40] Ruben Van de Vijver, Maarten K Sabbe, Marie-Françoise Reyniers, Kevin M Van Geem, and Guy B Marin. *Ab initio*derived group additivity model for intramolecular hydrogen abstraction reactions. *Phys. Chem. Chem. Phys.*, 20(16):10877–10894, 2018.

[41] Joan Banus. Perfluoroalkyl nitroso compounds. *Nature*, 171(4343):173–174, 1953.

[42] R N Haszeldine. 423. reactions of fluorocarbon radicals. part x. polyfluoroalkyl nitroso- and nitro-compounds. *J. Chem. Soc.*, page 2075, 1953.

[43] W A Severson and T J Brice. High temperature, vapor phase reactions of some fluorocarbon derivatives with oxidizing agents. *J. Am. Chem. Soc.*, 80(9):2313–2316, 1958.

[44] D A Barr, R N Haszeldine, and C J Willis. 260. perfluoroalkyl derivatives of nitrogen. part IX. the reaction of trifluoronitrosomethane with some unsymmetrical olefins. *J. Chem. Soc.*, page 1351, 1961.

[45] I L Knunyants, L S German, and I N Rozhkov. Aliphatic fluoro nitro compounds: Communication 1. conjugated nitrofluorination of olefins. *Russ Chem Bull*, 12(11):1794–1797, 1963.

[46] Richard M Scribner. Reactions of nitrogen dioxide with organic halogen compounds. i. synthesis of fluoro aldehydrols and fluoro ketols from fluoro alcohols. *J. Org. Chem.*, 29(2):279–283, 1964.

[47] I L Knunyants, B L Dyatkin, A V Fokin, and V A Komarov. Nitration of perfluoroisobutene. *Russ Chem Bull*, 13(8):1335–1338, 1964.

[48] R E Banks, M G Barlow, R N Haszeldine, and M K McCreath. 1326. perfluoroalkyl derivatives of nitrogen. part XIX. synthesis, pyrolysis, and nuclear magnetic resonance evidence for restricted inversion at the nitrogen atom of trisheptafluoro-n-propylhydroxyl-amine. *J. Chem. Soc.*, page 7203, 1965.

[49] R E Banks, M G Barlow, R N Haszeldine, M K McCreath, and H Sucliffe. 1327. perfluoroalkyl derivatives of nitrogen. part XX. thermal decomposition of trifluoronitrosomethane. *J. Chem. Soc.*, page 7209, 1965.

[50] I L Knunyants, A V Fokin, and V A Komarov. Nitration of hexafluoropropene with nitrogen dioxide, and investigation of the nitration products. *Russ Chem Bull*, 15(3):437–442, 1966.

[51] R. N. Haszeldine and B. J. H. Mattinson. *J. Chem. Soc.*, page 1741, 1957.

[52] J Mason (née Banus). 865. perfluoroalkyl compounds of nitrogen. part VI. the photolysis of trifluoronitrosomethane. *J. Chem. Soc.*, 0(0):4537–4544, 1963.

[53] R E Banks, W T Flowers, and R N Haszeldine. Perfluoroalkyl derivatives of nitrogen. part XLVI [1]. thermolysis and photolysis of heptafluoro-1-nitrosopropane. *J. Fluor. Chem.*, 13(3):267–271, 1979.

[54] K Pye and S Smith. The conversion of perfluoronitrosoalkanes to perfluoronitroalkanes and perfluoroazoalkanes catalysed by a living free-radical copolymer. *Eur. Polym. J.*, 27(2):155–158, 1991.

[55] A B Vakhtin, A V Baklanov, and A K Petrov. Absolute rate constants of R+NO(+M)→RNO(+M) reactions. II. measurements for R=C2F5, i-C3F7, n-C4F9, and t-C4F9 at T = 295 K. *Chem. Phys.*, 167(1-2):1–15, 1992.

[56] K Ludovici, D Naumann, G Siegemund, W Tyrra, H-G Varbelow, and H Wrubel. Neue syntheseverfahren für nitrosoperfluoralkane CnF2n+1NO (n=1, 2, 3, 6). *J. Fluor. Chem.*, 73(2): 273–274, 1995.

[57] A B Garmanov and A B Vakhtin. Photolysis of CF3NO as a source of CF3 radicals, rate constant of the CF3 + CF3NO reaction at 296 K. *Int. J. Chem. Kinet.*, 28(2):71–77, 1996.

[58] Vladimir O Smirnov, Marina I Struchkova, Dmitry E Arkhipov, Alexander A Korlyukov, and Alexander D Dilman. Synthesis of gem-difluorinated nitroso compounds. *J. Org. Chem.*, 79(23): 11819–11823, 2014.

[59] A V Fokin, A I Rapkin, and V A Komarov. Nitration of fluoroolefins with dinitrogen tetroxide, and the properties of the products. *Russ Chem Bull*, 31(8):1585–1608, 1982.

[60] David A Ellis, Jonathan W Martin, Amila O De Silva, Scott A Mabury, Michael D Hurley, Mads P Sulbaek Andersen, and Timothy J Wallington. Degradation of fluorotelomer alcohols: a likely atmospheric source of perfluorinated carboxylic acids. *Environ. Sci. Technol.*, 38(12):3316–3321, 2004.

[61] Suzanne A Gauthier and Scott A Mabury. Aqueous photolysis of 8:2 fluorotelomer alcohol. *Environ. Toxicol. Chem.*, 24(8):1837–1846, 2005.

[62] Mohd Faheem Khan and Cormac D Murphy. Fluorotelomer alcohols are efficiently biotransformed by cunninghamella elegans. *Environ. Sci. Pollut. Res. Int.*, 30(9):23613–23623, 2023.

[63] A D Becke. Density-functional exchange-energy approximation with correct asymptotic behavior. *Phys. Rev. A Gen. Phys.*, 38(6):3098–3100, 1988.

[64] C Lee, W Yang, and R G Parr. Development of the Colle-Salvetti correlation-energy formula into a functional of the electron density. *Phys. Rev. B Condens. Matter*, 37(2):785–789, 1988.

[65] J A Montgomery, Jr, M J Frisch, J W Ochterski, and G A Petersson. A complete basis set model chemistry. VI. use of density functional geometries and frequencies. *J. Chem. Phys.*, 110(6):2822–2827, 1999.

[66] R S Zhu and M C Lin. CH3NO2 decomposition/isomerization mechanism and product branching ratios: An ab initio chemical kinetic study. *Chem. Phys. Lett.*, 478(1-3):11–16, 2009.

[67] Ravin Fernando, Nuwandi M Ariyasingha, and Arthur G Suits. Imaging NO elimination in the infrared multiphoton dissociation of nitroalkanes and alkyl nitrites. *Chem. Phys. Lett.*, 645:76–83, 2016.

[68] Kirill Prozument, Yury V Suleimanov, Beat Buesser, James M Oldham, William H Green, Arthur G Suits, and Robert W Field. A signature of roaming dynamics in the thermal decomposition of ethyl nitrite: Chirped-pulse rotational spectroscopy and kinetic modeling. *J. Phys. Chem. Lett.*, 5(21): 3641–3648, 2014.

[69] Michael L Hause, Nuradhika Herath, Rongshun Zhu, M C Lin, and Arthur G Suits. Roaming-mediated isomerization in the photodissociation of nitrobenzene. *Nat. Chem.*, 3(12):932–937, 2011.

[70] Merrill W Beckstead, Karthik Puduppakkam, Piyush Thakre, and Vigor Yang. Modeling of combustion and ignition of solid-propellant ingredients. *Prog. Energy Combust. Sci.*, 33(6):497–551, 2007.

APPENDIX A

CHAPTER 2 SUPPORTING INFORMATION

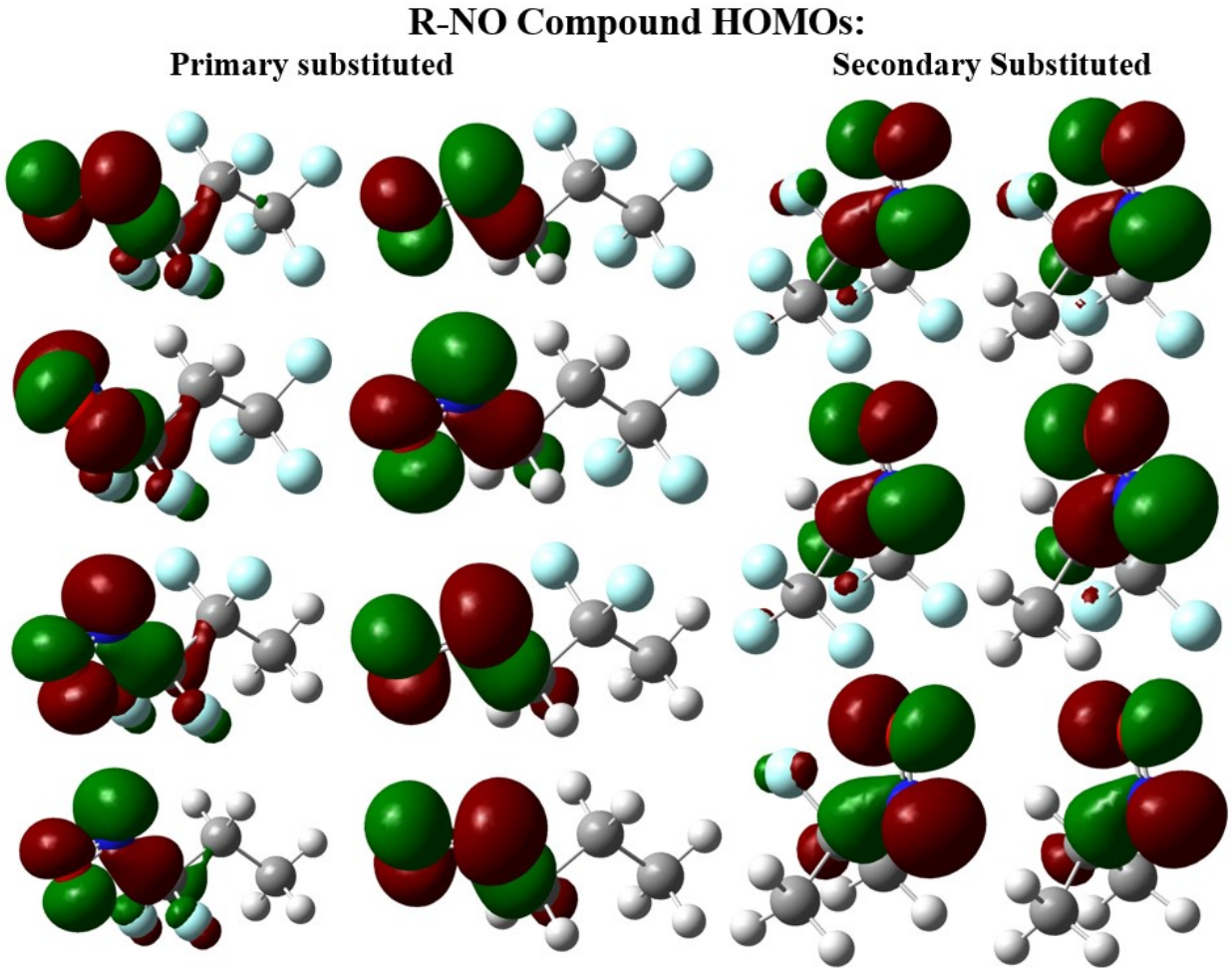


Figure A.1 HOMOs of all nitrosoalkanes (R-NO) under study.

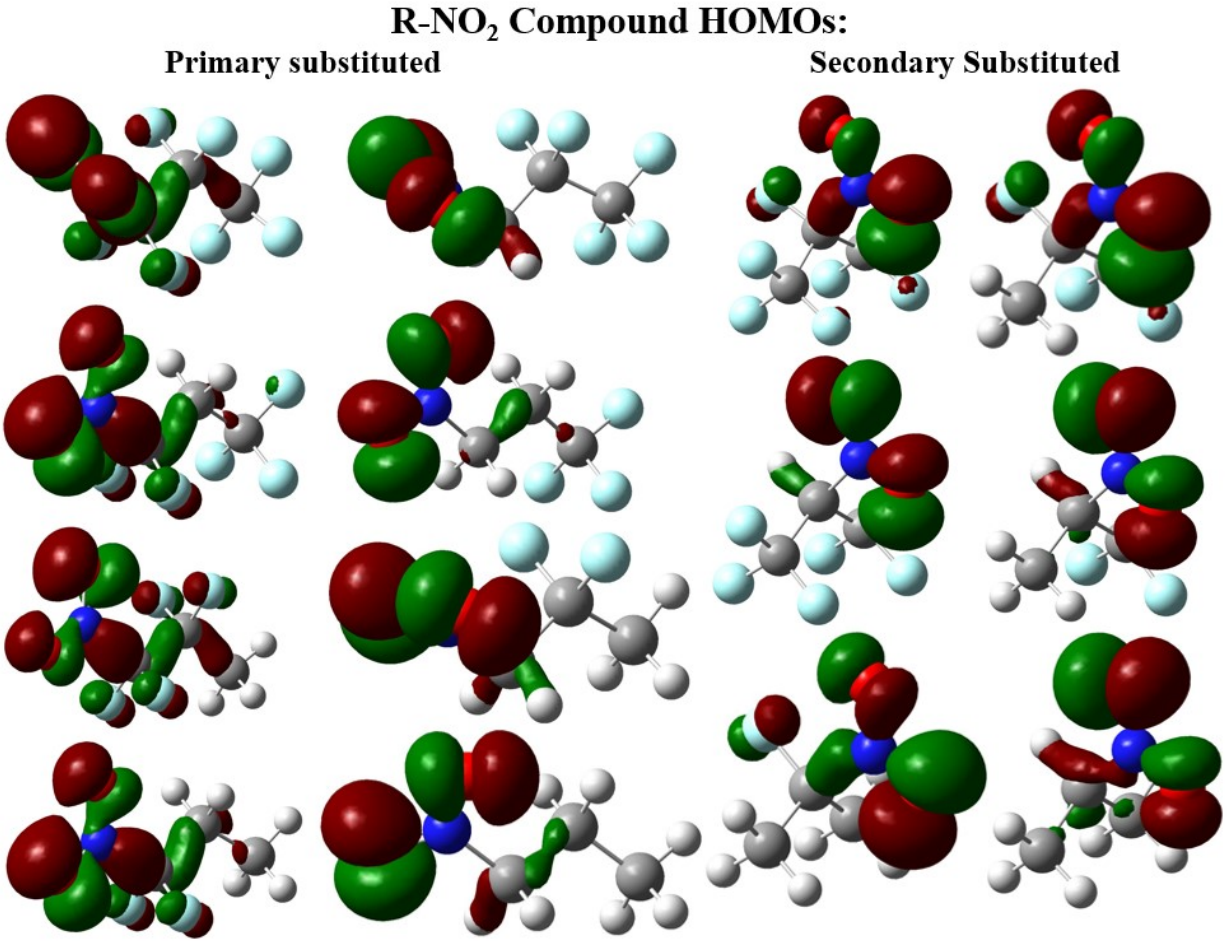


Figure A.2 HOMOs of all nitroalkanes (R-$NO_2$) under study.

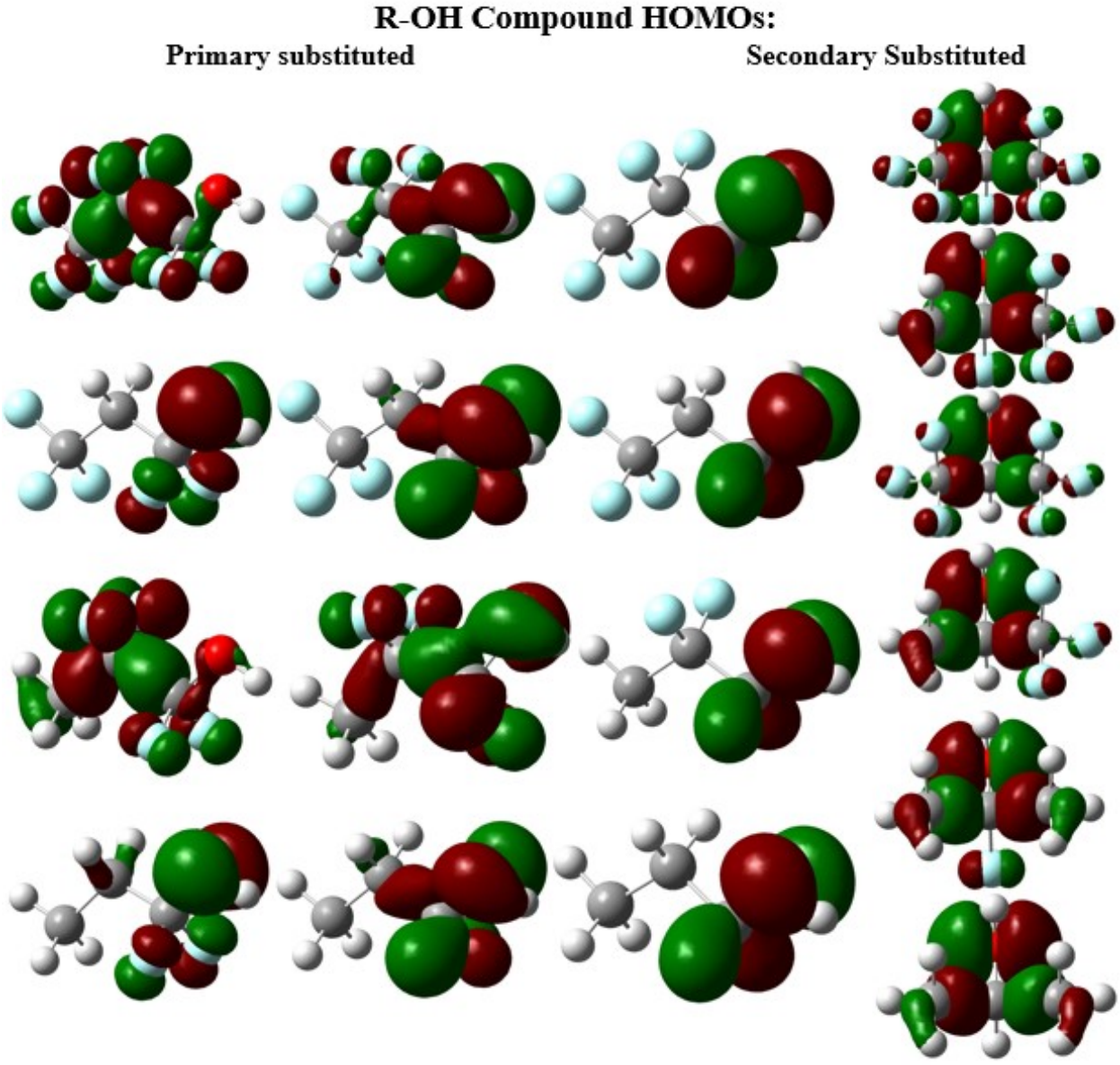


Figure A.3 HOMOs of all alcohols (R-OH) under study.

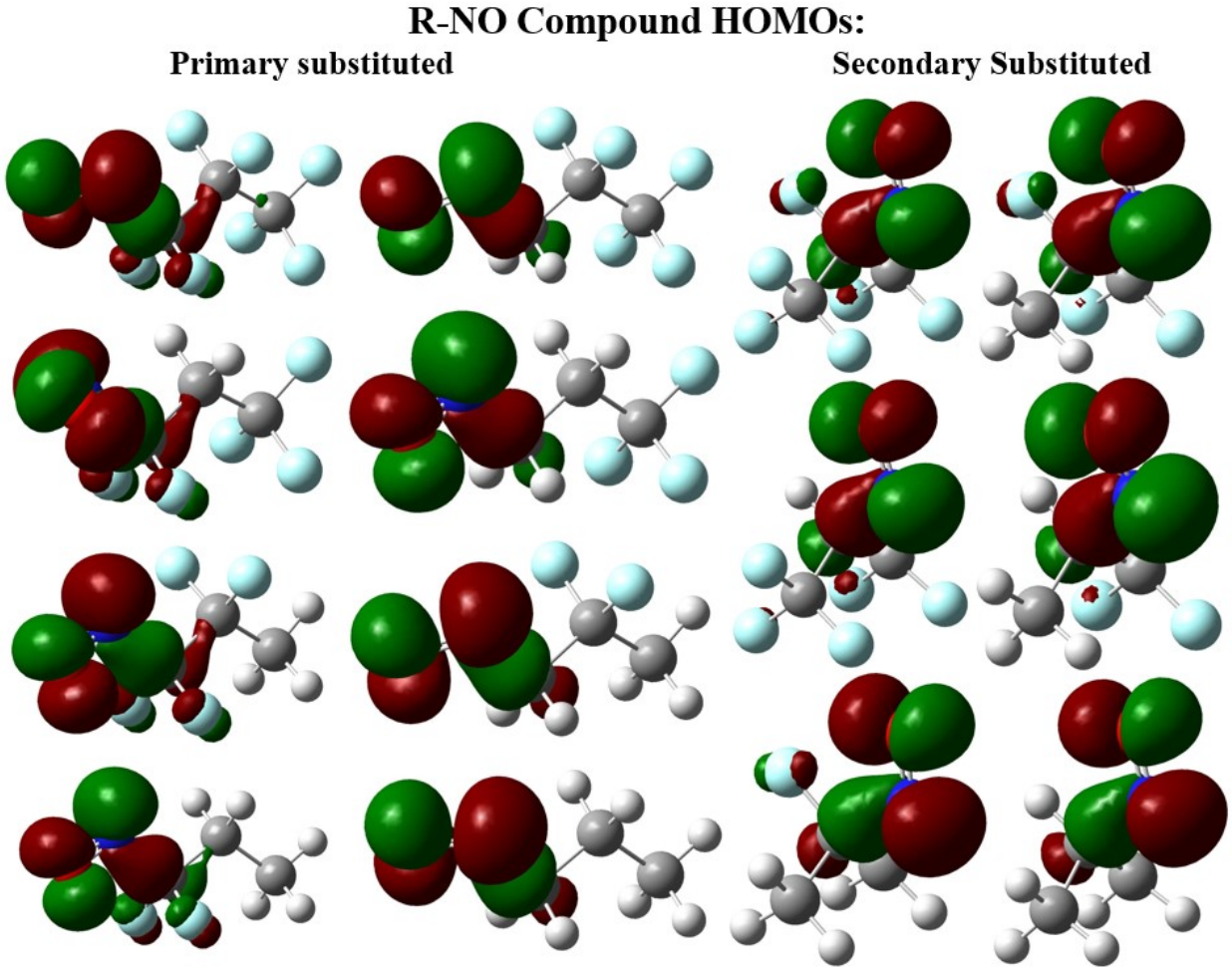


Figure A.4 HOMOs of all alkyl nitrites (R-ONO) under study.

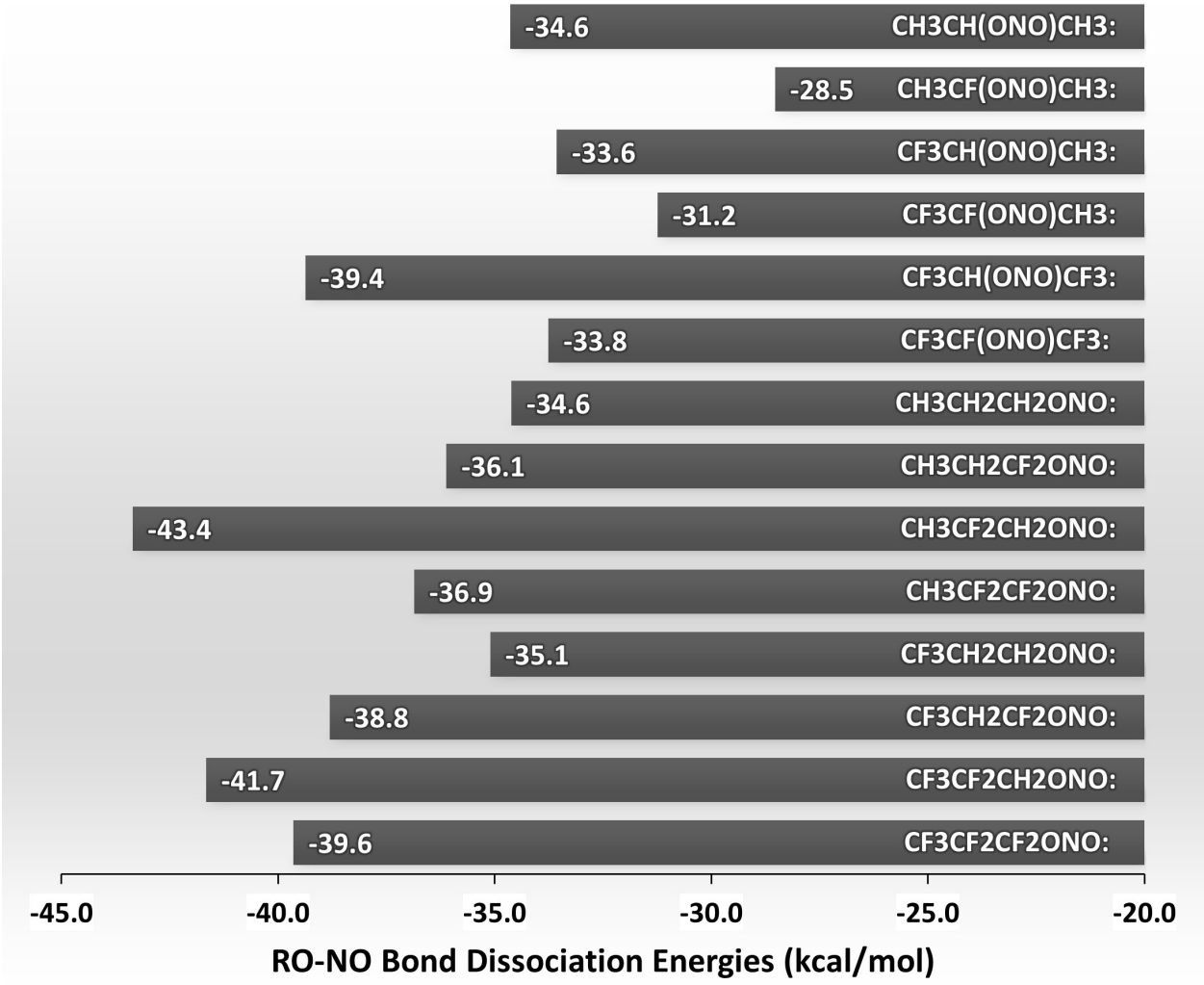


Figure A.5 BDEs for RO-NO bond in R-ONO compounds.

Table A.1 Miscellaneous bonding and atomic properties of compounds under study. The energy differences between the $\sigma$ and $\sigma^*$ orbitals and the percent s-character for the C-N bond in R-NO and R-$NO_2$ and the C-O bond in R-OH and R-ONO. Natural charge on nitrogen found from NBO analysis. C-F bond length based on distance from and character of substitution from optimized geometries.

| Species | $\sigma/\sigma^*$ Energy Difference (kcal/mol) | Percent s-character | Natural Charge on N | C-$F_\alpha$ Bond Length (Angstroms, Å) | C-$F_\beta$ Bond Length (Angstroms, Å) |
|---|---|---|---|---|---|
| $CH_3CH(NO_2)CH_3$ | -610.030 | 29.43% | 0.515 | n/a | n/a |
| $CH_3CF(NO_2)CH_3$ | -576.246 | 28.38% | 0.489 | 1.37019 | n/a |
| $CF_3CH(NO_2)CH_3$ | -609.177 | 28.77% | 0.513 | n/a | 1.3434 |
| $CF_3CF(NO_2)CH_3$ | -574.803 | 27.79% | 0.488 | 1.35616 | 1.33828 |
| $CF_3CH(NO_2)CF_3$ | -607.044 | 28.19% | 0.513 | n/a | 1.3427 |
| $CF_3CF(NO_2)CF_3$ | -570.460 | 27.27% | 0.489 | 1.34344 | 1.33641 |
| $CH_3CH_2CH_2NO_2$ | -624.952 | 29.59% | 0.523 | n/a | n/a |
| $CH_3CH_2CF_2NO_2$ | -562.278 | 27.75% | 0.473 | 1.34793 | n/a |
| $CH_3CF_2CH_2NO_2$ | -628.881 | 29.42% | 0.519 | n/a | 1.37167 |
| $CH_3CF_2CF_2NO_2$ | -565.076 | 27.59% | 0.473 | 1.33949 | 1.36209 |
| $CF_3CH_2CH_2NO_2$ | -621.783 | 29.21% | 0.526 | n/a | n/a |
| $CF_3CH_2CF_2NO_2$ | -556.084 | 27.41% | 0.474 | 1.34014 | n/a |
| $CF_3CF_2CH_2NO_2$ | -622.135 | 28.97% | 0.511 | n/a | 1.35838 |
| $CF_3CF_2CF_2NO_2$ | -553.562 | 27.09% | 0.469 | 1.32982 | 1.3517 |
| $CH_3CH(NO)CH_3$ | -623.007 | 24.55% | 0.107 | n/a | n/a |
| $CH_3CF(NO)CH_3$ | -599.319 | 23.50% | 0.112 | 1.38259 | n/a |
| $CF_3CH(NO)CH_3$ | -604.245 | 23.22% | 0.125 | n/a | 1.3474 |
| $CF_3CF(NO)CH_3$ | -579.559 | 22.48% | 0.091 | 1.36654 | 1.3435 |
| $CF_3CH(NO)CF_3$ | -570.247 | 21.48% | 0.138 | n/a | 1.34249 |
| $CF_3CF(NO)CF_3$ | -540.491 | 20.63% | 0.110 | 1.35161 | 1.33689 |
| $CH_3CH_2CH_2NO$ | -636.906 | 25.15% | 0.116 | n/a | n/a |
| $CH_3CH_2CF_2NO$ | -554.064 | 21.79% | 0.073 | 1.35873 | n/a |
| $CH_3CF_2CH_2NO$ | -625.266 | 24.31% | 0.113 | n/a | 1.3797 |
| $CH_3CF_2CF_2NO$ | -542.286 | 21.25% | 0.097 | 1.34829 | 1.36856 |
| $CF_3CH_2CH_2NO$ | -611.731 | 23.84% | 0.121 | n/a | n/a |
| $CF_3CH_2CF_2NO$ | -556.818 | 21.64% | 0.082 | 1.34321 | n/a |
| $CF_3CF_2CH_2NO$ | -611.988 | 23.64% | 0.128 | n/a | 1.36263 |
| $CF_3CF_2CF_2NO$ | -536.073 | 20.90% | 0.097 | 1.34357 | 1.34952 |
| $CH_3CH(OH)CH_3$ | -692.528 | 27.81% | n/a | n/a | n/a |
| $CH_3CF(OH)CH_3$ | -717.377 | 28.52% | n/a | 1.39048 | n/a |
| $CF_3CH(OH)CH_3$ | -707.255 | 27.43% | n/a | n/a | 1.35077 |

Table A.1 Continued.

| Species | $\sigma/\sigma^*$ Energy Difference (kcal/mol) | Percent s-character | Natural Charge on N | C-$F_\alpha$ Bond Length (Angstroms, Å) | C-$F_\beta$ Bond Length (Angstroms, Å) |
|---|---|---|---|---|---|
| $CF_3CF(OH)CH_3$ | -768.957 | 30.08% | n/a | 1.37345 | 1.34354 |
| $CF_3CH(OH)CF_3$ | -725.283 | 27.41% | n/a | n/a | 1.34166 |
| $CF_3CF(OH)CF_3$ | -763.492 | 29.48% | n/a | 1.35809 | 1.33481 |
| $CH_3CH_2CH_2OH$ | -689.146 | 27.28% | n/a | n/a | n/a |
| $CH_3CH_2CFHOH$ | -752.485 | 29.35% | n/a | 1.40901 | n/a |
| $CH_3CH_2CF_2OH$ | -790.311 | 30.91% | n/a | 1.38109 | n/a |
| $CH_3CF_2CH_2OH$ | -703.095 | 27.19% | n/a | n/a | 1.37662 |
| $CH_3CF_2CFHOH$ | -763.762 | 29.30% | n/a | 1.39976 | 1.36634 |
| $CH_3CF_2CF_2OH$ | -793.580 | 29.86% | n/a | 1.37195 | 1.36703 |
| $CF_3CH_2CH_2OH$ | -693.977 | 27.65% | n/a | n/a | n/a |
| $CF_3CH_2CFHOH$ | -752.661 | 29.14% | n/a | 1.39754 | n/a |
| $CF_3CH_2CF_2OH$ | -788.661 | 30.61% | n/a | 1.37098 | n/a |
| $CF_3CF_2CH_2OH$ | -715.394 | 27.68% | n/a | n/a | 1.3598 |
| $CF_3CF_2CFHOH$ | -771.536 | 29.45% | n/a | 1.38948 | 1.35014 |
| $CF_3CF_2CF_2OH$ | -806.959 | 30.91% | n/a | 1.363 | 1.35121 |
| $CH_3CH(ONO)CH_3$ | -665.313 | 26.59% | 0.330 | n/a | n/a |
| $CH_3CF(ONO)CH_3$ | -678.786 | 26.84% | 0.336 | 1.38471 | n/a |
| $CF_3CH(ONO)CH_3$ | -702.166 | 26.95% | 0.361 | n/a | 1.34271 |
| $CF_3CF(ONO)CH_3$ | -753.740 | 29.50% | 0.410 | 1.38752 | 1.34499 |
| $CF_3CH(ONO)CF_3$ | -725.553 | 27.45% | 0.389 | n/a | 1.343 |
| $CF_3CF(ONO)CF_3$ | -786.088 | 30.04% | 0.438 | 1.37967 | 1.33881 |
| $CH_3CH_2CH_2ONO$ | -674.864 | 26.21% | 0.346 | n/a | n/a |
| $CH_3CH_2CF_2ONO$ | -769.654 | 29.92% | 0.409 | 1.37294 | n/a |
| $CH_3CF_2CH_2ONO$ | -703.327 | 26.84% | 0.362 | n/a | 1.37781 |
| $CH_3CF_2CF_2ONO$ | -785.574 | 29.63% | 0.427 | 1.36886 | 1.36656 |
| $CF_3CH_2CH_2ONO$ | -691.474 | 26.66% | 0.347 | n/a | n/a |
| $CF_3CH_2CF_2ONO$ | -743.167 | 28.14% | 0.385 | 1.36651 | n/a |
| $CF_3CF_2CH_2ONO$ | -710.707 | 26.88% | 0.361 | n/a | 1.36112 |
| $CF_3CF_2CF_2ONO$ | -809.826 | 30.75% | 0.440 | 1.36297 | 1.35138 |

APPENDIX B

ATOMIC COORDINATES

Table B.1 Optimized Geometries of All Species Studied

| Species/Atom Number | Atom Name | Coordinates | | |
|---|---|---|---|---|
| | | X | Y | Z |
| Initial Radicals | | | | |
| CF3CF2CF2_R | | | | |
| 1 | C | 1.024109 | -0.383329 | -0.000089 |
| 2 | C | -1.525324 | 0.122893 | 0.000073 |
| 3 | F | 2.218440 | 0.212120 | -0.000133 |
| 4 | F | 0.925925 | -1.157595 | 1.087717 |
| 5 | F | 0.925704 | -1.157298 | -1.088113 |
| 6 | F | 0.042814 | 1.442626 | 1.105137 |
| 7 | F | -1.872876 | -0.530759 | 1.097112 |
| 8 | F | -1.873021 | -0.530142 | -1.097282 |
| 9 | C | -0.113398 | 0.677395 | 0.000148 |
| 10 | F | 0.042756 | 1.443075 | -1.104526 |
| CF3CF2CFH_R | | | | |
| 1 | C | -0.874789 | -0.331992 | 0.022340 |
| 2 | C | 1.608147 | 0.023246 | 0.582379 |
| 3 | F | -1.946001 | 0.279701 | -0.488358 |
| 4 | F | -0.641537 | -1.449826 | -0.676349 |
| 5 | F | -1.141934 | -0.672456 | 1.294505 |
| 6 | F | 0.573972 | 0.921775 | -1.323530 |
| 7 | F | 2.158333 | -1.004971 | -0.058348 |
| 8 | C | 0.371788 | 0.594564 | -0.016392 |
| 9 | F | 0.055335 | 1.721634 | 0.678472 |
| 10 | H | 1.845612 | 0.122385 | 1.632510 |
| CF3CF2CH2_R | | | | |
| 1 | C | -0.755818 | 0.047317 | 0.000000 |
| 2 | C | 1.467752 | 1.286243 | -0.000001 |
| 3 | C | 0.795652 | -0.030647 | 0.000000 |
| 4 | F | -1.305526 | -1.169535 | 0.000000 |
| 5 | F | -1.181215 | 0.708034 | 1.088953 |
| 6 | F | -1.181214 | 0.708033 | -1.088954 |
| 7 | F | 1.146220 | -0.754869 | 1.105754 |
| 8 | F | 1.146220 | -0.754871 | -1.105753 |
| 9 | H | 1.667065 | 1.775697 | 0.941721 |
| 10 | H | 1.667065 | 1.775696 | -0.941723 |
| CF3CFCF3_R | | | | |
| 1 | C | 1.325932 | -0.139300 | -0.023667 |
| 2 | C | 0.003232 | 0.541396 | -0.213114 |
| 3 | C | -1.333827 | -0.120523 | -0.025444 |
| 4 | F | 2.230662 | 0.335687 | -0.895516 |
| 5 | F | 1.815607 | 0.072874 | 1.214739 |
| 6 | F | 1.202927 | -1.460661 | -0.205896 |
| 7 | F | 0.030526 | 1.855922 | -0.048696 |

Table B.1 Continued.

| Species/Atom Number | Atom Name | Coordinates | | |
|---|---|---|---|---|
| | | X | Y | Z |
| 8 | F | -1.479460 | -0.610067 | 1.225761 |
| 9 | F | -2.313356 | 0.764858 | -0.238919 |
| 10 | F | -1.483797 | -1.146328 | -0.876657 |
| CF3CFCH3_R | | | | |
| 1 | C | -0.623788 | -0.059617 | -0.022717 |
| 2 | C | 0.842026 | 0.121747 | -0.233366 |
| 3 | F | -1.338038 | 0.913839 | -0.609876 |
| 4 | F | -1.020647 | -1.246566 | -0.527961 |
| 5 | F | -0.964971 | -0.058417 | 1.294693 |
| 6 | F | 1.248087 | 1.384118 | -0.002944 |
| 7 | C | 1.842282 | -0.943173 | -0.003802 |
| 8 | H | 1.455209 | -1.905700 | -0.337878 |
| 9 | H | 2.761950 | -0.719635 | -0.550296 |
| 10 | H | 2.099841 | -1.025165 | 1.062280 |
| CF3CH2CF2_R | | | | |
| 1 | C | 1.007651 | -0.000001 | -0.004461 |
| 2 | C | -1.498793 | -0.000001 | 0.475479 |
| 3 | F | -1.863170 | -1.096682 | -0.194121 |
| 4 | F | -1.863168 | 1.096684 | -0.194118 |
| 5 | C | -0.111638 | -0.000003 | 1.033090 |
| 6 | H | 0.018645 | -0.885648 | 1.656868 |
| 7 | H | 0.018647 | 0.885637 | 1.656876 |
| 8 | F | 2.209231 | -0.000008 | 0.611588 |
| 9 | F | 0.957404 | -1.086069 | -0.797148 |
| 10 | F | 0.957412 | 1.086080 | -0.797134 |
| CF3CH2CFH_R | | | | |
| 1 | C | 0.779296 | 0.018544 | -0.011005 |
| 2 | C | -1.661385 | -0.640610 | 0.091141 |
| 3 | F | 1.903267 | -0.111724 | -0.747898 |
| 4 | F | 0.532506 | 1.334724 | 0.123802 |
| 5 | F | 1.046440 | -0.470381 | 1.220201 |
| 6 | F | -2.365121 | 0.498556 | -0.053146 |
| 7 | C | -0.386498 | -0.718929 | -0.661786 |
| 8 | H | -1.846081 | -1.149690 | 1.028983 |
| 9 | H | -0.080428 | -1.763556 | -0.761727 |
| 10 | H | -0.515791 | -0.301355 | -1.663979 |
| CF3CH2CH2_R | | | | |
| 1 | C | -0.403281 | 0.010249 | -0.000000 |
| 2 | C | 2.118179 | -0.058237 | 0.000000 |
| 3 | C | 0.899844 | 0.799211 | -0.000000 |
| 4 | F | -1.471492 | 0.838607 | -0.000001 |
| 5 | F | -0.512938 | -0.782527 | -1.087247 |
| 6 | F | -0.512939 | -0.782526 | 1.087248 |
| 7 | H | 2.530269 | -0.426870 | -0.929517 |
| 8 | H | 2.530269 | -0.426869 | 0.929518 |
| 9 | H | 0.863664 | 1.442212 | -0.884101 |
| 10 | H | 0.863664 | 1.442213 | 0.884100 |
| CF3CHCF3_R | | | | |
| 1 | C | -0.044812 | 0.073477 | 1.306402 |
| 2 | F | -0.575604 | -1.153305 | -1.509371 |

Table B.1 Continued.

| Species/Atom Number | Atom Name | Coordinates | | |
|---|---|---|---|---|
| | | X | Y | Z |
| 3 | F | 1.291178 | -0.052250 | -1.394623 |
| 4 | C | -0.479317 | 0.645059 | 0.000000 |
| 5 | H | -1.276237 | 1.374194 | 0.000000 |
| 6 | F | -0.455025 | 0.865207 | 2.315163 |
| 7 | F | -0.575604 | -1.153305 | 1.509371 |
| 8 | F | 1.291178 | -0.052250 | 1.394623 |
| 9 | C | -0.044812 | 0.073477 | -1.306402 |
| 10 | F | -0.455025 | 0.865207 | -2.315163 |
| CF3CHCH3_R | | | | |
| 1 | C | -0.433896 | -0.037775 | -0.013121 |
| 2 | C | 0.870596 | -0.732202 | -0.087413 |
| 3 | H | 0.838854 | -1.809152 | 0.013670 |
| 4 | F | -1.456813 | -0.854536 | -0.339441 |
| 5 | F | -0.693343 | 0.436676 | 1.239668 |
| 6 | F | -0.491387 | 1.038193 | -0.836757 |
| 7 | C | 2.144145 | 0.026220 | -0.008608 |
| 8 | H | 2.401499 | 0.265996 | 1.034640 |
| 9 | H | 2.973724 | -0.552740 | -0.419269 |
| 10 | H | 2.074739 | 0.975436 | -0.545418 |
| CH3CF2CF2_R | | | | |
| 1 | C | 0.941233 | 0.000005 | 1.412012 |
| 2 | C | -0.889696 | 0.000001 | -0.368114 |
| 3 | F | 1.137000 | 1.104087 | -0.664805 |
| 4 | F | -1.525534 | 1.095964 | 0.043201 |
| 5 | F | -1.525544 | -1.095959 | 0.043205 |
| 6 | C | 0.600102 | -0.000002 | -0.061400 |
| 7 | F | 1.136998 | -1.104096 | -0.664796 |
| 8 | H | 2.026821 | -0.000010 | 1.519103 |
| 9 | H | 0.528542 | 0.890452 | 1.887319 |
| 10 | H | 0.528516 | -0.890414 | 1.887345 |
| CH3CF2CFH_R | | | | |
| 1 | C | -0.518289 | 1.451387 | -0.204548 |
| 2 | C | 0.957605 | -0.611125 | -0.347261 |
| 3 | F | 2.023268 | 0.116790 | 0.018339 |
| 4 | C | -0.376522 | -0.039143 | -0.022043 |
| 5 | H | 1.128866 | -1.678013 | -0.417222 |
| 6 | H | -0.347325 | 1.720900 | -1.247437 |
| 7 | H | 0.203616 | 1.972858 | 0.423951 |
| 8 | H | -1.528567 | 1.741096 | 0.085814 |
| 9 | F | -1.294336 | -0.709923 | -0.800568 |
| 10 | F | -0.710415 | -0.358373 | 1.293118 |
| CH3CF2CH2_R | | | | |
| 1 | C | -1.293942 | 0.725039 | -0.000000 |
| 2 | C | 1.247067 | 0.878001 | -0.000001 |
| 3 | C | 0.043830 | 0.008410 | 0.000000 |
| 4 | H | 1.654452 | 1.222292 | 0.939824 |
| 5 | H | 1.654452 | 1.222291 | -0.939826 |
| 6 | H | -1.385274 | 1.350174 | 0.889346 |
| 7 | H | -1.385274 | 1.350173 | -0.889347 |
| 8 | H | -2.091095 | -0.021285 | 0.000000 |

Table B.1 Continued.

| Species/Atom Number | Atom Name | Coordinates | | |
|---|---|---|---|---|
| | | X | Y | Z |
| 9 | F | 0.087278 | -0.821796 | 1.107792 |
| 10 | F | 0.087278 | -0.821797 | -1.107792 |
| CH3CFCH3_R | | | | |
| 1 | C | 0.204696 | -0.594274 | 1.314218 |
| 2 | C | 0.204696 | 0.097965 | -0.000000 |
| 3 | C | 0.204696 | -0.594274 | -1.314218 |
| 4 | H | -0.777596 | -1.042440 | -1.539673 |
| 5 | H | 0.433864 | 0.107786 | -2.120164 |
| 6 | H | 0.946651 | -1.395617 | -1.328170 |
| 7 | H | -0.777596 | -1.042440 | 1.539673 |
| 8 | H | 0.433864 | 0.107786 | 2.120164 |
| 9 | H | 0.946651 | -1.395617 | 1.328170 |
| 10 | F | -0.543373 | 1.244894 | -0.000000 |
| CH3CH2CF2_R | | | | |
| 1 | C | -1.720428 | 0.000000 | -0.510626 |
| 2 | C | 0.633848 | 0.000000 | 0.414209 |
| 3 | C | -0.823568 | 0.000000 | 0.743585 |
| 4 | H | -1.530518 | 0.884758 | -1.121418 |
| 5 | H | -1.530518 | -0.884758 | -1.121418 |
| 6 | H | -2.774412 | 0.000000 | -0.224658 |
| 7 | F | 1.074859 | 1.096284 | -0.229572 |
| 8 | F | 1.074859 | -1.096284 | -0.229572 |
| 9 | H | -1.025560 | 0.880662 | 1.358396 |
| 10 | H | -1.025560 | -0.880662 | 1.358396 |
| CH3CH2CFH_R | | | | |
| 1 | C | -1.518692 | -0.502876 | 0.137956 |
| 2 | C | 0.791223 | 0.538040 | 0.268863 |
| 3 | F | 1.504698 | -0.539041 | -0.151045 |
| 4 | C | -0.578905 | 0.647805 | -0.287898 |
| 5 | H | 1.068630 | 0.849939 | 1.271102 |
| 6 | H | -0.996305 | 1.608983 | 0.028574 |
| 7 | H | -0.517873 | 0.671575 | -1.382857 |
| 8 | H | -1.653451 | -0.519698 | 1.222608 |
| 9 | H | -1.103179 | -1.465577 | -0.166652 |
| 10 | H | -2.501860 | -0.391665 | -0.326897 |
| CH3CH2CH2_R | | | | |
| 1 | C | -1.218948 | -0.284576 | -0.000000 |
| 2 | C | 1.320599 | -0.241768 | 0.000000 |
| 3 | C | 0.071213 | 0.571067 | -0.000000 |
| 4 | H | 1.745463 | -0.609810 | -0.926645 |
| 5 | H | 1.745463 | -0.609809 | 0.926646 |
| 6 | H | 0.051542 | 1.225420 | -0.879133 |
| 7 | H | 0.051542 | 1.225421 | 0.879132 |
| 8 | H | -1.262040 | -0.927084 | -0.883344 |
| 9 | H | -1.262040 | -0.927083 | 0.883344 |
| 10 | H | -2.107116 | 0.354603 | -0.000001 |
| CH3CHCH3_R | | | | |
| 1 | C | 0.010210 | -0.197527 | 1.297855 |
| 2 | C | 0.010210 | 0.535225 | 0.000000 |
| 3 | H | -0.208529 | 1.597666 | 0.000000 |

Table B.1 Continued.

| Species/Atom Number | Atom Name | Coordinates | | |
|---|---|---|---|---|
| | | X | Y | Z |
| 4 | C | 0.010210 | -0.197527 | -1.297855 |
| 5 | H | -0.960500 | -0.682412 | -1.499567 |
| 6 | H | 0.215973 | 0.464784 | -2.142476 |
| 7 | H | 0.756899 | -1.001722 | -1.306907 |
| 8 | H | -0.960500 | -0.682412 | 1.499567 |
| 9 | H | 0.215973 | 0.464784 | 2.142476 |
| 10 | H | 0.756899 | -1.001722 | 1.306907 |
| NO2_R | | | | |
| 1 | N | 0.000000 | 0.323188 | -0.000000 |
| 2 | O | 1.100414 | -0.141395 | -0.000000 |
| 3 | O | -1.100414 | -0.141395 | 0.000000 |
| NO_R | | | | |
| 1 | N | 0.000000 | 0.000000 | -0.612432 |
| 2 | O | 0.000000 | 0.000000 | 0.535878 |
| OH_R | | | | |
| 1 | O | 0.000000 | 0.000000 | 0.108356 |
| 2 | H | 0.000000 | 0.000000 | -0.866852 |
| Primary Substitution | | | | |
| CF3CF2CF2OH | | | | |
| 1 | C | -1.255173 | 0.441901 | -0.000000 |
| 2 | C | 1.048054 | -0.835612 | 0.000000 |
| 3 | F | -1.750903 | 1.684485 | -0.000000 |
| 4 | F | -1.701242 | -0.194119 | -1.087496 |
| 5 | F | -1.701242 | -0.194119 | 1.087496 |
| 6 | F | 0.667376 | 1.215529 | -1.099914 |
| 7 | F | 0.667376 | -1.563260 | -1.087829 |
| 8 | F | 0.667376 | -1.563260 | 1.087829 |
| 9 | C | 0.297389 | 0.523391 | -0.000000 |
| 10 | F | 0.667376 | 1.215529 | 1.099914 |
| 11 | O | 2.371305 | -0.593458 | 0.000000 |
| 12 | H | 2.842885 | -1.437493 | 0.000000 |
| CF3CF2CFHOH | | | | |
| 1 | C | 1.189350 | 0.185282 | 0.055030 |
| 2 | C | -1.378015 | 0.326838 | 0.422798 |
| 3 | F | 2.171169 | -0.700851 | -0.139318 |
| 4 | F | 1.329555 | 1.174515 | -0.827533 |
| 5 | F | 1.316796 | 0.693216 | 1.296783 |
| 6 | F | -0.355988 | -0.851491 | -1.377926 |
| 7 | F | -1.322102 | 1.575239 | -0.184681 |
| 8 | C | -0.189658 | -0.510715 | -0.082132 |
| 9 | F | -0.140953 | -1.647763 | 0.662907 |
| 10 | H | -1.266976 | 0.494013 | 1.498255 |
| 11 | O | -2.523959 | -0.337640 | 0.082245 |
| 12 | H | -3.257708 | 0.012907 | 0.597525 |
| CF3CF2CH2OH | | | | |
| 1 | C | 0.895456 | -0.323445 | 0.022050 |
| 2 | C | -1.600693 | 0.041473 | 0.624490 |
| 3 | C | -0.336907 | 0.607319 | -0.027140 |
| 4 | F | 1.941216 | 0.202929 | -0.612109 |
| 5 | F | 1.240017 | -0.563802 | 1.297941 |

Table B.1 Continued.

| Species/Atom Number | Atom Name | Coordinates | | |
|---|---|---|---|---|
| | | X | Y | Z |
| 6 | F | 0.603710 | -1.512431 | -0.553173 |
| 7 | F | 0.012546 | 1.752438 | 0.630988 |
| 8 | F | -0.560326 | 0.918960 | -1.328141 |
| 9 | H | -2.314610 | 0.866066 | 0.654190 |
| 10 | H | -1.353357 | -0.237256 | 1.656098 |
| 11 | O | -2.199330 | -0.999554 | -0.106277 |
| 12 | H | -1.618993 | -1.767300 | -0.096035 |
| CF3CH2CF2OH | | | | |
| 1 | C | -1.286449 | 0.000030 | -0.077108 |
| 2 | C | 1.290209 | 0.000032 | -0.097416 |
| 3 | F | 1.365403 | -1.087402 | 0.734117 |
| 4 | F | 1.365375 | 1.086917 | 0.734825 |
| 5 | C | -0.006149 | 0.000273 | -0.889941 |
| 6 | H | -0.013190 | -0.884399 | -1.526823 |
| 7 | H | -0.013182 | 0.885323 | -1.526298 |
| 8 | F | -2.343524 | 0.000323 | -0.922268 |
| 9 | F | -1.403018 | -1.085902 | 0.707351 |
| 10 | F | -1.402989 | 1.085425 | 0.708075 |
| 11 | O | 2.331987 | 0.000331 | -0.969821 |
| 12 | H | 3.153594 | 0.000180 | -0.460410 |
| CF3CH2CFHOH | | | | |
| 1 | C | 1.121334 | -0.067124 | -0.018874 |
| 2 | C | -1.408138 | -0.081001 | 0.263266 |
| 3 | F | 2.148594 | -0.733512 | -0.589562 |
| 4 | F | 1.242166 | 1.226286 | -0.363080 |
| 5 | F | 1.295082 | -0.141873 | 1.324176 |
| 6 | F | -1.574414 | 1.247053 | -0.138896 |
| 7 | C | -0.198310 | -0.672708 | -0.438027 |
| 8 | H | -1.278044 | -0.043633 | 1.350044 |
| 9 | H | -0.155232 | -1.740007 | -0.216218 |
| 10 | H | -0.318117 | -0.545195 | -1.515088 |
| 11 | O | -2.507960 | -0.827539 | -0.114962 |
| 12 | H | -3.277099 | -0.507457 | 0.369034 |
| CF3CH2CH2OH | | | | |
| 1 | C | -0.909305 | 0.043224 | -0.000000 |
| 2 | C | 1.587068 | -0.436275 | 0.000001 |
| 3 | C | 0.484816 | 0.623187 | 0.000001 |
| 4 | F | -1.845166 | 1.016176 | -0.000001 |
| 5 | F | -1.134345 | -0.728612 | -1.087035 |
| 6 | F | -1.134346 | -0.728612 | 1.087033 |
| 7 | H | 1.483997 | -1.071512 | -0.884937 |
| 8 | H | 1.483997 | -1.071511 | 0.884940 |
| 9 | H | 0.570852 | 1.258774 | -0.886334 |
| 10 | H | 0.570851 | 1.258774 | 0.886336 |
| 11 | O | 2.890356 | 0.139634 | 0.000003 |
| 12 | H | 2.816690 | 1.097016 | -0.000013 |
| CH3CF2CF2OH | | | | |
| 1 | C | 1.521625 | 1.210207 | -0.123634 |
| 2 | C | -0.792493 | 0.054061 | 0.012390 |
| 3 | F | 1.056922 | -0.939188 | -1.014096 |

Table B.1 Continued.

| Species/Atom Number | Atom Name | Coordinates | | |
|---|---|---|---|---|
| | | X | Y | Z |
| 4 | F | -1.133675 | 0.814868 | -1.081339 |
| 5 | F | -1.195099 | 0.737650 | 1.102905 |
| 6 | C | 0.751345 | -0.072157 | 0.022473 |
| 7 | F | 1.103035 | -0.715620 | 1.173358 |
| 8 | H | 2.587030 | 0.982205 | -0.078550 |
| 9 | H | 1.284585 | 1.683018 | -1.075345 |
| 10 | H | 1.261339 | 1.886236 | 0.691217 |
| 11 | O | -1.438887 | -1.133319 | -0.001107 |
| 12 | H | -0.985357 | -1.716964 | -0.623289 |
| CH3CF2CFHOH | | | | |
| 1 | C | -0.924350 | 0.061423 | 1.427721 |
| 2 | C | 0.877147 | -0.010377 | -0.407480 |
| 3 | F | 1.423913 | -1.180517 | 0.118146 |
| 4 | C | -0.611805 | 0.018872 | -0.043972 |
| 5 | H | 0.986578 | -0.073948 | -1.494906 |
| 6 | H | -0.488708 | 0.956429 | 1.870452 |
| 7 | H | -0.509176 | -0.821296 | 1.913879 |
| 8 | H | -2.007290 | 0.074552 | 1.555236 |
| 9 | F | -1.158395 | 1.106695 | -0.682346 |
| 10 | F | -1.183340 | -1.091246 | -0.617496 |
| 11 | O | 1.483502 | 1.092504 | 0.145225 |
| 12 | H | 2.365029 | 1.190335 | -0.228818 |
| CH3CF2CH2OH | | | | |
| 1 | C | -0.660356 | 1.419163 | -0.302311 |
| 2 | C | 0.938669 | -0.595221 | -0.434893 |
| 3 | C | -0.409677 | -0.037147 | -0.002884 |
| 4 | H | 1.003081 | -1.615912 | -0.040515 |
| 5 | H | 0.951390 | -0.636813 | -1.531818 |
| 6 | H | 0.105795 | 2.025929 | 0.178840 |
| 7 | H | -0.631472 | 1.592074 | -1.379400 |
| 8 | H | -1.644114 | 1.693644 | 0.080409 |
| 9 | F | -0.564845 | -0.251111 | 1.348969 |
| 10 | F | -1.372044 | -0.813693 | -0.623090 |
| 11 | O | 1.954417 | 0.249535 | 0.078664 |
| 12 | H | 2.800157 | -0.192741 | -0.029213 |
| CH3CH2CF2OH | | | | |
| 1 | C | 1.754564 | -1.128896 | -0.000000 |
| 2 | C | -0.360175 | 0.272977 | 0.000000 |
| 3 | C | 1.151566 | 0.275893 | -0.000000 |
| 4 | H | 1.442709 | -1.688109 | 0.883964 |
| 5 | H | 1.442709 | -1.688109 | -0.883964 |
| 6 | H | 2.844848 | -1.071562 | -0.000000 |
| 7 | F | -0.851015 | -0.420283 | 1.088976 |
| 8 | F | -0.851015 | -0.420283 | -1.088976 |
| 9 | H | 1.468197 | 0.840029 | 0.880490 |
| 10 | H | 1.468197 | 0.840029 | -0.880490 |
| 11 | O | -0.851015 | 1.540379 | 0.000000 |
| 12 | H | -1.816005 | 1.489938 | 0.000000 |
| CH3CH2CFHOH | | | | |
| 1 | C | 2.005109 | 0.039343 | 0.100001 |

Table B.1 Continued.

| Species/Atom Number | Atom Name | Coordinates | | |
|---|---|---|---|---|
| | | X | Y | Z |
| 2 | C | -0.522900 | -0.011586 | 0.321129 |
| 3 | F | -0.595538 | 1.301411 | -0.184917 |
| 4 | C | 0.706227 | -0.692964 | -0.239052 |
| 5 | H | -0.471713 | 0.112625 | 1.411122 |
| 6 | H | 0.721980 | -1.715268 | 0.150310 |
| 7 | H | 0.568393 | -0.761622 | -1.322153 |
| 8 | H | 2.165585 | 0.090128 | 1.181413 |
| 9 | H | 1.985073 | 1.060455 | -0.285047 |
| 10 | H | 2.863833 | -0.473637 | -0.338425 |
| 11 | O | -1.647909 | -0.715625 | -0.070238 |
| 12 | H | -2.420652 | -0.309136 | 0.336474 |
| CH3CH2CH2OH | | | | |
| 1 | C | -1.900752 | -0.141107 | 0.000002 |
| 2 | C | 0.617654 | -0.486232 | 0.000001 |
| 3 | C | -0.521220 | 0.521558 | -0.000000 |
| 4 | H | 0.540888 | -1.131873 | -0.888142 |
| 5 | H | 0.540891 | -1.131869 | 0.888146 |
| 6 | H | -0.408428 | 1.165676 | -0.877903 |
| 7 | H | -0.408427 | 1.165679 | 0.877900 |
| 8 | H | -2.041525 | -0.771799 | -0.883409 |
| 9 | H | -2.041524 | -0.771797 | 0.883414 |
| 10 | H | -2.696163 | 0.607895 | 0.000001 |
| 11 | O | 1.846511 | 0.237530 | -0.000002 |
| 12 | H | 2.568107 | -0.397463 | -0.000001 |
| CF3CF2CF2ONO | | | | |
| 1 | C | -1.900270 | -0.180095 | 0.000003 |
| 2 | C | 0.737850 | -0.283395 | -0.000001 |
| 3 | F | -2.904606 | 0.704836 | -0.000013 |
| 4 | F | -2.011921 | -0.948714 | -1.087498 |
| 5 | F | -2.011931 | -0.948685 | 1.087522 |
| 6 | F | -0.533320 | 1.377395 | -1.100258 |
| 7 | F | 0.718965 | -1.099969 | -1.091120 |
| 8 | F | 0.718955 | -1.099987 | 1.091104 |
| 9 | C | -0.551031 | 0.592960 | -0.000002 |
| 10 | F | -0.533318 | 1.377403 | 1.100249 |
| 11 | O | 1.811375 | 0.528152 | 0.000010 |
| 12 | N | 3.189675 | -0.335165 | -0.000000 |
| 13 | O | 4.059571 | 0.385451 | 0.000007 |
| CF3CF2CH2ONO | | | | |
| 1 | C | 1.011081 | -0.759822 | 0.004844 |
| 2 | C | -0.620025 | 1.199400 | 0.537573 |
| 3 | C | 0.732905 | 0.761349 | -0.017363 |
| 4 | F | 2.249263 | -1.021273 | -0.420192 |
| 5 | F | 0.883029 | -1.224419 | 1.260720 |
| 6 | F | 0.143010 | -1.416153 | -0.776514 |
| 7 | F | 1.697384 | 1.353189 | 0.746362 |
| 8 | F | 0.886222 | 1.189256 | -1.295424 |
| 9 | H | -0.610227 | 2.291334 | 0.561670 |
| 10 | H | -0.734735 | 0.811757 | 1.553510 |
| 11 | O | -1.690606 | 0.769640 | -0.281025 |

Table B.1 Continued.

| Species/Atom Number | Atom Name | Coordinates | | |
|---|---|---|---|---|
| | | X | Y | Z |
| 12 | N | -2.506759 | -0.231439 | 0.441690 |
| 13 | O | -3.382101 | -0.596386 | -0.217965 |
| CF3CH2CF2ONO | | | | |
| 1 | C | -1.780132 | 0.352920 | -0.054282 |
| 2 | C | 0.621130 | -0.599450 | -0.030989 |
| 3 | F | 0.249660 | -1.794508 | -0.542997 |
| 4 | F | 0.616899 | -0.721020 | 1.325542 |
| 5 | C | -0.329551 | 0.505350 | -0.476229 |
| 6 | H | -0.300579 | 0.554526 | -1.565310 |
| 7 | H | 0.031576 | 1.453266 | -0.074831 |
| 8 | F | -2.494225 | 1.388136 | -0.553136 |
| 9 | F | -2.336768 | -0.779071 | -0.517611 |
| 10 | F | -1.932149 | 0.368701 | 1.281210 |
| 11 | N | 2.541902 | 0.852168 | 0.162516 |
| 12 | O | 1.922375 | -0.400426 | -0.473507 |
| 13 | O | 3.637157 | 0.939672 | -0.159685 |
| CF3CH2CH2ONO | | | | |
| 1 | C | 1.733467 | -0.097411 | -0.030006 |
| 2 | C | -0.678585 | 0.600440 | 0.248906 |
| 3 | C | 0.329860 | -0.198782 | -0.576167 |
| 4 | F | 2.603782 | -0.813728 | -0.768426 |
| 5 | F | 2.174954 | 1.181786 | -0.015230 |
| 6 | F | 1.811736 | -0.554878 | 1.241459 |
| 7 | H | -0.395381 | 1.652636 | 0.300187 |
| 8 | H | -0.757298 | 0.203345 | 1.263946 |
| 9 | H | 0.343967 | 0.164352 | -1.605769 |
| 10 | H | 0.052979 | -1.255108 | -0.592079 |
| 11 | O | -1.964035 | 0.543357 | -0.377357 |
| 12 | N | -2.852702 | -0.314286 | 0.381517 |
| 13 | O | -3.898223 | -0.382022 | -0.124334 |
| CH3CF2CF2ONO | | | | |
| 1 | C | 2.381251 | -0.267748 | -0.592303 |
| 2 | C | 0.077233 | 0.710564 | 0.040012 |
| 3 | F | 0.379065 | -1.525257 | -0.610580 |
| 4 | F | -0.052235 | 1.142880 | -1.252002 |
| 5 | F | 0.659309 | 1.715137 | 0.742161 |
| 6 | C | 1.036167 | -0.508643 | 0.040631 |
| 7 | F | 1.184237 | -0.905557 | 1.339031 |
| 8 | H | 2.965736 | -1.185617 | -0.521047 |
| 9 | H | 2.257307 | 0.007468 | -1.638946 |
| 10 | H | 2.898112 | 0.533828 | -0.064987 |
| 11 | O | -1.136740 | 0.465220 | 0.601196 |
| 12 | N | -2.124313 | -0.307582 | -0.396280 |
| 13 | O | -3.082292 | -0.546780 | 0.161480 |
| CH3CF2CH2ONO | | | | |
| 1 | C | -1.561401 | 1.412328 | -0.124364 |
| 2 | C | -0.020859 | -0.526729 | -0.852551 |
| 3 | C | -1.146512 | -0.026341 | 0.048992 |
| 4 | H | 0.198883 | -1.562879 | -0.581915 |
| 5 | H | -0.332329 | -0.477544 | -1.897230 |

Table B.1 Continued.

| Species/Atom Number | Atom Name | Coordinates | | |
|---|---|---|---|---|
| | | X | Y | Z |
| 6 | H | -0.702120 | 2.063447 | 0.036903 |
| 7 | H | -1.949725 | 1.573012 | -1.131401 |
| 8 | H | -2.339426 | 1.647314 | 0.602859 |
| 9 | F | -0.766183 | -0.233329 | 1.356988 |
| 10 | F | -2.224871 | -0.856826 | -0.179025 |
| 11 | O | 1.141601 | 0.278144 | -0.701891 |
| 12 | N | 2.127303 | -0.414940 | 0.134247 |
| 13 | O | 3.049113 | 0.261492 | 0.326508 |
| CH3CH2CF2ONO | | | | |
| 1 | C | 0.937682 | 2.674373 | 0.000000 |
| 2 | C | 0.154864 | 0.262866 | 0.000000 |
| 3 | C | -0.258638 | 1.720717 | 0.000000 |
| 4 | H | 1.559091 | 2.521747 | 0.884111 |
| 5 | H | 1.559091 | 2.521747 | -0.884111 |
| 6 | H | 0.592103 | 3.709948 | 0.000000 |
| 7 | F | 0.937682 | -0.023849 | 1.090856 |
| 8 | F | 0.937682 | -0.023849 | -1.090856 |
| 9 | H | -0.886270 | 1.875490 | 0.880691 |
| 10 | H | -0.886270 | 1.875490 | -0.880691 |
| 11 | O | -0.959195 | -0.543886 | -0.000000 |
| 12 | N | -0.567638 | -2.040432 | -0.000000 |
| 13 | O | -1.521554 | -2.673596 | -0.000000 |
| CH3CH2CH2ONO | | | | |
| 1 | C | -2.932348 | -0.197447 | 0.000005 |
| 2 | C | -0.412164 | -0.411725 | -0.000006 |
| 3 | C | -1.593006 | 0.545528 | -0.000003 |
| 4 | H | -0.422212 | -1.050712 | -0.888733 |
| 5 | H | -0.422203 | -1.050709 | 0.888724 |
| 6 | H | -1.519422 | 1.194095 | -0.878119 |
| 7 | H | -1.519414 | 1.194098 | 0.878111 |
| 8 | H | -3.036479 | -0.834109 | -0.883639 |
| 9 | H | -3.036472 | -0.834106 | 0.883652 |
| 10 | H | -3.766825 | 0.507089 | 0.000007 |
| 11 | O | 0.793311 | 0.382654 | -0.000013 |
| 12 | N | 1.942070 | -0.458983 | 0.000009 |
| 13 | O | 2.925895 | 0.175983 | 0.000008 |
| CF3CF2CF2NO | | | | |
| 1 | C | 1.559992 | -0.131678 | -0.146801 |
| 2 | C | -1.034907 | -0.401877 | 0.140385 |
| 3 | F | 2.538600 | 0.757028 | 0.041293 |
| 4 | F | 1.763854 | -1.177409 | 0.662072 |
| 5 | F | 1.594475 | -0.548633 | -1.414571 |
| 6 | F | 0.270730 | 1.083662 | 1.403040 |
| 7 | F | -1.012386 | -1.261674 | 1.172580 |
| 8 | F | -1.093116 | -1.076392 | -1.011310 |
| 9 | C | 0.192705 | 0.533946 | 0.173032 |
| 10 | F | -0.017127 | 1.517349 | -0.736483 |
| 11 | O | -3.051747 | 0.399873 | -0.574106 |
| 12 | N | -2.328291 | 0.450469 | 0.363366 |
| CF3CF2CH2NO | | | | |

Table B.1 Continued.

| Species/Atom Number | Atom Name | Coordinates | | |
|---|---|---|---|---|
| | | X | Y | Z |
| 1 | C | 1.109776 | -0.471989 | 0.012531 |
| 2 | C | -1.248134 | 0.417956 | 0.675892 |
| 3 | C | 0.076675 | 0.682399 | -0.018654 |
| 4 | F | 2.280750 | -0.060542 | -0.480147 |
| 5 | F | 1.298778 | -0.872194 | 1.284104 |
| 6 | F | 0.686973 | -1.516804 | -0.702849 |
| 7 | F | 0.665225 | 1.753262 | 0.586545 |
| 8 | F | -0.137993 | 1.005904 | -1.322672 |
| 9 | H | -1.826815 | 1.343202 | 0.713939 |
| 10 | H | -1.058557 | 0.047007 | 1.687075 |
| 11 | N | -2.036100 | -0.664570 | -0.017530 |
| 12 | O | -3.204430 | -0.411882 | -0.072719 |
| CF3CH2CF2NO | | | | |
| 1 | C | -1.549702 | -0.158330 | -0.055871 |
| 2 | C | 0.990586 | 0.207593 | -0.009003 |
| 3 | F | 1.166188 | 0.094294 | 1.317857 |
| 4 | F | 0.879915 | 1.520171 | -0.319738 |
| 5 | C | -0.175588 | -0.615266 | -0.517514 |
| 6 | H | -0.036620 | -1.646626 | -0.187204 |
| 7 | H | -0.164388 | -0.596007 | -1.608726 |
| 8 | F | -2.482607 | -1.020614 | -0.513991 |
| 9 | F | -1.651273 | -0.124695 | 1.283867 |
| 10 | F | -1.862779 | 1.061570 | -0.523468 |
| 11 | N | 2.259580 | -0.248982 | -0.770132 |
| 12 | O | 3.043397 | -0.799376 | -0.064944 |
| CF3CH2CH2NO | | | | |
| 1 | C | -1.308132 | 0.024629 | 0.000000 |
| 2 | C | 1.199714 | -0.270543 | -0.000001 |
| 3 | C | 0.035577 | 0.711046 | -0.000001 |
| 4 | F | -2.316672 | 0.918677 | -0.000000 |
| 5 | F | -1.469585 | -0.764364 | -1.087371 |
| 6 | F | -1.469584 | -0.764363 | 1.087372 |
| 7 | H | 1.203706 | -0.913208 | -0.884780 |
| 8 | H | 1.203708 | -0.913206 | 0.884780 |
| 9 | H | 0.078316 | 1.354554 | -0.881569 |
| 10 | H | 0.078317 | 1.354555 | 0.881567 |
| 11 | N | 2.497624 | 0.500797 | -0.000004 |
| 12 | O | 3.461525 | -0.211078 | 0.000004 |
| CH3CF2CF2NO | | | | |
| 1 | C | 2.065973 | 0.846846 | 0.000011 |
| 2 | C | -0.441918 | 0.308685 | -0.000002 |
| 3 | F | 1.121075 | -1.018980 | -1.102279 |
| 4 | F | -0.670128 | 1.060117 | -1.095980 |
| 5 | F | -0.670134 | 1.060109 | 1.095981 |
| 6 | C | 0.999723 | -0.216983 | 0.000000 |
| 7 | F | 1.121066 | -1.018992 | 1.102271 |
| 8 | H | 3.040028 | 0.356845 | 0.000010 |
| 9 | H | 1.971391 | 1.468568 | -0.890237 |
| 10 | H | 1.971386 | 1.468555 | 0.890267 |
| 11 | N | -1.464203 | -0.873011 | -0.000011 |

Table B.1 Continued.

| Species/Atom Number | Atom Name | Coordinates | | |
|---|---|---|---|---|
| | | X | Y | Z |
| 12 | O | -2.574120 | -0.444308 | 0.000006 |
| CH3CF2CH2NO | | | | |
| 1 | C | -1.225229 | 1.378468 | -0.161285 |
| 2 | C | 0.567960 | -0.420330 | -0.631752 |
| 3 | C | -0.768857 | -0.050536 | -0.002073 |
| 4 | H | 0.808209 | -1.469203 | -0.446982 |
| 5 | H | 0.523568 | -0.223488 | -1.708101 |
| 6 | H | -0.477150 | 2.054956 | 0.251771 |
| 7 | H | -1.375144 | 1.610333 | -1.216937 |
| 8 | H | -2.169069 | 1.504216 | 0.370388 |
| 9 | F | -0.696319 | -0.355893 | 1.340572 |
| 10 | F | -1.714803 | -0.899105 | -0.538028 |
| 11 | N | 1.652934 | 0.469739 | -0.107342 |
| 12 | O | 2.671987 | -0.114453 | 0.131127 |
| CH3CH2CF2NO | | | | |
| 1 | C | -2.440184 | 0.048255 | 0.000003 |
| 2 | C | 0.091757 | -0.030831 | -0.000001 |
| 3 | C | -1.131950 | 0.841248 | -0.000001 |
| 4 | H | -2.510537 | -0.588068 | -0.884142 |
| 5 | H | -2.510534 | -0.588064 | 0.884151 |
| 6 | H | -3.294815 | 0.727014 | 0.000003 |
| 7 | F | 0.155687 | -0.831592 | -1.095829 |
| 8 | F | 0.155690 | -0.831588 | 1.095829 |
| 9 | H | -1.060454 | 1.490770 | -0.877813 |
| 10 | H | -1.060451 | 1.490774 | 0.877808 |
| 11 | N | 1.377308 | 0.845779 | -0.000006 |
| 12 | O | 2.359438 | 0.170463 | 0.000005 |
| CH3CH2CH2NO | | | | |
| 1 | C | 2.342892 | -0.135280 | -0.123327 |
| 2 | C | -0.159301 | -0.500257 | 0.167823 |
| 3 | C | 0.966723 | 0.525188 | -0.007049 |
| 4 | H | 0.018003 | -1.096162 | 1.071550 |
| 5 | H | -0.279005 | -1.156222 | -0.700167 |
| 6 | H | 0.947734 | 1.214957 | 0.842177 |
| 7 | H | 0.761787 | 1.122311 | -0.901647 |
| 8 | H | 2.584629 | -0.708548 | 0.776446 |
| 9 | H | 2.386651 | -0.818452 | -0.976204 |
| 10 | H | 3.123748 | 0.616893 | -0.259320 |
| 11 | N | -1.436765 | 0.222850 | 0.425034 |
| 12 | O | -2.298510 | -0.009079 | -0.381595 |
| CF3CF2CF2NO2 | | | | |
| 1 | C | -1.770425 | -0.097071 | -0.050816 |
| 2 | C | 0.788872 | -0.441036 | 0.354901 |
| 3 | F | -2.662616 | 0.855401 | -0.323427 |
| 4 | F | -1.931874 | -1.101151 | -0.913273 |
| 5 | F | -1.980480 | -0.547851 | 1.191764 |
| 6 | F | -0.092134 | 0.769503 | -1.465457 |
| 7 | F | 0.626213 | -1.677107 | -0.103136 |
| 8 | F | 0.837131 | -0.442788 | 1.683841 |
| 9 | C | -0.336174 | 0.500279 | -0.163513 |

Table B.1 Continued.

| Species/Atom Number | Atom Name | Coordinates | | |
|---|---|---|---|---|
| | | X | Y | Z |
| 10 | F | -0.301422 | 1.644919 | 0.540266 |
| 11 | O | 2.687793 | -0.549474 | -1.056859 |
| 12 | N | 2.178657 | 0.079274 | -0.160064 |
| 13 | O | 2.587507 | 1.069938 | 0.404585 |
| CF3CF2CH2NO2 | | | | |
| 1 | C | -1.143492 | -0.566692 | 0.124065 |
| 2 | C | 0.925970 | 0.652007 | -0.882925 |
| 3 | C | -0.401481 | 0.768022 | -0.138065 |
| 4 | F | -2.342592 | -0.333926 | 0.658032 |
| 5 | F | -1.306179 | -1.230034 | -1.031114 |
| 6 | F | -0.436267 | -1.331475 | 0.963819 |
| 7 | F | -1.214006 | 1.532437 | -0.921937 |
| 8 | F | -0.246214 | 1.396546 | 1.047693 |
| 9 | H | 1.311123 | 1.660476 | -1.021210 |
| 10 | H | 0.776893 | 0.143010 | -1.830562 |
| 11 | N | 1.975217 | -0.121170 | -0.112747 |
| 12 | O | 2.493891 | 0.451368 | 0.827060 |
| 13 | O | 2.219459 | -1.248524 | -0.505295 |
| CF3CH2CF2NO2 | | | | |
| 1 | C | -1.785601 | 0.157604 | -0.000013 |
| 2 | C | 0.724766 | -0.282918 | 0.000010 |
| 3 | F | 0.712446 | -1.064165 | -1.088780 |
| 4 | F | 0.712427 | -1.064023 | 1.088904 |
| 5 | C | -0.383072 | 0.747541 | -0.000069 |
| 6 | H | -0.279238 | 1.378615 | -0.881889 |
| 7 | H | -0.279228 | 1.378763 | 0.881643 |
| 8 | F | -2.683001 | 1.163834 | -0.000115 |
| 9 | F | -2.021369 | -0.598453 | -1.085948 |
| 10 | F | -2.021371 | -0.598235 | 1.086073 |
| 11 | N | 2.139920 | 0.404883 | -0.000018 |
| 12 | O | 3.078295 | -0.356598 | -0.000050 |
| 13 | O | 2.165490 | 1.622154 | -0.000001 |
| CF3CH2CH2NO2 | | | | |
| 1 | C | -1.605026 | 0.026624 | 0.000001 |
| 2 | C | 0.837963 | -0.514821 | 0.000001 |
| 3 | C | -0.203385 | 0.592831 | 0.000001 |
| 4 | F | -2.524880 | 1.007661 | 0.000001 |
| 5 | F | -1.833853 | -0.745564 | -1.087263 |
| 6 | F | -1.833853 | -0.745564 | 1.087265 |
| 7 | H | 0.774598 | -1.150515 | -0.882632 |
| 8 | H | 0.774600 | -1.150513 | 0.882636 |
| 9 | H | -0.096757 | 1.226905 | -0.880590 |
| 10 | H | -0.096757 | 1.226906 | 0.880590 |
| 11 | N | 2.255143 | 0.025864 | -0.000001 |
| 12 | O | 3.138658 | -0.811863 | 0.000001 |
| 13 | O | 2.413126 | 1.235559 | -0.000004 |
| CH3CF2CF2NO2 | | | | |
| 1 | C | -2.313469 | -0.673011 | 0.000010 |
| 2 | C | 0.225936 | -0.524213 | 0.000001 |
| 3 | F | -1.138235 | 1.044450 | -1.104954 |

Table B.1 Continued.

| Species/Atom Number | Atom Name | Coordinates | | |
|---|---|---|---|---|
| | | X | Y | Z |
| 4 | F | 0.309891 | -1.295866 | -1.091666 |
| 5 | F | 0.309891 | -1.295860 | 1.091672 |
| 6 | C | -1.116568 | 0.248274 | -0.000001 |
| 7 | F | -1.138228 | 1.044467 | 1.104939 |
| 8 | H | -3.209003 | -0.050972 | 0.000008 |
| 9 | H | -2.307521 | -1.299856 | -0.891172 |
| 10 | H | -2.307515 | -1.299843 | 0.891201 |
| 11 | N | 1.513000 | 0.362314 | -0.000001 |
| 12 | O | 2.544652 | -0.274153 | -0.000003 |
| 13 | O | 1.376320 | 1.565834 | 0.000004 |
| CH3CF2CH2NO2 | | | | |
| 1 | C | -1.358391 | 1.397529 | 0.103106 |
| 2 | C | 0.248070 | -0.460159 | -0.792112 |
| 3 | C | -0.998466 | -0.062441 | 0.004264 |
| 4 | H | 0.301622 | -1.543835 | -0.842017 |
| 5 | H | 0.220521 | -0.017668 | -1.786602 |
| 6 | H | -0.565445 | 1.952352 | 0.600465 |
| 7 | H | -1.512362 | 1.813697 | -0.893368 |
| 8 | H | -2.284256 | 1.478554 | 0.673919 |
| 9 | F | -0.874533 | -0.593905 | 1.265317 |
| 10 | F | -2.030749 | -0.743589 | -0.607610 |
| 11 | N | 1.525638 | 0.011864 | -0.141170 |
| 12 | O | 2.302431 | -0.842783 | 0.239924 |
| 13 | O | 1.692657 | 1.220498 | -0.061814 |
| CH3CH2CF2NO2 | | | | |
| 1 | C | -1.011358 | -2.417167 | 0.000000 |
| 2 | C | -0.281694 | -0.013019 | 0.000000 |
| 3 | C | 0.175635 | -1.447220 | -0.000000 |
| 4 | H | -1.634575 | -2.277742 | 0.884946 |
| 5 | H | -1.634575 | -2.277742 | -0.884946 |
| 6 | H | -0.645680 | -3.445126 | 0.000000 |
| 7 | F | -1.011358 | 0.297806 | 1.089901 |
| 8 | F | -1.011358 | 0.297806 | -1.089901 |
| 9 | H | 0.807641 | -1.593650 | 0.877476 |
| 10 | H | 0.807641 | -1.593650 | -0.877476 |
| 11 | N | 0.902867 | 1.016760 | -0.000000 |
| 12 | O | 0.578025 | 2.183256 | -0.000000 |
| 13 | O | 2.033027 | 0.563558 | -0.000000 |
| CH3CH2CH2NO2 | | | | |
| 1 | C | 2.656974 | -0.121444 | 0.022314 |
| 2 | C | 0.184354 | -0.474958 | 0.390484 |
| 3 | C | 1.243039 | 0.329173 | -0.356025 |
| 4 | H | 0.272896 | -0.341149 | 1.471277 |
| 5 | H | 0.204844 | -1.536079 | 0.150555 |
| 6 | H | 1.102358 | 1.386958 | -0.126977 |
| 7 | H | 1.087416 | 0.210544 | -1.432986 |
| 8 | H | 2.846928 | 0.017127 | 1.090712 |
| 9 | H | 2.819930 | -1.177109 | -0.212993 |
| 10 | H | 3.402880 | 0.458887 | -0.524826 |
| 11 | N | -1.215649 | -0.008011 | 0.049528 |

Table B.1 Continued.

| Species/Atom Number | Atom Name | Coordinates | | |
|---|---|---|---|---|
| | | X | Y | Z |
| 12 | O | -2.030301 | -0.860829 | -0.263799 |
| 13 | O | -1.436437 | 1.190863 | 0.126037 |
| Secondary Substitution | | | | |
| CF3CFOHCF3 | | | | |
| 1 | C | -1.307311 | -0.246080 | 0.015991 |
| 2 | C | 0.000000 | 0.595687 | -0.007427 |
| 3 | C | 1.307312 | -0.246078 | 0.015991 |
| 4 | F | -2.357589 | 0.583376 | -0.049034 |
| 5 | F | -1.369440 | -1.086409 | -1.023774 |
| 6 | F | -1.392463 | -0.955103 | 1.146342 |
| 7 | F | -0.000001 | 1.291553 | -1.192659 |
| 8 | F | 1.369431 | -1.086418 | -1.023765 |
| 9 | F | 2.357589 | 0.583376 | -0.049052 |
| 10 | F | 1.392474 | -0.955090 | 1.146349 |
| 11 | O | 0.000003 | 1.455327 | 1.066700 |
| 12 | H | -0.000038 | 2.358639 | 0.729418 |
| CF3CFOHCH3 | | | | |
| 1 | C | 0.768114 | -0.067842 | 0.012279 |
| 2 | C | -0.772493 | 0.072143 | 0.009429 |
| 3 | F | 1.344329 | 1.153111 | -0.065707 |
| 4 | F | 1.192698 | -0.644765 | 1.150088 |
| 5 | F | 1.209354 | -0.802804 | -1.016528 |
| 6 | F | -1.073905 | 0.575492 | -1.261113 |
| 7 | C | -1.491442 | -1.241451 | 0.205177 |
| 8 | H | -1.259209 | -1.656642 | 1.185382 |
| 9 | H | -2.562773 | -1.052622 | 0.137702 |
| 10 | H | -1.198479 | -1.947227 | -0.571605 |
| 11 | O | -1.172490 | 0.969895 | 0.971598 |
| 12 | H | -0.676976 | 1.790918 | 0.853759 |
| CF3CHOHCF3 | | | | |
| 1 | C | -1.297460 | -0.135094 | -0.030957 |
| 2 | F | 1.442727 | -1.346724 | -0.637227 |
| 3 | F | 1.321819 | -0.360877 | 1.296062 |
| 4 | C | -0.004063 | 0.547517 | -0.493551 |
| 5 | H | -0.001831 | 0.495307 | -1.589786 |
| 6 | F | -2.352349 | 0.459544 | -0.611969 |
| 7 | F | -1.302985 | -1.431481 | -0.396424 |
| 8 | F | -1.462905 | -0.072993 | 1.293982 |
| 9 | C | 1.276360 | -0.165044 | -0.024924 |
| 10 | F | 2.333066 | 0.619864 | -0.358741 |
| 11 | O | -0.047337 | 1.859652 | -0.005085 |
| 12 | H | 0.717145 | 2.337198 | -0.344087 |
| CF3CHOHCH3 | | | | |
| 1 | C | -0.635283 | 0.022529 | -0.012459 |
| 2 | C | 0.822773 | -0.099351 | -0.446227 |
| 3 | F | -1.372704 | -1.014525 | -0.441833 |
| 4 | F | -0.769267 | 0.095474 | 1.324578 |
| 5 | F | -1.177582 | 1.149203 | -0.535442 |
| 6 | C | 1.653917 | 1.084556 | 0.039035 |
| 7 | H | 1.663262 | 1.110523 | 1.129817 |

Table B.1 Continued.

| Species/Atom Number | Atom Name | Coordinates | | |
|---|---|---|---|---|
| | | X | Y | Z |
| 8 | H | 2.682837 | 0.983180 | -0.316304 |
| 9 | H | 1.257779 | 2.028974 | -0.338525 |
| 10 | H | 0.797826 | -0.121904 | -1.544458 |
| 11 | O | 1.278177 | -1.334631 | 0.079032 |
| 12 | H | 2.200419 | -1.441496 | -0.170612 |
| CH3CFOHCH3 | | | | |
| 1 | C | -0.407786 | 0.688946 | 1.281508 |
| 2 | C | 0.005592 | -0.021876 | 0.000000 |
| 3 | C | -0.407786 | 0.688946 | -1.281508 |
| 4 | H | 0.008992 | 1.697439 | -1.315929 |
| 5 | H | -0.037601 | 0.119066 | -2.134607 |
| 6 | H | -1.496833 | 0.762007 | -1.350300 |
| 7 | H | 0.008992 | 1.697439 | 1.315929 |
| 8 | H | -0.037601 | 0.119066 | 2.134607 |
| 9 | H | -1.496833 | 0.762007 | 1.350300 |
| 10 | F | 1.393662 | -0.103630 | -0.000000 |
| 11 | O | -0.407786 | -1.371319 | 0.000000 |
| 12 | H | -1.369904 | -1.389903 | 0.000000 |
| CH3CHOHCH3 | | | | |
| 1 | C | -1.272740 | -0.666536 | 0.098677 |
| 2 | C | 0.000000 | 0.037486 | -0.371153 |
| 3 | H | 0.000000 | 0.076819 | -1.464657 |
| 4 | C | 1.272740 | -0.666536 | 0.098677 |
| 5 | H | 1.329200 | -1.689622 | -0.284696 |
| 6 | H | 2.154118 | -0.118306 | -0.240446 |
| 7 | H | 1.302930 | -0.718233 | 1.193372 |
| 8 | H | -1.329200 | -1.689622 | -0.284696 |
| 9 | H | -2.154118 | -0.118306 | -0.240446 |
| 10 | H | -1.302930 | -0.718233 | 1.193372 |
| 11 | O | 0.000000 | 1.413732 | 0.023085 |
| 12 | H | 0.000000 | 1.439158 | 0.986313 |
| CF3CFONOCF3 | | | | |
| 1 | C | 0.098670 | 1.362099 | 0.087308 |
| 2 | C | 0.011187 | -0.156084 | -0.255893 |
| 3 | C | -1.364482 | -0.798345 | 0.103584 |
| 4 | F | 1.349960 | 1.798106 | -0.142779 |
| 5 | F | -0.738316 | 2.088487 | -0.657239 |
| 6 | F | -0.182791 | 1.570914 | 1.379435 |
| 7 | F | 0.137481 | -0.244266 | -1.626944 |
| 8 | F | -2.370926 | -0.112256 | -0.454927 |
| 9 | F | -1.397680 | -2.050118 | -0.362769 |
| 10 | F | -1.552321 | -0.828628 | 1.426380 |
| 11 | O | 0.967991 | -0.879111 | 0.394088 |
| 12 | N | 2.450901 | -0.709236 | -0.255157 |
| 13 | O | 3.177356 | -1.306079 | 0.371623 |
| CF3CFONOCH3 | | | | |
| 1 | C | -0.971763 | -0.578389 | 0.045784 |
| 2 | C | -0.137203 | 0.724990 | -0.049170 |
| 3 | F | -0.348627 | -1.617913 | -0.528860 |
| 4 | F | -1.194233 | -0.891197 | 1.335630 |

Table B.1 Continued.

| Species/Atom Number | Atom Name | Coordinates | | |
|---|---|---|---|---|
| | | X | Y | Z |
| 5 | F | -2.163586 | -0.424250 | -0.555196 |
| 6 | F | 0.002909 | 0.981349 | -1.406637 |
| 7 | C | -0.830383 | 1.898231 | 0.613856 |
| 8 | H | -0.946901 | 1.715956 | 1.681611 |
| 9 | H | -0.212629 | 2.783120 | 0.463169 |
| 10 | H | -1.808851 | 2.053639 | 0.159006 |
| 11 | O | 3.065035 | -0.426555 | 0.271204 |
| 12 | O | 1.111427 | 0.564176 | 0.538740 |
| 13 | N | 2.074946 | -0.336367 | -0.292940 |
| CH3CFONOCH3 | | | | |
| 1 | C | 0.994704 | -1.284308 | 0.734085 |
| 2 | C | 0.752193 | -0.000002 | -0.033938 |
| 3 | C | 0.994728 | 1.284309 | 0.734069 |
| 4 | H | 2.026031 | 1.314537 | 1.089650 |
| 5 | H | 0.820859 | 2.134483 | 0.073039 |
| 6 | H | 0.320175 | 1.350884 | 1.589256 |
| 7 | H | 2.026007 | -1.314552 | 1.089667 |
| 8 | H | 0.820820 | -2.134486 | 0.073065 |
| 9 | H | 0.320151 | -1.350861 | 1.589273 |
| 10 | F | 1.579058 | -0.000016 | -1.144664 |
| 11 | O | -0.562524 | 0.000008 | -0.634549 |
| 12 | N | -1.606767 | 0.000026 | 0.356794 |
| 13 | O | -2.655969 | -0.000012 | -0.153555 |
| CF3CHONOCF3 | | | | |
| 1 | C | -0.034376 | 1.403716 | -0.030766 |
| 2 | F | -2.282311 | -0.341638 | 0.226367 |
| 3 | F | -0.625651 | -1.401740 | 1.158347 |
| 4 | C | -0.119714 | 0.014500 | -0.704677 |
| 5 | H | -0.519831 | 0.196603 | -1.704819 |
| 6 | F | 1.042350 | 2.063647 | -0.485593 |
| 7 | F | -1.125095 | 2.126244 | -0.341709 |
| 8 | F | 0.049788 | 1.344730 | 1.306820 |
| 9 | C | -1.104146 | -0.944114 | -0.008571 |
| 10 | F | -1.330529 | -2.004353 | -0.801220 |
| 11 | N | 1.982451 | -0.651117 | 0.374515 |
| 12 | O | 2.953879 | -1.214704 | 0.151107 |
| 13 | O | 1.125511 | -0.605972 | -0.903584 |
| CF3CHONOCH3 | | | | |
| 1 | C | -1.064520 | -0.411587 | -0.006517 |
| 2 | C | -0.039044 | 0.671235 | -0.346080 |
| 3 | F | -0.572827 | -1.640235 | -0.249912 |
| 4 | F | -1.445631 | -0.370962 | 1.282219 |
| 5 | F | -2.172014 | -0.255567 | -0.766416 |
| 6 | C | -0.543909 | 2.071643 | -0.033398 |
| 7 | H | -0.732965 | 2.176570 | 1.035685 |
| 8 | H | 0.208747 | 2.802668 | -0.330482 |
| 9 | H | -1.467682 | 2.274839 | -0.577743 |
| 10 | H | 0.187078 | 0.555525 | -1.411282 |
| 11 | O | 1.144989 | 0.413612 | 0.404675 |
| 12 | N | 2.176241 | -0.177051 | -0.461056 |

Table B.1 Continued.

| Species/Atom Number | Atom Name | Coordinates | | |
|---|---|---|---|---|
| | | X | Y | Z |
| 13 | O | 3.126287 | -0.433252 | 0.149596 |
| CH3CHONOCH3 | | | | |
| 1 | C | -1.350646 | -1.280230 | -0.280207 |
| 2 | C | -0.948800 | -0.000000 | 0.445653 |
| 3 | H | -1.388190 | -0.000000 | 1.445740 |
| 4 | C | -1.350633 | 1.280236 | -0.280202 |
| 5 | H | -2.438745 | 1.332265 | -0.372114 |
| 6 | H | -1.011347 | 2.156614 | 0.276253 |
| 7 | H | -0.919394 | 1.315608 | -1.282643 |
| 8 | H | -2.438758 | -1.332247 | -0.372119 |
| 9 | H | -1.011368 | -2.156613 | 0.276245 |
| 10 | H | -0.919407 | -1.315602 | -1.282648 |
| 11 | O | 0.476551 | -0.000007 | 0.759169 |
| 12 | N | 1.272340 | 0.000003 | -0.416254 |
| 13 | O | 2.413613 | -0.000004 | -0.144969 |
| CF3CFNOCF3 | | | | |
| 1 | C | -1.304145 | -0.434056 | 0.057237 |
| 2 | C | 0.000000 | 0.348148 | -0.211111 |
| 3 | C | 1.304145 | -0.434056 | 0.057237 |
| 4 | F | -2.348489 | 0.375016 | -0.172370 |
| 5 | F | -1.406603 | -1.492403 | -0.753126 |
| 6 | F | -1.359548 | -0.853005 | 1.324540 |
| 7 | F | 0.000000 | 0.762547 | -1.497623 |
| 8 | F | 1.406600 | -1.492407 | -0.753122 |
| 9 | F | 2.348489 | 0.375014 | -0.172376 |
| 10 | F | 1.359550 | -0.853000 | 1.324541 |
| 11 | N | 0.000000 | 1.567002 | 0.771949 |
| 12 | O | 0.000001 | 2.594363 | 0.184000 |
| CF3CFNOCH3 | | | | |
| 1 | C | -0.955197 | -0.210587 | 0.040327 |
| 2 | C | 0.456068 | 0.389709 | -0.085215 |
| 3 | F | -0.982176 | -1.473849 | -0.406652 |
| 4 | F | -1.356495 | -0.206157 | 1.322489 |
| 5 | F | -1.838674 | 0.504804 | -0.675887 |
| 6 | F | 0.804101 | 0.356269 | -1.406266 |
| 7 | C | 0.566902 | 1.795317 | 0.469997 |
| 8 | H | 0.337779 | 1.807105 | 1.535267 |
| 9 | H | 1.586446 | 2.152810 | 0.316794 |
| 10 | H | -0.125439 | 2.451905 | -0.058056 |
| 11 | N | 1.385432 | -0.503890 | 0.746019 |
| 12 | O | 2.306968 | -0.920103 | 0.116257 |
| CH3CFNOCH3 | | | | |
| 1 | C | -0.493736 | 1.286211 | 0.760364 |
| 2 | C | -0.340613 | 0.000003 | -0.031023 |
| 3 | C | -0.493783 | -1.286181 | 0.760396 |
| 4 | H | -1.478628 | -1.314807 | 1.229534 |
| 5 | H | -0.399485 | -2.145242 | 0.092989 |
| 6 | H | 0.277547 | -1.344217 | 1.529695 |
| 7 | H | -1.478565 | 1.314870 | 1.229533 |
| 8 | H | -0.399442 | 2.145251 | 0.092929 |

Table B.1 Continued.

| Species/Atom Number | Atom Name | Coordinates | | |
|---|---|---|---|---|
| | | X | Y | Z |
| 9 | H | 0.277621 | 1.344254 | 1.529636 |
| 10 | F | -1.260086 | 0.000006 | -1.072216 |
| 11 | N | 1.006172 | -0.000046 | -0.738952 |
| 12 | O | 1.933415 | -0.000005 | 0.022484 |
| CF3CHNOCF3 | | | | |
| 1 | C | -1.288269 | -0.365358 | -0.033063 |
| 2 | F | 1.393320 | -1.498550 | -0.745411 |
| 3 | F | 1.371846 | -0.675442 | 1.265268 |
| 4 | C | 0.000009 | 0.383794 | -0.375736 |
| 5 | H | 0.000031 | 0.621647 | -1.440645 |
| 6 | F | -2.341467 | 0.415890 | -0.342013 |
| 7 | F | -1.393624 | -1.498276 | -0.745568 |
| 8 | F | -1.371876 | -0.675452 | 1.265224 |
| 9 | C | 1.288196 | -0.365515 | -0.033057 |
| 10 | F | 2.341494 | 0.415523 | -0.342189 |
| 11 | N | 0.000084 | 1.695674 | 0.435191 |
| 12 | O | 0.000314 | 2.654734 | -0.269044 |
| CF3CHNOCH3 | | | | |
| 1 | C | -0.872553 | -0.174197 | -0.022607 |
| 2 | C | 0.516997 | 0.335883 | -0.370253 |
| 3 | F | -0.982536 | -1.491323 | -0.284454 |
| 4 | F | -1.178131 | 0.011852 | 1.273524 |
| 5 | F | -1.808168 | 0.466088 | -0.758005 |
| 6 | C | 0.714713 | 1.804370 | 0.008641 |
| 7 | H | 0.627997 | 1.938498 | 1.088003 |
| 8 | H | 1.703152 | 2.135429 | -0.312499 |
| 9 | H | -0.038751 | 2.420889 | -0.483743 |
| 10 | H | 0.696589 | 0.160031 | -1.433648 |
| 11 | N | 1.517967 | -0.472576 | 0.429826 |
| 12 | O | 2.493728 | -0.752837 | -0.205145 |
| CH3CHNOCH3 | | | | |
| 1 | C | -1.071376 | -1.275217 | -0.042817 |
| 2 | C | -0.310125 | 0.000000 | 0.326799 |
| 3 | H | -0.023206 | 0.000000 | 1.383487 |
| 4 | C | -1.071376 | 1.275217 | -0.042817 |
| 5 | H | -2.028483 | 1.304532 | 0.483486 |
| 6 | H | -0.502287 | 2.166226 | 0.232502 |
| 7 | H | -1.266636 | 1.309919 | -1.117658 |
| 8 | H | -2.028483 | -1.304532 | 0.483486 |
| 9 | H | -0.502287 | -2.166226 | 0.232502 |
| 10 | H | -1.266636 | -1.309919 | -1.117658 |
| 11 | N | 0.952507 | -0.000000 | -0.486177 |
| 12 | O | 1.958466 | -0.000000 | 0.172013 |
| CF3CFNO2CF3 | | | | |
| 1 | C | -1.316370 | -0.552691 | 0.079473 |
| 2 | C | -0.000001 | 0.143176 | -0.373076 |
| 3 | C | 1.316368 | -0.552696 | 0.079466 |
| 4 | F | -2.353514 | 0.217214 | -0.271811 |
| 5 | F | -1.424229 | -1.727390 | -0.548564 |
| 6 | F | -1.355969 | -0.760889 | 1.391838 |

Table B.1 Continued.

| Species/Atom Number | Atom Name | Coordinates | | |
|---|---|---|---|---|
| | | X | Y | Z |
| 7 | F | -0.000005 | 0.192174 | -1.715623 |
| 8 | F | 1.424261 | -1.727353 | -0.548648 |
| 9 | F | 2.353508 | 0.217250 | -0.271743 |
| 10 | F | 1.355932 | -0.760977 | 1.391816 |
| 11 | O | -0.000020 | 2.476569 | -0.688168 |
| 12 | N | 0.000005 | 1.612316 | 0.151956 |
| 13 | O | 0.000035 | 1.728027 | 1.360136 |
| CF3CFNO2CH3 | | | | |
| 1 | C | -1.063118 | -0.296223 | -0.085271 |
| 2 | C | 0.195197 | 0.594970 | 0.067913 |
| 3 | F | -0.946096 | -1.115607 | -1.136888 |
| 4 | F | -1.284537 | -1.031121 | 1.009833 |
| 5 | F | -2.130801 | 0.494258 | -0.280524 |
| 6 | F | 0.247982 | 1.397122 | -1.024300 |
| 7 | C | 0.225747 | 1.401845 | 1.344334 |
| 8 | H | 0.252353 | 0.742834 | 2.209426 |
| 9 | H | 1.110704 | 2.039466 | 1.339442 |
| 10 | H | -0.664685 | 2.030207 | 1.386009 |
| 11 | N | 1.447340 | -0.331545 | 0.003763 |
| 12 | O | 2.185983 | -0.196688 | -0.942792 |
| 13 | O | 1.569563 | -1.102951 | 0.938271 |
| CF3CHNO2CF3 | | | | |
| 1 | C | -1.298160 | -0.531808 | -0.045752 |
| 2 | F | 1.399785 | -1.721501 | -0.660720 |
| 3 | F | 1.365962 | -0.730688 | 1.269094 |
| 4 | C | 0.000047 | 0.157556 | -0.497113 |
| 5 | H | 0.000118 | 0.193124 | -1.583959 |
| 6 | F | -2.346470 | 0.222972 | -0.415406 |
| 7 | F | -1.400763 | -1.720618 | -0.661412 |
| 8 | F | -1.366185 | -0.730730 | 1.268857 |
| 9 | C | 1.297912 | -0.532352 | -0.045605 |
| 10 | F | 2.346603 | 0.221678 | -0.415704 |
| 11 | N | 0.000375 | 1.614863 | -0.037142 |
| 12 | O | 0.001097 | 2.447139 | -0.922272 |
| 13 | O | -0.000088 | 1.811917 | 1.161322 |
| CF3CHNO2CH3 | | | | |
| 1 | C | -1.018083 | -0.247865 | 0.003962 |
| 2 | C | 0.200642 | 0.482619 | -0.564247 |
| 3 | F | -0.907790 | -1.577748 | -0.150817 |
| 4 | F | -1.221417 | 0.003517 | 1.303809 |
| 5 | F | -2.116039 | 0.158075 | -0.669296 |
| 6 | C | 0.198916 | 1.969360 | -0.243948 |
| 7 | H | 0.239798 | 2.123227 | 0.833181 |
| 8 | H | 1.058275 | 2.454212 | -0.708806 |
| 9 | H | -0.710953 | 2.423345 | -0.639131 |
| 10 | H | 0.225324 | 0.280588 | -1.633028 |
| 11 | N | 1.467997 | -0.176053 | -0.019506 |
| 12 | O | 2.135524 | -0.810964 | -0.815741 |
| 13 | O | 1.718220 | -0.005072 | 1.160298 |
| CH3CFNO2CH3 | | | | |

Table B.1 Continued.

| Species/Atom Number | Atom Name | Coordinates | | |
|---|---|---|---|---|
| | | X | Y | Z |
| 1 | C | 1.075735 | -0.567464 | -1.286333 |
| 2 | C | 0.572238 | 0.057838 | -0.000010 |
| 3 | C | 1.075744 | -0.567129 | 1.286472 |
| 4 | H | 2.164581 | -0.496824 | 1.309633 |
| 5 | H | 0.671315 | -0.026449 | 2.143905 |
| 6 | H | 0.777410 | -1.612792 | 1.344912 |
| 7 | H | 2.164574 | -0.497182 | -1.309512 |
| 8 | H | 0.671315 | -0.026994 | -2.143903 |
| 9 | H | 0.777384 | -1.613136 | -1.344508 |
| 10 | F | 0.863158 | 1.396788 | -0.000185 |
| 11 | N | -0.984264 | -0.041564 | 0.000009 |
| 12 | O | -1.430975 | -1.179165 | 0.000154 |
| 13 | O | -1.624957 | 0.985885 | -0.000116 |
| CH3CHNO2CH3 | | | | |
| 1 | C | 1.272789 | -1.276573 | 0.024761 |
| 2 | C | 0.599590 | 0.000001 | -0.468848 |
| 3 | H | 0.503547 | 0.000005 | -1.553631 |
| 4 | C | 1.272792 | 1.276572 | 0.024768 |
| 5 | H | 2.298748 | 1.310231 | -0.348733 |
| 6 | H | 0.749175 | 2.164660 | -0.335650 |
| 7 | H | 1.294489 | 1.299350 | 1.115201 |
| 8 | H | 2.298745 | -1.310232 | -0.348741 |
| 9 | H | 0.749170 | -2.164658 | -0.335663 |
| 10 | H | 1.294487 | -1.299358 | 1.115194 |
| 11 | N | -0.851321 | 0.000002 | 0.015315 |
| 12 | O | -1.726474 | 0.000004 | -0.835270 |
| 13 | O | -1.036043 | -0.000006 | 1.222862 |
| Transition States | | | | |
| CH3CHNO2CH3_to_ONO | | | | |
| 1 | C | 1.471498 | -1.293019 | 0.019191 |
| 2 | C | 0.949173 | 0.000005 | -0.484442 |
| 3 | H | 0.668908 | 0.000008 | -1.529501 |
| 4 | C | 1.471468 | 1.293034 | 0.019208 |
| 5 | H | 2.417129 | 1.484567 | -0.514112 |
| 6 | H | 0.797916 | 2.116064 | -0.219266 |
| 7 | H | 1.661545 | 1.272152 | 1.090313 |
| 8 | H | 2.417140 | -1.484544 | -0.514164 |
| 9 | H | 0.797946 | -2.116055 | -0.219261 |
| 10 | H | 1.661611 | -1.272138 | 1.090289 |
| 11 | N | -1.225766 | 0.000010 | -0.227076 |
| 12 | O | -2.426618 | -0.000004 | -0.321264 |
| 13 | O | -0.722715 | -0.000027 | 0.956450 |
| CH3CH2CH2NO2_to_ONO | | | | |
| 1 | C | -2.812366 | -0.185970 | 0.010445 |
| 2 | C | -0.466981 | 0.224265 | 0.667596 |
| 3 | C | -1.341805 | -0.165020 | -0.468488 |
| 4 | O | 2.553235 | -0.658930 | 0.000191 |
| 5 | N | 1.431297 | -0.235324 | 0.009255 |
| 6 | O | 1.247714 | 1.015401 | -0.254756 |
| 7 | H | -0.547171 | 1.242354 | 1.027321 |

Table B.1 Continued.

| Species/Atom Number | Atom Name | Coordinates | | |
|---|---|---|---|---|
| | | X | Y | Z |
| 8 | H | -0.314425 | -0.507374 | 1.451982 |
| 9 | H | -1.055633 | -1.149223 | -0.842483 |
| 10 | H | -1.223935 | 0.554239 | -1.279674 |
| 11 | H | -3.135227 | 0.795769 | 0.365231 |
| 12 | H | -2.965085 | -0.909437 | 0.815011 |
| 13 | H | -3.458276 | -0.470477 | -0.822970 |
| CH3CH2CF2NO2_to_ONO | | | | |
| 1 | C | -2.610140 | 0.732893 | -0.170220 |
| 2 | C | -0.374753 | -0.364787 | 0.004177 |
| 3 | C | -1.128725 | 0.906811 | 0.218818 |
| 4 | O | 2.768326 | 0.447885 | -0.519127 |
| 5 | N | 1.635265 | 0.219691 | -0.201538 |
| 6 | O | 1.331608 | 0.273466 | 1.048746 |
| 7 | H | -3.087170 | -0.051757 | 0.420496 |
| 8 | H | -2.720626 | 0.490220 | -1.227937 |
| 9 | H | -3.136069 | 1.669191 | 0.023495 |
| 10 | F | -0.556110 | -1.344013 | 0.851233 |
| 11 | F | -0.438362 | -0.869824 | -1.211114 |
| 12 | H | -0.657065 | 1.680673 | -0.385963 |
| 13 | H | -1.013437 | 1.178062 | 1.266010 |
| CH3CFNO2CH3_to_ONO | | | | |
| 1 | C | 1.009548 | -0.675959 | 1.329155 |
| 2 | C | 0.879761 | 0.058026 | 0.045338 |
| 3 | C | 0.918243 | 1.537575 | -0.090726 |
| 4 | H | 1.975080 | 1.840214 | -0.061657 |
| 5 | H | 0.516342 | 1.834249 | -1.059851 |
| 6 | H | 0.365445 | 2.027158 | 0.705516 |
| 7 | H | 2.077859 | -0.694927 | 1.586827 |
| 8 | H | 0.674302 | -1.704231 | 1.200835 |
| 9 | H | 0.444549 | -0.193268 | 2.121428 |
| 10 | F | 1.546787 | -0.530926 | -0.937333 |
| 11 | N | -1.302015 | 0.037670 | 0.088544 |
| 12 | O | -2.467509 | 0.313131 | 0.249227 |
| 13 | O | -0.995724 | -0.827181 | -0.796667 |
| CH3CF2CH2NO2_to_ONO | | | | |
| 1 | C | -2.397408 | 0.870723 | -0.102705 |
| 2 | C | 0.080894 | 0.825093 | -0.273709 |
| 3 | C | -1.150520 | 0.000267 | 0.017196 |
| 4 | O | 3.155508 | 0.269577 | 0.134947 |
| 5 | N | 1.981739 | 0.305026 | -0.080018 |
| 6 | O | 1.321614 | -0.797462 | -0.126960 |
| 7 | H | 0.193362 | 1.108007 | -1.311842 |
| 8 | H | 0.211588 | 1.638242 | 0.430039 |
| 9 | H | -2.497166 | 1.271494 | -1.112330 |
| 10 | H | -2.372811 | 1.688519 | 0.618140 |
| 11 | H | -3.257682 | 0.234433 | 0.111595 |
| 12 | F | -1.090266 | -0.513003 | 1.282555 |
| 13 | F | -1.261316 | -1.045808 | -0.847451 |
| CH3CF2CF2NO2_to_ONO | | | | |
| 1 | C | 2.455375 | 0.484929 | -0.204680 |

Table B.1 Continued.

| Species/Atom Number | Atom Name | Coordinates | | |
|---|---|---|---|---|
| | | X | Y | Z |
| 2 | C | -0.059833 | 0.576415 | 0.119710 |
| 3 | C | 1.181876 | -0.331255 | -0.087926 |
| 4 | O | -3.065558 | -0.229344 | -0.382598 |
| 5 | N | -1.925845 | -0.041432 | -0.095612 |
| 6 | O | -1.259364 | -0.984563 | 0.482142 |
| 7 | H | 2.606660 | 1.080120 | 0.696516 |
| 8 | H | 2.410709 | 1.136848 | -1.075636 |
| 9 | H | 3.283668 | -0.215841 | -0.314251 |
| 10 | F | 0.980171 | -1.052642 | -1.220735 |
| 11 | F | 1.279126 | -1.181952 | 0.955578 |
| 12 | F | -0.117689 | 1.152734 | 1.289107 |
| 13 | F | -0.106637 | 1.484041 | -0.845764 |
| CF3CHNO2CH3_to_ONO | | | | |
| 1 | C | -1.143973 | -0.275447 | -0.055311 |
| 2 | C | 0.017534 | 0.610460 | -0.471316 |
| 3 | F | -0.988039 | -1.545844 | -0.431137 |
| 4 | F | -1.428102 | -0.230876 | 1.245817 |
| 5 | F | -2.228417 | 0.217329 | -0.724277 |
| 6 | C | 0.054921 | 1.978988 | 0.105152 |
| 7 | H | 0.033437 | 1.946414 | 1.193096 |
| 8 | H | 0.931993 | 2.525083 | -0.237131 |
| 9 | H | -0.842163 | 2.508387 | -0.243724 |
| 10 | H | 0.175673 | 0.523663 | -1.539592 |
| 11 | N | 1.922086 | -0.050911 | -0.201139 |
| 12 | O | 3.054046 | -0.409392 | -0.328015 |
| 13 | O | 1.255528 | -0.465189 | 0.821834 |
| CF3CHNO2CF3_to_ONO | | | | |
| 1 | C | 0.603821 | -1.314324 | -0.040661 |
| 2 | F | 1.499377 | 1.354344 | -1.133978 |
| 3 | F | 1.504239 | 1.317747 | 1.038206 |
| 4 | C | -0.167155 | 0.013713 | -0.092010 |
| 5 | H | -0.667543 | 0.036900 | -1.074251 |
| 6 | F | -0.270485 | -2.330281 | -0.182735 |
| 7 | F | 1.495005 | -1.400628 | -1.047447 |
| 8 | F | 1.260440 | -1.493417 | 1.110680 |
| 9 | C | 0.713994 | 1.272585 | -0.041583 |
| 10 | F | -0.075347 | 2.362422 | -0.027426 |
| 11 | O | -3.593602 | 0.112693 | -0.239589 |
| 12 | O | -1.111951 | 0.046662 | 0.945004 |
| 13 | N | -2.473009 | 0.080677 | -0.191323 |
| CF3CH2CH2NO2_to_ONO | | | | |
| 1 | C | -1.691175 | -0.063039 | -0.066481 |
| 2 | C | 0.665783 | 0.215283 | 0.669357 |
| 3 | F | -2.490976 | -0.406403 | -1.089169 |
| 4 | F | -1.960786 | -0.895419 | 0.963700 |
| 5 | F | -2.036533 | 1.181357 | 0.326249 |
| 6 | C | -0.228100 | -0.138539 | -0.477004 |
| 7 | O | 3.591497 | -0.689082 | -0.046167 |
| 8 | N | 2.480871 | -0.249856 | -0.071087 |
| 9 | O | 2.318375 | 1.021630 | -0.257009 |

Table B.1 Continued.

| Species/Atom Number | Atom Name | Coordinates | | |
|---|---|---|---|---|
| | | X | Y | Z |
| 10 | H | 0.567569 | 1.217836 | 1.064614 |
| 11 | H | 0.813385 | -0.542626 | 1.428209 |
| 12 | H | -0.030934 | -1.148731 | -0.835054 |
| 13 | H | -0.079488 | 0.564076 | -1.297007 |
| CF3CH2CF2NO2_to_ONO | | | | |
| 1 | C | -1.876797 | 0.229869 | -0.074622 |
| 2 | C | 0.567587 | -0.394038 | 0.148684 |
| 3 | C | -0.445480 | 0.716380 | 0.158473 |
| 4 | O | 3.655778 | 0.374042 | -0.588971 |
| 5 | N | 2.532343 | 0.188780 | -0.230253 |
| 6 | O | 2.041957 | 0.982364 | 0.665086 |
| 7 | F | 0.708464 | -1.109024 | 1.223534 |
| 8 | F | 0.492624 | -1.174242 | -0.904795 |
| 9 | F | -2.204897 | -0.765305 | 0.772335 |
| 10 | F | -2.069262 | -0.216853 | -1.325856 |
| 11 | F | -2.726007 | 1.250445 | 0.135137 |
| 12 | H | -0.393234 | 1.213432 | 1.123981 |
| 13 | H | -0.195211 | 1.435401 | -0.619541 |
| CF3CFNO2CH3_to_ONO | | | | |
| 1 | C | -1.146942 | -0.372179 | -0.020328 |
| 2 | C | -0.000706 | 0.657257 | -0.066433 |
| 3 | F | -0.932794 | -1.399788 | -0.836151 |
| 4 | F | -1.378652 | -0.810543 | 1.214320 |
| 5 | F | -2.263446 | 0.271756 | -0.439502 |
| 6 | F | 0.052184 | 1.136374 | -1.308689 |
| 7 | C | 0.072343 | 1.707747 | 0.981352 |
| 8 | H | 0.011900 | 1.269502 | 1.973167 |
| 9 | H | 0.994778 | 2.276576 | 0.873839 |
| 10 | H | -0.772043 | 2.388609 | 0.818803 |
| 11 | N | 1.881341 | -0.129860 | -0.101160 |
| 12 | O | 2.996504 | -0.485932 | -0.329882 |
| 13 | O | 1.222519 | -0.734418 | 0.830503 |
| CF3CFNO2CF3_to_ONO | | | | |
| 1 | C | -1.430674 | -0.135663 | 0.228411 |
| 2 | C | -0.063206 | -0.075022 | -0.499755 |
| 3 | C | 1.103301 | -0.906691 | 0.098401 |
| 4 | F | -2.392828 | 0.326497 | -0.557771 |
| 5 | F | -1.686540 | -1.431117 | 0.495800 |
| 6 | F | -1.422933 | 0.536403 | 1.375049 |
| 7 | F | -0.176352 | -0.408136 | -1.772057 |
| 8 | F | 0.908660 | -2.202270 | -0.190311 |
| 9 | F | 2.260489 | -0.528455 | -0.445459 |
| 10 | F | 1.161149 | -0.768669 | 1.420749 |
| 11 | O | -0.116536 | 1.879243 | -0.880891 |
| 12 | N | 0.699018 | 1.652682 | 0.090723 |
| 13 | O | 1.314729 | 2.547909 | 0.564464 |
| CF3CF2CH2NO2_to_ONO | | | | |
| 1 | C | 1.711513 | -0.289414 | -0.006267 |
| 2 | C | -0.768296 | -0.669977 | -0.115950 |
| 3 | F | 2.677261 | 0.617811 | 0.098770 |

Table B.1 Continued.

| Species/Atom Number | Atom Name | Coordinates | | |
|---|---|---|---|---|
| | | X | Y | Z |
| 4 | F | 1.820603 | -1.160145 | 1.011166 |
| 5 | F | 1.872064 | -0.965042 | -1.157037 |
| 6 | F | 0.211509 | 1.054690 | 1.191915 |
| 7 | C | 0.305313 | 0.388451 | 0.019445 |
| 8 | F | 0.280645 | 1.277637 | -0.995393 |
| 9 | O | -3.883057 | -0.565919 | 0.069133 |
| 10 | N | -2.705671 | -0.432071 | -0.035772 |
| 11 | O | -2.211053 | 0.756960 | -0.081320 |
| 12 | H | -0.790406 | -1.135188 | -1.092256 |
| 13 | H | -0.766920 | -1.367563 | 0.712006 |
| CF3CF2CF2NO2_to_ONO | | | | |
| 1 | C | -1.900270 | -0.180093 | -0.000003 |
| 2 | C | 0.737850 | -0.283398 | 0.000005 |
| 3 | F | -2.904604 | 0.704840 | -0.000001 |
| 4 | F | -2.011927 | -0.948694 | -1.087515 |
| 5 | F | -2.011928 | -0.948700 | 1.087506 |
| 6 | F | -0.533313 | 1.377397 | -1.100254 |
| 7 | F | 0.718959 | -1.099985 | -1.091105 |
| 8 | F | 0.718958 | -1.099977 | 1.091119 |
| 9 | C | -0.551029 | 0.592958 | 0.000001 |
| 10 | F | -0.533319 | 1.377399 | 1.100254 |
| 11 | O | 4.059567 | 0.385455 | -0.000001 |
| 12 | N | 3.189674 | -0.335164 | -0.000011 |
| 13 | O | 1.811375 | 0.528148 | 0.000002 |